Anti-bacterial and Anti-adhesive Nanostructured Coatings for Improved Implant Biocompatibility

Dissertation

zur

Erlangung des Doktorgrades

der Naturwissenschaften

(Dr.rer.nat.)

dem

Fachbereich Pharmazie

der Phillipps-Universität Marburg

vorgelegt von

Eyas Dayyoub

aus Latakia/Syrien

Marburg an der Lahn 2012

Vom Fachbereich Pharmazie der Philipps-Universität Marburg als Dissertation am 14.02.2012 angenommen

Erstgutachter: Prof.Dr. Udo Bakowsky
Zweitgutachter: Prof.Dr. Michael Keusgen

Tag der mündlichen Prüfung am 20.03.2012

Die vorliegende Arbeit entstand
auf Anregung und unter Leitung von

Herrn Prof. Dr. Udo Bakowsky

am Institut für Pharmazeutische Technologie und Biopharmazie
der Philipps-Universität Marburg.

Meiner Familie

In Liebe und Dankbarkeit

“It’s not the idea that I am extraordinarily intelligent, but everything in it, that I spend more time in solving the problems!”

“If A equals success, then the formula is: A = X + Y + Z

X is work, Y is play, and Z is keeping your mouth shut!”

Albert Einstein

Danksagung

Mein besonderer Dank gilt meinem Doktorvater Herrn ***Prof. Dr. Udo Bakowsky*** für die fortwährend geduldige Betreuung, die unermüdliche Anregung und Motivation, die Freiheit bei der Umsetzung sowie seine stete Diskussionsbereitschaft während der gesamten Promotion.

Ich danke meinen Kollegen ganz herzlich für die Unterstützung, besonders Johannes Sitterberg für die technische Unterstützung während der AFM-Messungen, Dr. Jens Schäfer für den lehrreichen Erfahrungsaustausch und die administrative Unterstützung , Elena Marxer für die wertvolle Freundschaft, Aybike Özcetin für die angenehme Unterhaltung, Jana Brüßler für die stete Hilfsbereitschaft, Nico Harbach für die Hilfe bei der deutschen Sprache, Thomas Betz für die Einführung in die saarländische Küche, Maria Solovey für die englische Korrektur, Boris Strehlow für die Unterstützung bei den REM-Messungen, Mario Bandulik für die nette Gesellschaft beim Shisha rauchen. Allen anderen, Bassam Al Meslmani, Anett Sommerwerk, Leonie Baginski und Susanne Lüttebrandt danke ich ebenfalls für die gute Zusammenarbeit.

Weiterhin bedanke ich mich beim Herrn Prof. Dr. Michael Keusgen, der mir stets Ansprechpartner für unser Kooperationsprojekt war, für die Erstellung des Zweitgutachtens.

Ich danke Herrn Prof. Dr. Thomas Kissel sowie seinen Mitarbeitern Dr. Moritz Beck-Broichsitter, Dr. Nadja Bege, Dr. Markus Benfer, Dr. Heiko Debus, Thomas Endres, Klaus Keim, Dr. Tobias Lebhardt, Dr. Sascha Maretschek, Dr. Olivia Merkel, Eva Mohr, Frank Morell, Dr. Thomas Renette, Dr. Regina Reul, Dr. Susanne Rösler, Olga Samsonova, Dr. Christoph Schweiger, Nina Seidel, Dr. Nan Zhao, Dr. Claudia Packhäuser, Prof. Dr. Oliver Germershaus, Dr. Michael Neu, Dr. Juliane Nguyen, Dr. Terry Steele, Dr. Erik Rytting, Dr. Yu Liu und Dr. Cuifang Cai für die nette Zeit im Institut und ihre Freundschaften.

Prof. Dr. Klaus Liefeith und Dr. Marion Frant von dem IBA/Heiligenstadt danke ichfür die erfolgreiche Zusammenarbeit.

Den Mitarbeitern des AK Keusgen, besonders Dr. Elvira Belz, Nina Dassinger, Christian Hobler und Doru Gheorghe Marcel Vornicescu danke ich für die erfolgreiche Zusammenarbeit.

Ich möchte Herrn Prof. Dr. Torsten Steinmetzer und Herrn Prof. Dr. Klaus Kuschinsky dafür danken, dass sie die Aufgaben der Nebenfachprüfer übernommen haben.

Von tiefsten Herzen möchte ich meinen Eltern und Geschwistern danken.Meinem Vater für sein Vertrauen und die finanzielle Unterstützung, meiner Mutter für ihre Geduld und Liebe, meinen beiden Brüder und meiner Schwester für die herrliche alte Zeit.

Table of Contents

Chapter 3

Highly Ordered Self-Organized Polymer Coatings for Reduced Bacteria Adhesion……... 71

Chapter 4

A novel Method for Designing Nanostructured Polymer Surfaces for Reduced Bacteria Adhesion…… 93

1 Introduction

Biofilm

Formation and Architecture

Growth of bacteria is characterized by two forms of life, one being as single cells (planktonic) and the other being in sessile aggregates [1]. These aggregates are called Biofilms. Like many other communities, the existing of bacteria in groups offers the members of the population advantages they would not achieve when they are in a single form. Examples of other sociobiology existingare easy to find innature; Herds of mammals, flocks of birds, schools of fish, and colonies of insects are prime examples where life of members becomes simpler with protection of the groups [2].

Bacterial biofilms are described as cells bound together by extracellular polymeric substances (EPS) and attached together and to biotic or abiotic surface, the extracellular matrix consists of different kinds of substances such as protein, DNA and polysaccharides [1,3,4]. In nature, probably 99% of the bacteria exist in biofilm form. Bacteria attach to surface and secrete extracellular matrix that protect the bacteria from environment dangers like white blood cells, antibodies and therapeutic antibiotics [5]. Most of biofilms have water channels which are employed as distribution systems for water and nutrients [1].

Biofilm formation is not a random process; it is an ancient and integral componentof the prokaryotic life cycle [6,7] (Fig 1). In the firstphase, bacteria are transported to surfaces by sedimentation, liquid flow,brownian motionand active motion. In this phase, motile bacteriacan use their appendages such as flagella and fimbriae (or pilli) for active swimming [6]. This transport provides direct contact of bacteria with the surface. The attachment of bacteria in this stage depends mainly on favorable bacteria-surface interaction to overcome the repulsive forces occur between bacteria surface and the surface to be colonized [8] and therefore the structure of bacterial surface plays major roll in this stage. In the case of flagellated bacteria, flagellum is not only responsible for motility which may be necessary to

reach the surface; it can also promote recognition and initial adhesion to surface.Studies compared between various bacterial species and have shown that flagella are either completely necessary for, or quicken initial attachment [6,9-12]. The explanation depends on the hypothesis that flagella help the bacteria to overcome the repulsive forces between bacterial surface and substratum [13]. In addition to flagellum, bacterial fimbriae/pili can also promote and accelerate surface attachment [14,15].

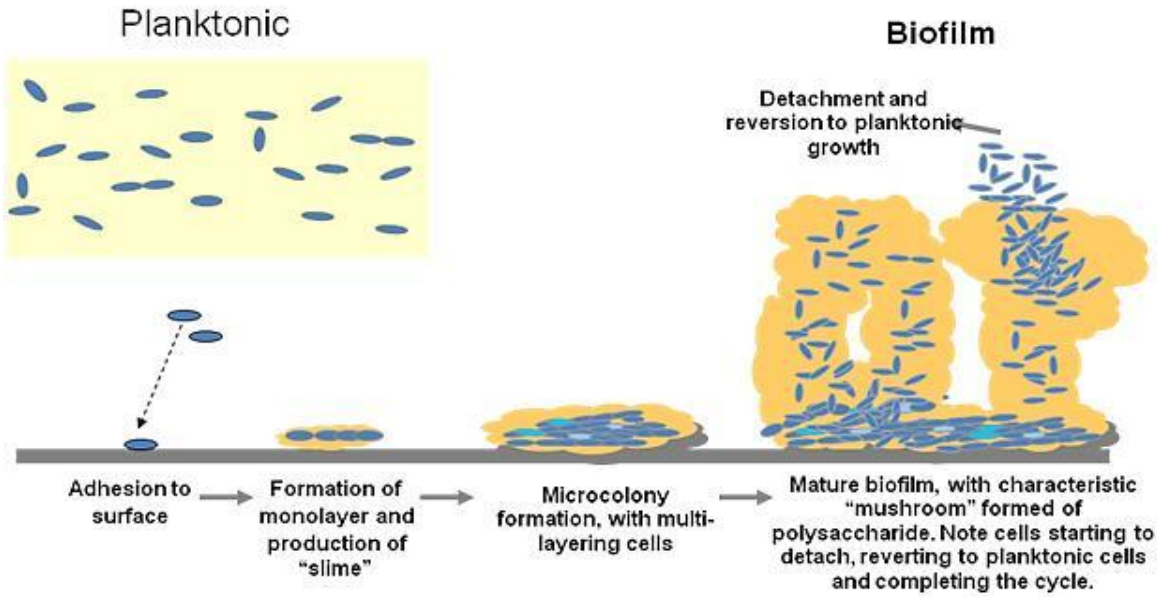

Fig. 1. Steps of biofilm formation (ref: http://biotuesdays.com/2010/10/19/innovotech-targets-personalized-medicine-for-bacteria/).

Further key parameters that influence bacterial initial adhesion are the bacterial membrane molecules such as lipopolysaccharide, lipoproteins, membrane protein, adhesins, etc [16] and the interactions between these molecules and the colonized surface. When membrane molecules come in contact with the conditioning film, short and long range forces like electrostatic, hydrophobic and van der Waals forces in addition to hydrogen bonds, dipole-dipole and coulomb interactions can take place [17]. In aquatic environment, organic

materials attach to the substratum surface before the bacteria, these organic substances form a conditioning film which covers the original surface. Indeed the initial adhesion of bacteria depends on the nature of the conditioning film and not of the original one [18].

If the forces are attractive, a weak and reversible attachment occurs.The influence of the environment must be considered since some factors like ionic strength and pH of the medium can alter surface charge of both bacteria and substratum surfaces resulting in changes of the interactions between the two [19-23]. At the end of this phase, bacteria form monolayer weakly attached to the surface.

In the second step, irreversible attachment is constructed and the bacteria undergo significant changes and initiate lifestyle switch. In the case of non-motile species, the secretion of adhesins increases which promote the cell-cell and cell-surface adherence [24] while in the case of motile species; extracellular matrix is produced to hold the cells together and strengthening the adhesion to surface [25]. These EPS are not only associated with cell surface, they are also excreted in the bacterial growth medium and therefore, they can be presented on the surface to be colonized when secreted from bacteria [26]

It is believed that stimulation of sensory protein bound to membrane leads to producing of EPS [27]. The process continues resulting in three dimensional architecture. In this step, bacteria of the biofilm can interact with their neighbor in the local environment by releasing small diffusible molecules, this system is called Quorum-sensing [28]. It depends on self-generated molecules which are used as signals to coordinate gene expression in correlation to population density [29].

The next step is the surface colonization, bacteria grow and divide inside the biofilm; entrapment of other planktonic cells can also take place leading to the formation of a biofilm [30].The composition of this biofilm is complicated, it differs between the various species of bacteria, it mainly consists of biofilm bacteria entrapped in EPS with high preamble water channels which carry nutrients and waste products [31]. EPS differ between gram-positive

and gram negative bacteria as it contains different EPS polysaccharide. These polysaccharides are neutral or polyanionic in the gram-negative bacteria while gram negative bacteria have cationic polysaccharide. The biofilm structure and architecture can also be affected by parameters like available nutrition in the environment [32] and hydrodynamic conditions [33]. The last step is the detachment of bacteria from biofilm, this happens in the case of unfavorable environment conditions like nutrition limitation [6], the released bacteria attached on other surface and begin again to form another biofilm.

Biofilm on Implant Surfaces

The Food and Drug Administration (FDA) defines an implant as a "device that is placed into a surgically or naturally formed cavity of the human body if it is intended to remain there for a period of 30 days or more." [34]. Implants can be classified in regards to the application site, they also vary due to materials they made from.

Dental implants, neural, orthopedic and urologic prostheses, vascular graft, venous and urinary catheter are well-known examples for medical implants. The used materials vary between polyethylene terephthalate (PET or Dacron), polytetrafluoroethylene (PTFE), polyurethane (PUR), polyimide, silicon and titanium. According to implant type, implant surface encounter one or more body fluids like saliva, urine, blood and gastrointestinal secretions. Human tissues come also in contact with the implant resulting in different kinds of interactions.

Biocompatibility of the implant depends on the tissue-implant and body fluid-implant interactions.Undesired interactions canadversely affect body and cell functions, the effect can appear like inflammation, cell proliferation,coagulation, encrustation and biofilm formation.

Biofilms and the associated infections at the site of implantation present a serious problem for the patients. Bacteria come in contact with implant surface and construct biofilm, the formed biofilms are highly resistant to both immune system of the host and systematic antibiotic [35]. When the bacteria exist in biofilm, they become 10-1000 times more resistance against antibacterial agents [36,37]. Hypotheses suggested mechanisms resistance developments; the first theory suggested that the biofilm glycocalyx prevents diffusion of the antibiotic in the film[38] the second hypotheses depends on the altering of bacterial growth rate which dictate the response to antimicrobial agents [39] while the third one supposed that microenvironment in the biofilm has influence on the antimicrobial activity [40]. The bacteria get into human body and reach implant surface through different ways; the possible sources are the ambient

atmosphere, surgical tools, clothes, bacteria on the patient`s skin and bacteria already in the body [41]

In spite of theefforts, made to develop new implants materials for reduced bacterial adhesion, the rate of implant-associated infections is still high. In the United State, 2.6 million orthopedic implants are inserted in humans annually and 4.3% of them become infected,the medical costs for implant-associated infections exceed about $ 3 billion yearly in the USA alone [42]. In addition to the human pain and suffering because of the infections, these infections can sometimes only be treated by removal of the implant.

To reduce or prevent biofilm formation, effective strategies were followed. They depend on i) preventing or reduction of bacterial adhesion by physiochemical modifying of implant surface ii) systematical or local controlled release of antibiotic.

Strategies to Resist Biofilm

Between the four steps of biofilm formation, the initial adhesion is a determining step. If the initial adhesion is prevented, the bacteria fail to build biofilm and are less capable to cause infections since bacterial attachment is the first step of infection development. The planktonic bacteria are more easily killed by antibacterial agents or host immune system than the bacteria in biofilm as described previously.

Characteristics of surfaces of both bacteria and substratum exert significant influence over the tendency of bacteria to attach to different surfaces [43,44] since the forces that affect bacterial adhesion are the interaction forces at the interfaces between the two surfaces.

There have been a number of studies concerning the influence of substratum surface characteristics on bacterial attachment.

Some of these studies have concentrated on the influence of micro- and nanostructured surfaces on the bacterial adhesion and they showed evidences that bacteria can response to micro- and nanoscale surface features[45-50]. The mechanisms that regulate this response are still less well understood. The effect of this factor is extensively discussed in the next section.

Other studies concentrated on the chemical structure of the surface. Biofuctionalization, coating and chemical modifying of the implant surface showed interesting potential to resist bacterial adhesion and biofilm formation [51-56]. Plasma treatment of the surface results in changing of surface free energy. Upon this fact, the treated surface can decrease the tendency of bacteria to adhere and form biofilm [57,58].

Localized administration of antimicrobial agents is also desirable choice to resist the risk of bacterial adhesion and biofilm formation. As described previously, bacteria within biofilm can develop high resistance against antibacterial agents; therefore, the admisitration of antibacterial agents locally rather than systematically can prevent or reduce the biofilm formation which in turn inhibits creation of antibacterial-resistant strains in the film. In

addition to the last advantage,The high required over-kill dosage in the case of systematical application exposures human body to different risks like side-effects and develompemt of resistant strains in the body in addition to the need to take the drug more than one time daily and the pain caused by intravenous application in some cases.

Different antibiotic like aminoclycosides, cyphalosporines, penicillins and quinolones in addition to inorganic antibacterial agents like silver and nitric oxide were incorporated in coatings or implant materials to be released in the site of implantation [59-66]. More explanation is described in the next sections.

Surface Morphology

The fast development of biomedical industry and bio-interfaces analyzing techniques accompanied with large increasing of studies concerning on the enhancement of implant biocompatibility. These new techniques allow more understanding of biological response to implants and its mechanisms at micro-, nano- and molecular scale.The advances in micor- and nanotechnology have allowed the fabrication of appropriate structured substrates and the aim was controlling the biological response by altering the unfavorable human-implant interactions.

It has been shown that surface topography is an important key to modulate human cell response to this surface. Cells react to macro, micro- and nanostructures. Human cells attach to surface using different molecules; the most common ones are integrins [67], clusters of integrins link the cell to extracellular matrix (ECM). The clustering of integrins is essential in the formation of mutant focal adhesions [68,69]. The cells can expand and bend their membrane when they adhere to surfaces.

Recently, increasing number of scientist investigated the mechansims by which human cells adhere to surface. Comparisons were also done between bacteria and human cells regarding their adhesion to surface; but, till now less is known about the capability of bacteria to sense the surface and thedriving mechanisms than that of eukaryotic cells [67].

Bacterial cells are more rigid and can’t change their form which is partly due to the external layer of peptidoglycan; this layer is thick in gram-positive bacteria while gram-negative bacteria have thin layer which is covered by additional polysaccharide outer layer [70]. They also have variety of surface structures and different outer membrane proteins; some of them express flagella or pili depending on the strain and species [71,72] which renders them very motile and promote surface attachment as described previously.

Bacteria vary significantly in size and shape, their size range between under 1µm to several tens of micrometers and their shape can be spherical, twisted or rod one [70].

This variety of membrane structures, rigidity, shape, motility resulted in different bacterial reaction to topography of the surface they colonized. In contrast, surface topography is characterized by surface roughness, feature shapes (holes, graves, tubes, fibers, micro- and nanoparticles), feature size and distance between the features.

Roughness may influences surface properties like water contact angle [73,74]. Measured zeta potential may also depend on surface roughness; electrical forces at peaks are different than that at valleys [75]. Upon these factors one can expect dissimilar response of bacteria to rough and flat surface.

Evaluation of surface geometry is very complicated; for accurate description, many parameters must be considered. Surface roughness parameters are defined in three groups: amplitude, spacing and hybrid parameters.Among the three, amplitude parameters are the most important one for characterization of surface topography, amplitude includes many parameters such as: arithmetic average height (R_a), root mean square roughness (R_q or RMS), ten-point height (R_z), maximum height of peaks (R_p), maximum height of valleys (R_v) and many other parameters. R_a, also known as centre line average (CLA), is the most universally employed parameter for control of general quality andamongst the used parameters, $R_a$is widely used to characterize surface roughness.

$R_a$is the average of absolute deviation of the roughness irregularities over one sampling length (Fig 2); it offers good description regarding height variations but its main disadvantages is the low sensitivity to small changes in the profile and that it doesn’t provide any information about the wavelength [76].

$R_a$is defined mathematically as:

$$R_a = \frac{1}{l}\int_0^l |y(x)|\,dx$$ (seeFig 2)

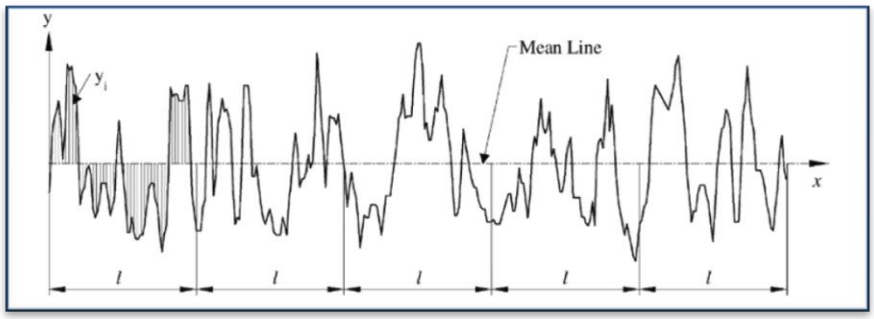

Fig. 2. Definition of arithmetic average height [ref:76]

In addition to arithmetic average height, $R_q$is frequently used in literatures to measure surface roughness. It is defined as standard deviation of surface height distribution.Comparison to R_a, it shows more sensibility to large deviation from the mean line [76]. Its mathematical definition is:

$$R_q = \sqrt{\frac{1}{l}\int_0^l \{y(x)\}^2\,dx}$$ [ref:76]

Recently, atomic force microscopy (AFM) is extensively employedto visualization of surface topography; it is also utilized to determine three-dimensional topographical parameters at the micrometer and nanometer range [77].

Surface roughening has typically used to reduce bacterial adhesion to implant materials [78]. some reports described positive correlation between bacterial adhesion and surface roughness, the explanations are the higher contact surface for the attachment, the protection from shear forces and the increasing in convection mass transport[79-83], this explanation could be right in the case of microstructured surface and not nanostructured one where the contact surface

issmaller and there is no protection from shear forces.Other reports showed negative correlation between surface roughness and bacterial adhesion [84,85], or they didn't find any significant correlation[86].One possible reason for the conflict in some researches is that most of these studies considered only one or two roughness parameters, another failure resource may be the measurement of surface roughness of very limited area (pair of microns), some surfaces have micro-features and these features are nanostructured. In such cases, the bacteria are exposed to the influence of micro-roughness (protection of shear force) and nano-roughness (reduced contact surface).Therefore, more research is required to understand the relation between bacteria and surface roughness by analyzing the underlying factors for bacterial behavior on rough surfaces.

Recently, many investigations of the effect of textured and patterned surfaces on bacterial adhesion were done. Accurate patterned and structured surface were utilized and the influences of feature size, shape and distance between the features were examined. In these researches micro, sub-micro and nano-features were constructed. It is evident that bacteria react to topography that is larger than the bacteria for example they prefer to adhere to the bottom of crevices than to the top [79]. Similar effect was also noticed on surface with scratches. When scratches with different micro-sizes were prepared, the bacterial tended to localize in the bottom of the bigger scratches which provide more bacteria-surface contact and more generically favorable for the adhesion [80]. Under flow conditions, non-motile bacteria adhere less than motile ones suggesting that transport from bulk phase to substratum, especially transport due to motility,plays a predominate roll in initial adhesion. Flagella help bacteria to transport into grooves and/or to recognize the feature topography [81]. Sub-micrometer textures (pillars sizes 400 and 500 nm) significantly reduced bacterial adhesion up to 90% compared to smooth surface of the same chemical nature [87]. The authors described this phenomenon as the effect of reduced surface contact area which accessed 27.5% and 24.5% for the 400 and 500 nm pillars, respectively.

It could be useful to compare the effect of the previous feature with each other. A work done by Puckett et al [85] investigated the effect of nanofeature shape and organization on bacterial adhesion. The used methods enabled the production of nanorough, nanotextured and nanotubular titanium surfaces. Bacterial adhesion tests on the three surfaces were done and compared with unmodified titanium surface. The results showed different bacterial adhesion behavior depending on feature shape. Nanorough surface had more potential to inhibit bacterial adhesion than unmodified surface while nanotextured and nanotubular were more colonized than unmodified surface. However,analyzing and charachterization of the surface energy, contact angle and chemical analysis showed clear differences among the surfaces due to the different steps of modification methods (electron beam evaporation and anodization). Therefore, the chemical nature of the surface must be more considered [67].

The behavior of bacteria on textured and patterned surface needs more investigation to understand the factual and effective factors that drive this behavior and enable designing of ideal anti-bacterial adhesion surfaces.

Coatings for Release of Anti-bacterial Agents

Coating of implants is a versatile method for controlled local delivery of therapeutic agents. Implantation process is mostly associated with a number of complications resulting from undesired reactions of the body at the interfaces. Releasing of active molecules locally at the implantation site improves implant longevity and integration into the body. These molecules can encourage implant acceptance by the body and reduce accompanying rejection responses. The coating act as reservoir for the drugs and allows drug release after the implantation. In order to achieve an optimal effect of the drugs, the coating must have the potential to release operative concentrations of the drugs during the implantation time so many factors that influence the release rate and durations must be considered. Drug/coating affinity and interaction are the most important factors.Coating material, chemical nature, porosity, thickness, homogeneity and preparation methods are also influencing factors. In addition to these factors, drug solubility in water, molecular weight and drug loading affect its release from the coating. Release mechanisms varied due to the used coating material and drugs. Most of the coatings provide diffusive release of the drugs. However,in many coatings that are diffusion-based, degradation, swelling or erosion of coating material allow and/or enhance drug diffusion through the coating matrix. [88-93]. For accurate and regulated release, pH and temperature-sensitive polymer and polymer-blends coating provide the ability to control release profile according to environment parameters [94-96].

Antibiotic delivery systems from implant coating have found increasing interest for inhibition of bacterial adhesion and local therapy of implant-related infections,it is one of the oldest choices used to avoid or alleviate the accompanying infections. As previously described, implant/bacteria interaction process is determining factor for bacterial attachment on implant surface and dealing with this problem requires the development of newimplant materials that are unfavorable for bacterial attachment or coating the implants with anti-adhesive films.

Nevertheless releasing of anti-bacterial agents from the surface is an alternative opportunity which has its advantages over the option of altering implant/bacteria interfaces. Characteristics of bacterial surface and the mechanisms they used to attach to surfacesare diverse due to the variety of bacteria strain and spices andso designing of new surfaces or coatings that resist the adhesion of the different bacteria strains requires taking into account the surface properties and adhesions mechanisms of all probable colonizing bacteria. The construct of such a surface is very hard to achieve and in many cases, the prepared surface were adhesion-resistant against certain kind to bacteria while other strains could survive and form biofilm. In the case of anti-bacterial release coating, one or more wide-spectrum anti-bacterial molecules can be loaded and release for targeting of wide range of bacteria.

The released molecules have not only the potential to kill the bacteria that attempt to attach to the surface, but they can also acts as therapeutic drugs for treatment of the possible infections in the surrounding tissues.

Large number of antibiotics can be incorporated in a coating and applied on implant surfaces. For example: ciprofloxacin, norfloxacin, vancomycin, tobramycin, gentamycin, carbenicillin, amoxicillin, cephalothin, cephamandol, rifampin were loaded in films to release after the implantation. Anti-bacterial agents and antiseptics were also employed such as: chlorhexidine, nitric oxide, silver ions etc. The method used to prepare the films varied between: dipping, spray, solvent evaporation, layer-by-layer (LBL), precipitation and sol-gel methods and the shape of the yielded films were smooth, porous, nanoparticle-containing, fiber-containing or multi-layered films [97-103].

Protein Adsorption on Implant Surfaces

Proteins are an essential component of the human body, they play critical role for the building of the muscles and organs in the human body and they are required for the growth and repair the cells. Their structure consists of hundreds or thousands of amino-acids; the sequence of these amino-acids varies between the different types of proteins and determines their functions. Proteins perform different functions: they are main component of the body; enzymes are proteins that promote chemical reactions in the body. Some proteins from an important part of immune system like antibodies. Due to their complex structure, the proteins can also bind various kinds of molecules so that they play a role as transporting molecules. Hormones are also proteins which regulate the functions of some organs. Many other functions are also known for the proteins.

When an implant is inserted in the body, within seconds, conditioning film of organic components is formed on its surface.Largepart of this film consists ofproteins adsorbed from body fluids. The protein film alters the physiochemical properties of the implants surface like, roughness, charge density and surface tension [104] which in turn, can impact the biological response like cell and bacterial adhesion because these films create the interfaces and affect the subsequence adhesion of human cells and bacteria. Upon this fact, protein adhesion is of crucial importance for designing biocompatible implants.

Fibrinogen, fibronectin, vitronectin, collagen, albumin and immunoglobulin are the most-known proteins adsorbed to implant surface. Fibronectin can regulate cell adhesion and tissue attachment to implant surface and this can promote tissue regeneration [105], vitronectin was found to be able to enhance cell adhesion and the reorganization of the actin microfilaments [106,107]. The adhesion of such proteins could be useful for bone or tooth implant where cell adhesion is required for the growth of the bones and forming strong binding between implant and bones. This phenomenon is undesired for catheter or contact lenses where low adhesion

of the tissues and cells is required [108]. Studies also showed that protein adsorption on biomaterials is the first step of serial events which lead to thrombosis or failure of the biomaterials [109,110].

While some proteins enhance cell adhesion, other proteins inhibit the adhesion like albumin. Its anti-adhesive properties against osteoblast cells were investigated and found to be crucial problem for bone implants [111]. The adverse effect of protein adsorption was particularly noticed in the implants which are in contact with blood.The adhesion of plasma proteins was found to be the initial phase for sequent adhesion of platelet and for coagulation and complement activation [112]. Another disadvantage of protein adsorption is the adsorption of tear protein on contact lenses which cause discomfort to the patients. Adhesion of protein on implant surface alters the surface topography so that the biological responses will depend on the morphology of the new adsorbed layer.

Protein adsorption on implant surface can limit their efficiency and biocompatibility and therefore theinvestigations of this phenomenon gain more concern.

Factors Influence Protein Adsorption

Proteins are small colloids with complex structure; they are composed of sequences of different kinds of amino-acids. Their interactions with surfaces depend mainly on their structure, surface characteristics and environment parameters. Here many interaction forces are known like ionic, van der Waals, solvation and donor-receptor interactions. These forces play major role in protein tendency to attach at solid/liquid interfaces [113].

Molecular properties of proteins determine the adsorption activity of their surface. Hydrophobic forces were reported to be one of the most important forces driving adsorption process, hydrophobic surfaces were considered to be more favorable for protein adsorption than hydrophilic surfaces. [114,115]. In the case of charged surfaces like metals, protein and surface charges are critical for adsorption process. pH value and ionic strength of aqueous medium are determined for charge of protein and surface and so that they influence protein adsorption to surfaces [116,117]. Van der Waals, steric hindering, and donor receptor interactions have showed impact on protein adsorption. The role, these forces play, varies widely between the different proteins and surfaces and so each case must be lonely considered.

Attention must be also given to the composition and conformation of the adsorbed protein film because of the fact that the interaction of cells and other biological component can be governed by the nature and composition of the protein layer [118].

Surface nanotopography is a key factor influencing thickness of the formed layer; it can also control the conformation and orientation of adsorbed proteins and therefore it is critical for cell integrins and adhesion [119-121]. Coating of surfaces with nanostructured films is an innovative method to modulate protein adsorption for improved biocompatibility of implant; this will be discussed in the next section.

Strategies to Resist Protein Adsorption

Resistance of protein adsorption was the aim of many investigations in the last decades.

Literatures describe two main strategies to enhance the anti-fouling properties of biomaterials against protein adsorption. The first one depends on structuring of the biomaterial surface to gain nanostructured surface while the second one exploits the benefits provided by the advanced chemical techniques to modify the biomaterial surface with molecules that repel proteins and reduce their adhesion.

Poly (ethylene oxide) (PEO) is one of the most effective polymers used to control protein adsorption. It is widely used as anti-fouling coatings for implants and biomaterials [123-124]. Its anti-fouling properties against proteins have been attributed to the high mobility of the molecules resulting in steric repulsion and to its neutral charge which minimalizes the electrostatic interactions [125-126]. It can also bind water through hydrogen bonds, this leads to barrier and reduced protein adsorption [127]. Take advantages of polymers that bind water, another kind of polymers were synthesized and used as anti-fouling coating [128]. Increasing of surface wettability by polymer coatings is another possible method to minimize protein adsorption [129]. Examination of new synthesized polymer regards their ability to reduce protein adhesion showed some promising polymers like dextran-based graft copolymers [130] and many other polymers.

Recently, increasing number of studies concern on the impact of surface topography at nanoscale on protein adsorption. The results showed clear evidences that proteins react to nanostructured surface with sizes comparable to protein dimensions [120-122]. In spite of the fact that rough surfaces presents more contact area to protein, decreasing protein adsorption on nanostructured surfaces was noticed [131,119] interactions between nanoscaled surface and proteins are complex because of the combination of attractive and repulsive forces

administered by local changes of surface properties[119] and more investigation in this field must be done for deep understanding of these interactions.

References

1. Bjarnsholt T. Introduction to biofilms. in:Bjarnsholt T, Moser C, Jensen PØ, Høiby N. Biofilm infections. New York Dordrecht Heidelberg London: Springer.P 1-11.

2. *Pseudomonas* biofilm matrix composition and niche biology, Ethan E. Mann and Daniel J. Wozniak. FEMS Microbiology Reviews 2011.Accepted article.

3.Karunakaran E, Mukherjee J, Ramalingam B, Biggs CA. "Biofilmology": a multidisciplinary review of the study of microbial biofilms. Appl Microbiol Biotechnol 2011;90:1869–1881.

4. Davey ME, O'Toole GA. Microbial biofilms: from ecology to molecular genetics. Microbiol Mol Biol Rev 200;64:847-867.

5.Wolcott R, Dowd S. The role of biofilms: Are we hitting the right target. Plastic and ReconstructiveSurgery2010;127: 28–35.

6. Kierek-Pearson K, Karatan E.Biofilm Development in Bacteria ,Adv Appl Microbiol 2005;57:79-104.

7. Zhang X, Wyss UP, Pichora D, Goosen MF. Biodegradable controlled antibiotic release devices for osteomyelitis: Optimization of release properties. J. Pharm. Pharmacol 1994;46:718 – 724 .

8. Geesey GG. Bacterial behavior at surfaces.Curr Opin Microbiol 2001;4:296–300.

9. Piette JP, Idziak ES. Role of flagella in adhesion of Pseudomonas fluorescens to tendon slices.Appl. Environ. Microbiol 1991;57:1635-1639.

10. Prigent-Combaret C, Prensier G, Le Thi TT, Vidal O, Lejeune P, Dorel C. Developmental pathway for biofilm formation in curli-producing Escherichia coli strains: Role of flagella, curli and colanic acid. Environ. Microbiol 2000;2:450–464.

11. O'Toole GA, Kolter R. Flagellar and twitching motility are necessary for Pseudomonas aeruginosa biofilm development. Mol. Microbiol 1998;30:295–304.

12. O'Toole, GA, Kolter R. Initiation of biofilm formation in Pseudomonas fluorescens WCS365 proceeds via multiple, convergent signalling pathways: A genetic analysis. Mol. Microbiol 1998;28:449–461.

13. Lejeune P. Contamination of abiotic surfaces: What a colonizing bacterium sees and how to blur it. Trends Microbiol 2003;11:179–184.

14.Pratt LA, Kolter R. Genetic analysis of Escherichia coli biofilm formation: Roles ofm flagella, motility, chemotaxis and type I pili. Mol. Microbiol 1998;30:285–293.

15. Meibom KL, Li XB, Nielsen AT, Wu CY, Roseman S, Schoolnik GK.The Vibrio cholerae chitin utilization program. Proc. Natl. Acad. Sci. USA 2004;101:2524–2529.

16. Sutherland IW. Bacterial exopolysaccharides. Adv. Microb. Physiol 1972;8:143–212.

17. Hannig C, Hannig M. The oral cavity: a key system to understand substratumdependent bioadhesion on solid surfaces in man. Clin Oral Invest 2009;13: 123–39.

18. Hwang G, Kang S, Gamal El-Din M, Liu Y.Impact of conditioning films on the initial adhesion of Burkholderia cepacia. Colloids and Surfaces B: Biointerfaces 2012;91:181– 188.

19. Fang B, Gon S, Park M, Kumar KN, Rotello VM, Nusslein K, Santore MM. Bacterial adhesion on hybrid cationic nanoparticle–polymer brush surfaces:Ionic strength tunes capture from monovalent to multivalent binding. Colloids and Surfaces B: Biointerfaces 2011;87: 109– 115.

20. Katsikogianni MG, Missirlis YF.Interactions of bacteria with specific biomaterial surface chemistries under flow conditions. Acta Biomaterialia 2010;6:1107–1118.

21. Kalasina S, Dabkowskic J, Nüssleinb K, Santorec MM,The role of nano-scale heterogeneous electrostatic interactions in initial bacterial adhesion from flow: A case study with Staphylococcus aureus. Colloids and Surfaces B: Biointerfaces 2010;76:489–495.

22. Mi L, Bernards MT, Cheng G, Yu Q, Jiang S. pH responsive properties of non-fouling mixed-charge polymer brushes based on quaternary amine and carboxylic acid monomers, , Biomaterials2010;31:2919–2925.

23. Sheng X , Ting YP , Pehkonen SO.The influence of ionic strength, nutrients and pH on bacterial adhesion to metals.Journal of Colloid and Interface Science 2008;321:256–264.

24. Gotz F. *Staphylococcus* and biofilms. Mol Microbiol 2002;43:1367-1378.

25.Lemon KP, Earl AM, Vlamakis HC, Aguilar C, Kolter R.Biofilm Development with an Emphasison Bacillus subtilis. In: Romeo T. Bacterial Biofilms. Berlin Heidelberg: Springer-Verlag; 2008. P 1-16.

26. Jain A, Bhosle NB, Biochemical composition of the marine conditioning film:implications for bacterial adhesion, Biofouling: The Journal of Bioadhesion andBiofilm Research 2009; 25:13–19.

27. Boyd A,Chakrabarty AM. *Pseudomonas aeruginosa* biofi lms: role of the alginate exopolysaccharide.J. Indust. Microbio 1995;15:162 – 168 .

28. Davies DG.Understanding biofilm resistance to antibacterial agents.Nature Reviews Drug Discovery 2003;2:114 – 122 .

29. Shunmugaperumal T, Introdcution and overwniew of biofilm. In:Biofilm eradication and prevention. Hoboken, New Jersey: John Wiley & Sons; 2010. p 3-35.

30. Costerton JW, Lewandowski Z, De Beer D, Caldwell D, Korber D, James G. Biofilms, the customised microniche.J. Bacteriol 1994;76:2137–2142 .

31. Stoodley P, De Beer D, Lewandowski Z. Liquid fl ow in biofilm Systems. Appl. Environ. Microbiol 1994;60:2711–2716 .

32 Heydorn A, Ersboll B, Kato J, Hentzer M, Parsek MR, Tolker-Nielsen T, Givskov M, Molin S. Statistical analysis of Pseudomonas aeruginosa biofilm development: Impact of mutations in genes involved in twitchingmotility, cell-to-cell signaling, and stationary-phase sigma factor expression. Appl. Environ. Microbiol2002;68:2008–2017.

33. Purevdorj B, Costerton JW, Stoodley P. Influence of hydrodynamics and cell signaling on the structure and behavior of Pseudomonas aeruginosa biofilms. Appl. Environ. Microbiol 2002;68:4457–4464.

34. U.S. food and drug administration, code of federal regulations, title 21, volume 8.

35. Hetrick EM, Schoenfisch MH.Reducing implant-related infections: active release strategies.Chem. Soc. Rev;2006:35:780–789.

36.Prosser BL,Taylor D,Dix BA, Cleeland R. Method of evaluatingeffects of antibiotics on bacterial biofilm.Antimicrob. Agents Chemother 1987;31:1502–1506

37. Nickel JC,Ruseska I,Wright J B, Costerton JW. Tobramycin resistance of*Pseudomonas aeruginosa* cells growing as abiofilm on urinary tract catheter. Antimicrob. Agents Chemother 1985;27:619–624

38. John GT, Litton I, Rinde H. Economic Impact ofBiofilms on TreatmentCosts. in: Pace JL, Rupp ME, Finch RG. Biofilms, Infection, and Antimicrobial Therapy. Florida, USA: Taylor & Francis Group; 2006. P 21-38.

39. Eng RH, Padberg FT, Smith SM, Tan EN, Cherubin CE. Bactericidal effects of antibiotics on slowly growing and nongrowing bacteria.Antimicrob.Agents Chemother 1991;35:1824-1828.

40. Dunne WMJr. Bacterial adhesion: seen any good biofilms lately? Clin.Microbiol. Rev2002;15:155–166.

41. An YH, FriedmanRJ. Prevention of sepsis in total joint arthroplasty. J. Hosp. Infect 1996;33:93-108.

42.Rabih O, Darouiche MD. New Engl. J. Med 2004;350:1422-1429.

43. Riedewald F. Bacterial adhesion to surfaces: the influence of surface roughness. PDA J Pharma Sci Technol 2006;60:164–171.

44. Shellenberger K, Logan BE. Effect of molecular scaleroughness of glass beads on colloidal and bacterial deposition.Environ Sci Technol 2002;36:184–189.

45. Colon G, Ward BC, Webster TJ. Increased osteoblast and decreasedStaphylococcus epidermidis functions on nanophase ZnO and TiO2. J BiomedMater Res A 2006;78:595–604.

46. Ploux L, Anselme K, Dirani A, Ponche A, Soppera O, Roucoules V. Oppositeresponses of cells and bacteria to micro/nanopatterned surfaces prepared bypulsed plasma polymerization and UV-irradiation. Langmuir 2009;25:8161–8169.

47. Bruinsma GM, Rustema-Abbing M, de Vries J, Stegenga B, van der Mei HC, vander Linden ML, et al. Influence of wear and overwear on surface properties ofEtafilcon a contact lenses and adhesion of Pseudomonas aeruginosa. InvestOphthalmol Vis Sci 2002;43:3646–3652.

48. Whitehead KA, Colligon J, Verran J. Retention of microbial cells in substratumsurface features of micrometer and sub-micrometer dimensions. ColloidsSurf B Biointerfaces 2005;41:129–138.

49. Campoccia D, Montanaro L, Agheli H, Sutherland DS, Pirini V, Donati ME, Arciola CR. Study of Staphylococcus aureus adhesion on a novel nanostructured surface bychemiluminometry. Int J Artif Organs 2006;29:622–629.

50. Diaz C, Schilardi PL, Salvarezza RC, Lorenzo Fernandez, de Mele M. Nano/Microscale Order Affects the Early Stages of Biofilm Formation on Metal Surfaces. Langmuir 2007;23:11206–11210.

51. Lopez AI, Kumar A, Planas MR, Li Y, Nguyen TV, Cai C. Biofunctionalization of silicone polymers using poly(amidoamine) dendrimersand a mannose derivative for prolonged interference against pathogen colonization. Biomaterials 2011;32:4336-4346.

52. Wanga H, Wanga L, Zhangb P, Yuana L, Yua Q, Chena H. High antibacterial efficiency of pDMAEMA modified silicon nanowire arrays Colloids and Surfaces B: Biointerfaces 2011;83:355–359.

53. Yuan S, Wan D, Liang B, Pehkonen SO, Ting YP, Neoh KG, Kang ET. Lysozyme-Coupled Poly(poly(ethylene glycol)methacrylate)-Stainless Steel Hybrids and Their Antifoulingand Antibacterial Surfaces. Langmuir 2011;27:2761–2774.

54. Belcarz A, Bieniaś J, Surowska B , Ginalska G. Studies of bacterial adhesion on TiN, SiO2–TiO2 and hydroxyapatite thin layersdeposited on titanium and Ti6Al4V alloy for medical applications.Thin Solid Films 2010;519:797–803.

55. Sisti L, Cruciania L, Totaroa G, Vanninia M, Berti C , Aloisio I, Di Gioia D. Antibacterial coatings on poly(fluoroethylenepropylene) films via grafting of 3-hexadecyl-1-vinylimidazolium bromide. Progress in Organic Coatings 2012;73:257–263.

56. Travan A, Marsich E, Donati I, Benincasa M, Giazzon M , Felisari L, Paoletti S. Silver–polysaccharide nanocomposite antimicrobial coatings for methacrylic thermosets. Acta Biomaterialia 2011;7:337–346.

57. TriandafilluaK, BalazsbDJ, AronssoncBO, DescoutscP, Tu QuocdP, van DeldendC, MathieubHJ, Harms H. Adhesion of Pseudomonas aeruginosa strains to untreated and oxygen-plasma treated poly(vinyl chloride) (PVC) from endotracheal intubation devices. Biomaterials 2003;24:1507–1518.

58. KatsikogianniaM, AmanatidesbE, MatarasbD, MissirlisYF. *Staphylococcus epidermidis* adhesion to He, He/O2 plasma treated PET films and aged materials: Contributions of surface free energy and shear rate. Colloids and Surfaces B: Biointerfaces 2008;65:257–268.

59 Simchi A, Tamjid E, Pishbin F, BoccacciniAR.Recent progress in inorganic and composite coatings with bactericidal capability for orthopaedic applications.Nanomedicine: Nanotechnology, Biology, and Medicine 2011;7:22–39.

60. Shukla A, Fuller RC, Hammond PT.Design of multi-drug release coatings targeting infection and inflammation.J Control Release 2011;155:159–166.

61. Ewald A , Hösel D , Patel S , Grover LM, Barralet JE , Gbureck U.Silver-doped calcium phosphate cements with antimicrobial activity. Acta Biomaterialia 2011;7:4064–4070.

62.Popata KC, Eltgrothc M, LaTempad TJ, Grimesd CA, Desai TA.Decreased Staphylococcus epidermis adhesion and increased osteoblast functionality on antibiotic-loaded titania nanotubes, Biomaterials 2007;28:4880–4888.

63.Minelli EB, Bora TD, Benini A.Different microbial biofilm formation on polymethylmethacrylate (PMMA) bone cement loaded with gentamicin and vancomycin. Anaerobe 2011;17:380-383.

64. Shukla A, Fleming KE, Chuang HF, Chau TM, Loose CR, Stephanopoulos GN, Hammond PT. Controlling the release of peptide antimicrobial agents from surfaces. Biomaterials 2010;31:2348–2357.

65.StigteraM, BezemeraJ, de GrootbK, LayrolleP, Incorporation of different antibiotics into carbonated hydroxyapatite coatings on titanium implants, release and antibiotic efficacy. J Control Release 2004;99127–137.

66. Malcher M, Volodkin D, Heurtault B, André P, Schaaf P , Möhwald H , Voegel JC, Sokolowski A, Ball V, Boulmedais F, Frisch B.Embedded Silver Ions-Containing Liposomes in Polyelectrolyte Multilayers: Cargos Films for Antibacterial Agents,Langmuir 2008;24:10209–10215.

67. Anselme K, Davidson P, Popa AM, Giazzon M, Liley M, Ploux L. The interaction of cells and bacteria with surfaces structured at the nanometre scale. Acta Biomaterialia 2010;6:3824–3846.

68. Hersel U, Dahmen C, Kessler H. RGD modified polymers:biomaterials for stimulated cell adhesion and beyond. Biomaterials 2003;24:4385–415.

69. Spatz PS. Cell-nanostructure interactions. Nanobiotechnology.Weinheim: Wiley-VCH; 2004. p. 53–65.

70. Srivastava S, Srivastava PS. Understanding bacteria. Dordrecht: Kluwer Academic; 2003.

71.Proft T, Baker EN. Pili in Gram-negative and Gram-positive bacteria structure, assembly and their role in disease. Cell Mol Life Sci 2009;66:613–635.

72. Van Houdt R, Michiels CW. Role of bacterial cell surface structures in Escherichia coli biofilm formation. Res Microbiol 2005;156:626–633.

73. Cassie ABD, Baxter S,Wettability of porous surfaces, Transactions of the Faraday Society 1944;40:546–550.

74. WenzelRN. Resistance of solid surfaces to wetting by water, Industrial and Engineering Chemistry 1936;28:988–994.

75. BowenWR, DonevaTA.Atomic force microscopy studies ofmembranes: effect of surface roughness on double-layer interactions and particle adhesion, J Colloid Interface Sci 2000;229:544–549.

76. Gadelmawla ES, koura MM, Maksoud TMA, Elewa IM, Soliman HH. Roughness parameters.journal of material processing technology 2002;123:133-145.

77. De Chi1reL.Industrial Survey on ISO surface texture parameters.Annals of the CIRP 1999;48:74–77.

78. Wu Y, Zitelli JP, Kevor S. TenHuisen KS, Yu X, Libera MR. Differential response of Staphylococci and osteoblasts to varying titanium surface roughness Biomaterials 2011;32: 951-960.

79. Characklis WG. Fouling biofilm development: a process analysis. Biotechnol Bioeng 1981;23:1923–60.

80. Edwards KJ, Rutenberg AD. Microbial response to surface microtopography: the role of metabolism in localized mineral dissolution. Chem Geol 2001;180:19–32.

81.Scheuerman TR, Camper AK, Hamilton MA. Effects of substratum topography on bacterial adhesion. J Colloid Interface Sci 1998;208:23–33.

82. Whitehead KA, Verran J. The effect of surface topography on the retention of microorganisms. Food Bioprod Process 2006;84:253–9.

83. Flint SH, Brooks JD, Bremer PJ. Properties of the stainless steel substrate, influencing the adhesion of thermo-resistant streptococci 2000;43:235-242.

84.Truong VK, Lapovok R, Estrin YS, Rundell S, Wang JY, Fluke CJ, Crawford RG. Ivanova IP.The influence of nano-scale surface roughness on bacterial adhesion to ultrafine-grained titanium. Biomaterials 2010;31:3674–3683.

85. Puckett SD , Taylor E, Raimondo T, Webster TJ.The relationship between the nanostructure of titanium surfaces and bacterial attachment, , Biomaterials 2010;31:706–713.

86. Hilberta LR, Bagge-Ravnb D, Koldc J, Gramb L.Influence of surface roughness of stainless steel on microbial adhesion and corrosion resistance. International Biodeterioration & Biodegradation 2003;52:175 – 185.

87.Xu LC, Siedlecki CA.Submicron-textured biomaterial surface reduces staphylococcal bacterial adhesion and biofilm formation. Acta Biomaterialia 2012;8:72–81.

88. Abarrategi A, Civantos A, Ramos V, Casado JVS, López-Lacomba JL. Chitosan film as rhBMP2 carrier: delivery properties for bone tissue application.Biomacromolecules2008:2:711–718.

89. Wang LC, Chen XG, Zhong DY, Xu QC. Study on poly(vinyl alcohol)/carboxymethyl-chitosan blend film as local drug delivery system. J Mater Sci Mater Med 2007; 18:1125-1133.

90. Grant J, Blicker M, Piquette-Miller M,Allen C. Hybrid films from blends of chitosan and egg phosphatidylcholine for localized delivery of paclitaxel. J Pharm Sci 2005;94:1512–1527.

91. Price JS, Tencer AF, Arm DM,Bohach GA. Controlled release of antibiotics from coated orthopedic implants.J Biomed Mater Res 1996;30 281–286.

92. Klugherz BD, Jones PL, Cui X, Chen X, Meneveau NF, DeFelice S,Jeanne Connolly J, Wilensky RL, Levy RJ. Gene delivery from a DNA controlledrelease stent in porcine coronary arteries.Nature 2000;18 1181-1184.

93. C. J. Pan, J. J. Tang, Y. J. Weng, J. Wang und N. Huang. Preparation and characterization of rapamycin-loaded PLGA coating stent.J Mater Sci Mater Med 2007;18:2193-219.

94. Burke SE, Barrett CJ.pH-Dependent Loading and Release Behavior of Small Hydrophilic Molecules in Weak Polyelectrolyte Multilayer Films. Macromolecules2004;37:5375–5384.

95. Chung AJ, Rubner MF.Methods of Loading and Releasing Low Molecular Weight Cationic Molecules in Weak Polyelectrolyte Multilayer Films.Langmuir2002;18:1176–1183.

96. Yoshizawa T, Shin-ya Y, Hong KJ, Kajiuchi T. pH- and temperature-sensitive release behaviors from polyelectrolyte complex films composed of chitosan and PAOMA copolymer.Eur J Pharm Biopharm 2005;59:307-313.

97. Verraedt E, Braem A, Chaudhari A, Thevissen K, Adams E, Van Mellaert L, Cammue BPA, Duyck J, Anné J, Vleugels J, Martens JA. Controlled release of chlorhexidine antiseptic from microporous amorphous silica applied in open porosity of an implant surface, Int J Pharm2011;419:28– 32.

98. ParkPIP , Makoid M, Jonnalagadda S. The design of flexible ciprofloxacin-loaded PLGA implants using a reversedphase separation/coacervation method, Eur J Pharm Biopharm 2011;77:233–239.

99. Ravelingien M, Mullens S, Luyten J, D'Hondt M , Boonen J, De Spiegeleer B , Coenye T, Vervaet C, Remon JP. Vancomycin release from poly(D,L-lactic acid) spray-coated hydroxyapatite fibers, Eur J Pharm Biopharm2010;76:366–370.

100. Shukla A, Fuller RC, Hammond PT. Design of multi-drug release coatings targeting infection and inflammation.J Control Release2011;155:159–166.

101. Stigtera M, BezemeraJ, de GrootbK, LayrolleP. Incorporation of different antibiotics into carbonated hydroxyapatite coatings on titanium implants, release and antibiotic efficacy.J Control Release2004;99:127–137.

102. StigteraM, de GrootaK, LayrolleP. Incorporation of tobramycin into biomimetic hydroxyapatitecoating on titanium, Biomaterials 2002;23:4143–4153.

103. Nablo BJ, Rothrock AR, Schoenfisch MH.Nitric oxide-releasing sol–gels as antibacterial coatings for orthopedic implants. Biomaterials 2005;26:917–924.

104. Xu LC, LoganBE. Interaction forces between colloids and protein-coatedsurfaces measured using an atomic force microscope, Environmental Science & Technology 2005;39:3592–3600.

105. Wan L. Cytological study on the effect of fibronectin in promoting periodontal regeneration. J Stomatology 1994;29:175-177.

106. Degasne I, Basle MF, Demais V, Hure G, Lesourd M, Grolleau B, Mercier L, Chappard D. Effects of roughness, "bronectin and vitronectin on attachment, spreading and proliferation of human osteoblast-like cells (Saos-2) on titanium surfaces. Calcif Tissue Int 1999;64:499-507.

107. Grinnell F, Feld MK. Fibronectin adsorption on hydrophilic and hydrophobic surfaces detected by antibody binding and analysed during cell adhesion in serum-containing medium. J Biol Chem 1982;257:4888-4893.

108. Galli C, Coen M C, Hauert R, KatanaevV L, Wymann M P, Groning P, Schlapbach L. Protein adsorption on topographically nanostructured titanium. Surface Science 2001;474:L180-L184.

109. Horbett TA. Principles underlying the role of adsorbed plasma proteins in blood interactions with foreign materials. Cardiovasc Pathol 1993;2:1375-1485.

110. Andrade JD,Nagaoka S, Cooper S, Okano T, Kim SW. Surfaces and blood complatibility: current hypotheses. Am Soc Artif Inter Org J 1987;10:75-84.

111. Klinger A, Steinberg D, Kohavi D, Sela MN. Mechanism of adsorption of human albumin to titanium in vitro, J. Biomed.Mater.Res 1997;36:387–392.

112. Brash JL. Exploiting the current paradigm of blood-material interactions for the rational design of blood-compatible materials.J Biomater Sci Polym Edn 2000;11:1135–1146.

113. Haynes CA, Norde W. Globular proteins at solid/liquid interfaces. Colloids Surf B 1994;2:517–566.

114. Krisdhasima V,Mcguire J, Sproull R. Surface hydrophobic influences on β-lactoglobulin adsorption kinetics. J Colloid Interface Sci1992;154:337-350.

115. Buijs J, Hlady VV. Adsorption Kinetics, Conformation, and Mobility of the Growth Hormone and Lysozyme on Solid Surfaces, Studied with TIRF. J Colloid Interface Sci. 1997;190:171-81.

116. Pasche S, Vörös J, Griesser HJ, Spencer ND, Textor M. Effects of Ionic Strength and Surface Charge on Protein Adsorption at PEGylated Surfaces. J. Phys. Chem. B 2005:109:17545–17552.

117. Burns NL,Holmberg K, Brink C. Influence of Surface Charge on Protein Adsorption at an Amphoteric Surface: Effects of Varying Acid to Base Ratio. J Colloid Interface1996;178:116–122.

118. Lynch I, Dawson KA. Are there generic mechanisms governing interactions between nanoparticles and cells? Random epitope mapping for the outer layer of the protein–material interface.Physica A 2007;373:511-520.

119. Lorda MS, Fossb M, Besenbacherb F. Influence of nanoscale surface topography on protein adsorption and cellular response. Nano Today 2010;5:66-78.

120. DeligianniDD, KatsalaN, LadasS, SotiropoulouD, AmedeeJ, MissirlisYF. Efect of surface roughness of the titanium alloy Ti-6Al-4V on human bone marrow cell response and on protein adsorption. Biomaterials 2001;22:1241-1251.

121. Denis FA, Hanarp P, Sutherland DS, Gold J,‡ Mustin C, Rouxhet PG, Dufrêne YF. Protein Adsorption on Model Surfaces with Controlled Nanotopography and Chemistry. Langmuir2002;18:819–828.

122. Galli C,Coen MC, Hauert R, Katanaev VL, Gröning P, Schlapbach L. Creation of nanostructures to study the topographical dependency of protein adsorption. Colloids Surf B Biointerfaces2002;26:255–267.

123. Hamilton-Brown P, Gengenbach T, Griesser H,Meagher L. End Terminal, Poly(ethylene oxide) Graft Layers: Surface Forces and Protein Adsorption. Langmuir 2009;25:9149–9156.

124. Sofia SJ, Premnath V, Merrill EW. Poly(ethylene oxide) Grafted to Silicon Surfaces: Grafting Density and Protein Adsorption. Macromolecules1998;31:5059–5070.

125. Jeon SI, Andrade JD.Protein—surface interactions in the presence of polyethylene oxide: II. Effect of protein size. J. Colloid Interface Sci. 1991;142:159–166.

126. Jeon SI, Lee JH, Andrade JD, de Gennes PG. Protein—surface interactions in the presence of polyethylene oxide: I. Simplified theoryJ. Colloid Interface Sci. 1991;142:149-158.

127. Gombotz WR, Wang G, Horbett TA, Hoffman AS.Protein adsorption topoly(ethylene oxide) surfaces, J. Biomed. Mater.Res. A 1991;25:1547–1562.

128. Liua PS, Chena Q, Wua SS, Shena J, Lina SC. Surface modification of cellulose membranes with zwitterionic polymers for resistance to protein adsorption and platelet adhesion. Journal of Membrane Science 2010;350:387–394.

129. Huang B, Wu H, Kim S, Zare N. Coating of poly(dimethylsiloxane) with n-dodecyl-b-D-maltoside to minimize nonspecific protein adsorption. Lab Chip 2005;5:1005–1007.

130. Perrino C,Lee S,Choi SW,Maruyama A,Spencer ND. A Biomimetic Alternative to Poly(ethylene glycol) as an Antifouling Coating: Resistance to Nonspecific Protein Adsorption of Poly(L-lysine)-graft-dextran. Langmuir2008;24:8850-8856.

131. KocY,.de Mello J, McHale G, Newton I, Roach P,Shirtcliffe NJ. Nano-scale superhydrophobicity: suppression of protein adsorption and promotion of flow-induced detachment. Lab on a Chip 2008;8:582-586.

2 Anti-bacterial and Anti-encrustation Hydrophobic Biodegradable Polymer Coating for Urinary Catheter

In preparation for Journal of Controlled Release

Abstract

Bacterial biofilm and crystalline deposits are the common causes of failure of long-term indwelling urinary catheter. Bacteria colonize the catheter surface causing serious infections in the urinary tract and encrustations that can block the catheter and induce trauma in patients. In this study, the strategy used to resist bacterial adhesion and encrustation represents a combination of the anti-bacterial effects of norfloxacin and silver nanoparticles and the PLGA-based neutralization of alkalic products of urea hydrolysis gained through the degradation of the polymer in an aqueous milieu. Silver nanoparticles were coated with Tetraether lipids (TEL) to avoid the aggregation when dispersed in acetone and during the film formation. The polymer films loaded with the two anti-bacterial agents were applied on glass which was used as catheter surface model. It was shown that the release of norfloxacin from the films was diffusion-controlled and lasted over ~2 months. We also demonstrated the anti-bacterial and anti-adhesion effectiveness of the coatings whereby glass, unloaded polymer films and copper were used as a control. Using artificial urine and a new *in vitro*-encrustation model, it was shown that the coatings resist the encrustation for at least 2 weeks. This combination of a degradable polymer and wide-range anti-bacterial agents represents a potentially attractive biocompatible coating for urinary catheters.

Introduction

Indwelling urinary catheters are medical devices employedin both hospital and nursing home settings to allow the drain of patient's urine in case of urinaryretention and to relieve the urinary incontinence [1]. These catheters are one of the most commonly used medical devices in urology [2]. More than 30 million urinary catheters were utilized in the United States yearly and a quarter of the hospitalized patients receive an indwelling urinary catheter [3].

The main serious complication related to urinary catheterisation is the catheter-associated urinary tract infections (CUTI). Millions of CUTI happen per annum, two million nosocomial infections happen yearly in the United States and 40% involve the urinary tract infection [4] and the costs are averagely 3,000 US $ to 4,000 US $ each [5]. Up to 50% of short-term urinary catheterization cases (7 days) and virtually all long-term catheterization cases (28-30 days) lead to the development of CUTI. These CUTI are the most significantly notable nosocomial infections in hospitals and nursing homes [6].

After catheterisation, the bacteria capture in the urinary tract through three main routes: A) Bacteria which colonise the distal urethra can be picked up on the catheter's tip and pushed into the bladder through the insertion of the catheter. B) Bacteria of distal urethra can ascend the outside of the catheter through growth or motility. C) Bacteria may contaminate and colonise the catheter bag, which can lead to contamination of catheter lumen and due to the junction between catheter and catheter bag, bacteria can also grow in the urine residual in the bladder. Urine can fill the bladder until it reaches the eye-hole above the catheter balloon and then it drains which means that there is constant volume of urine in the bladder. This urine pool may provide a reservoir in which bacteria can grow [7].

In order to cause an infection, the bacteria must first adhere to the urinary tract or/and catheter surface. For adhesion on the epithelia that line the urinary tract, they use specific adhesions. Most likely this adhesion is the prerequisite to initiate and continue the infection [8].

Adhesion of bacteria on catheter surface can also take place on the host-derived protein and other molecules adsorbed on the catheter surface after catheterisation and the adhered bacteria form biofilm [9]. This biofilm provides protection for the bacteria against antibiotics, antibodies and defences of the human body [10].

Encrustation of urinary catheter is another common problem combined with CUTI [11, 12]. Among the bacteria related to CUTI, *proteus mirabilis* has a dominant role in the encrustation process [13], other urease producing bacteria like *pseudomonas aeruginusa*, *klebsiella pneumoniae*, *morganella morganii*, *proteus* species, some *providencia* species and some strains of *staphylococcus aureus* and coagulates-negative staphylococci are also responsible for crystalline biofilm [14, 15]. This crystalline biofilm generally consists of two main types of crystals, struvite (magnesium ammonium phosphate) and apatite (hydroxylated form of calcium phosphate) [16]. Urease producing bacteria can hydrolyze urea in the residual bladder urine resulting in two molecules of ammonia to every molecule of carbon dioxide which leads to rise in pH of the urine and this, in turn, causes the crystallization of magnesium and calcium phosphate [17]. These crystalline deposits can scratch the urethral mucosa when the catheter is withdrawn causing pain and haematuria in the patient [2]. It can also block the catheter which is a major problem in patients undergoing long-term indwelling bladder catheterisation since these bacteria have the ability to colonise all available types of indwelling catheter and generate alkaline urine [18].

Due to these complications related to urethral catheters, scientists, clinical investigators and manufactures are attempting for more than 50 years to optimize the development process of the catheters and to modify their surfaces to reduce the crystalline film formation and bacterial adhesion onto catheter surface [19, 20]. These attempts have focused on combining the catheter with antimicrobial agents. A simple method includes immersion of the catheter into an antimicrobial solution prior to catheterization. This method provides only a short-term

protection against infection since the antimicrobial agent is loosely adsorbed to/or absorbed in the catheter surface and the release is rapid [20-22]. It is common knowledge that the most effective choice is coating of catheter surface with antimicrobial agents or polymer film loaded with antimicrobial agents. Silver and it salts have been the most commonly applied antimicrobial agents for coating of catheter surface [23-29]. In the USA three antimicrobial catheters, coated with a silver alloy, were launched to the market [30]. The ionised form of silver is well-known as broad-spectrum antibacterial agents against both gram-positive and gram-negative strains. It can attack broad sites within the bacterial cell and therefore it is improbable that bacteria can develop resistance against it. On the other hand the large increase of antibiotic-resistant strains of bacteria leads to a great interest in using silver as an antibacterial agent [31, 32].

The antibacterial effectiveness of silver imbedded into coatings was found to be higher than the silver coating alone since surface silver can be rapidly de-activated by protein anions [33] and the impregnation of silver facilitates continuous release of silver ions [32], researchers investigated numerous numbers of methodologies to construct silver impregnated coatings. These trials involve the use of silver nanoparticles distributed in a hydrogel coating [34-36] and silver nanoparticles embedded in a polyelectrolyte multilayer [37, 38].

The aim of this work was the development of TEL-coated silver nanoparticles distributed in a film of poly(lactic-co-glycolic acid) (PLGA) loaded with norfloxacin. Fig. 1 shows schematic representation of the film.

Tetraether lipids are the main part of cell membrane of archaeon Thermoplasma acidiphilum, this kind of archaea grow in sulphuric acid milieu at pH 2 and 56 °C and since they have no cell wall, it is the lipid composition of their membrane that provides high chemical and thermal stability [39-44]. The hydrocarbon chains of these lipids have no double bonds and are bond and are bond to the glycerol residues via ether bonds instead of ester bonds. These

properties provides long-term resistance against both hydrolytic and oxidative agents and (bio)chemical degradation [39].

Norfloxacin (1-ethyl-6-fluoro-1,4-dihydro-4-oxo-7-(1-piperazinyl)-3-quinolinecarboxylic acid (NF) is broad-spectrum fluoroquinolone antibacterial agent which is frequently used for the treatment of urinary tract infections (UTI) caused by both gram-positive and gram-negative bacteria [45, 46]. This bactericidal agent builds a complex with enzyme DNA-gyrase enzyme which is required for synthesis of the bacterial DNA [50].

It is of high importance to select the optimum coating formulation by choosing the compatible and suitable polymers which have the potential to control the release rate over the whole catheterization period. Various studies focused on producing hydrogel coatings for urinary catheter [34-36]. Hydrogel coatings can significantly decrease the damage of the urethral mucosa and the trauma when the catheter is withdrawn [48-50], it also unlikely to cause discomfort to the patient due to its soft and lubricant nature. However, it is still not evident that they promote the anti-encrustation properties [51-53].

In this work, incorporating of the above mentioned anti-bacterial agents was achieved by employment of PLGA film. PLGA is an FDA-approved, biocompatible and biodegradable polymer [54-56]. It degrades in water via chemical hydrolysis of the ester bonds resulting in oligomers with carboxyl end groups or lactic and glycolic acids [57]. The yielded acids have the ability to decrease the pH in the surrounding microenvironment [58]. This effect can be exploited to neutralize the alkaline products produced from urea hydrolysis and upgrade the coating effectiveness against encrustation.

In this study, we developed a new methodology to design anti-bacterial and anti-encrustation coating for urinary catheter. Glass slides were chosen as a model for catheter surface. Since the films must be still attached to the surface during the release and bacterial adhesion experiments, further modification of the glass surface was needed to improve the glass-PLGA

interaction. The films were loaded with both norfloxacin and TEL-coated silver nanoparticles. The release rate of norfloxacin in phosphate buffered saline (PBS) was assessed. The anti-encrustation potent of the films was tested in synthetic human urine. Finally, quantitative assays of both dead and live adhered bacteria (five strains) in an *in vitro* urinary tract infection model were performed.

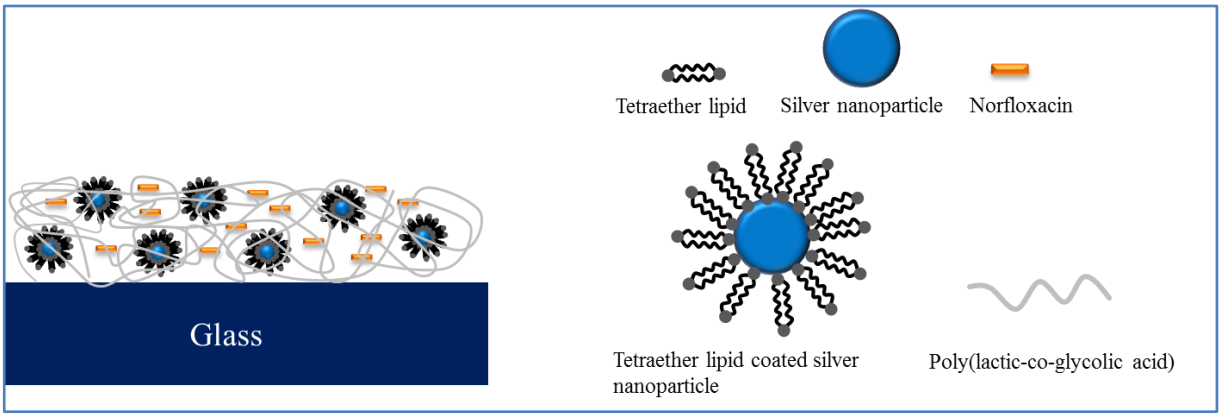

Fig. 1 Schematic representation of PLGA-NF-Ag construction

Materials and Methods

Materials

Poly($_{D,L}$-lactide-co-glycolide) (PLGA), Types Resomer® RG 503H was purchased from Boehringer Ingelheim, Ingelheim, Germany. (3-Aminopropyl)triethoxysilane (APTES), ≥ 98%, Norfloxacin, sodium dodecyl sulfate (95%) and urease (type II from jack beans) were obtained from Sigma-Aldrich (Sigma-Aldrich Chemie GmbH, Germany). Silver nitrate and glass slides (76 x 26 mm) were purchased from Carl Roth, Germany. *Escherichia coli* (*E.coli*) (DSMZ Nr. 498), *Staphylococcus aureus* (DSMZ Nr. 20231), *Staphylococcus epidermides* (DSMZ Nr. 3269), *Enterococcus faecalis* (DSMZ Nr. 2570) and *Pseudomonas aeruginosa* DSMZ Nr. 1117) were purchased from the DSMZ (Braunschweig, Germany). All other chemicals and solvents were of high analytical grade and commercially available.

Methods

TEL Extraction and Activation

Extraction and purifying of TEL were done according to the method described elsewhere [40,43]. For this purpose two-step chromatography with DEAE-cellulose and silica columns eluted with chloroform and methanol (2:1, v:v) was used. The lipids were then lyophilized at 10^{-2} torr and stored at -20 °C. TEL were activated by cyanuric chloride, equimolar amount of cyanuric chloride and TEL were allowed to react overnight at 40 °C in chloroform and N,N-diisopropylethylamine was employed as catalyzer. Activated lipids were purified with thin layer chromatography and then stored at 4 °C.

Preparation of Lipid coated Silver Nanoparticle

Silver nanoparticles were prepared as described elsewhere [59]. Briefly: 4 ml of sodium hydroxide solution (0.1 molar) were added to 0.8 ml of ethylenediaminetetracetic acid (EDTA) 0.1 molar. Distilled water was added to the mixture to get a final volume of 100 ml.

1.3 ml silver nitrate (0.1 molar) and 0.3 ml HCL (0.1 molar) were added to the mixture when the mixture started to boil. After 90 seconds of boiling the mixture was cooled down to room temperature and the silver nanoparticles were stored under light exclusion.

Coating of the silver nanoparticles with TEL was done according to the method described in our previous work [39], briefly: 15 ml of the previous silver nanoparticle dispersion was diluted up to 50 ml with distilled water. The dispersion was centrifuged (2000 rpm, 5 min) followed by re-dispersion in 15 ml distilled water and then transferred to a flask.

2 mg of activated TEL were dissolved in 1 ml of chloroform in a flask; the chloroform was allowed to evaporate and the TEL formed a thin film on the bottom of the flask. The 15 ml purified silver nanoparticle dispersion and 100 µl sodium dodecyl sulfate (SDS) (30%) were added to TEL in the flask. Ultrasonic treatment was applied on the mixture and TEL films were formed surrounding the silver nanoparticles. SDS was eliminated by dialysis the dispersion in water for 12 h, the coated nanoparticles were then stored at 4 °C under light exclusion.

Polymer Film Preparation

Aminolysis on Substrate Surface

Glass slides were washed with chloroform, acetone and distilled water and dried in flow nitrogen. Glass surface was modified by APTES to get an amino-terminated layer as described by Emoto at al [60]. Briefly, 1 ml APTES were dissolved in 100 ml toluene under stirring, the glass slides were incubated in this solution for 4 h and then washed with toluene

to remove the loosely physisorbed APTES from the surface. The modified glass slides were heated at 160 ℃ for 20 h in vacuum and then stored at 4 ℃.

Coating of aminated Surface with PLGA

First, unloaded polymer films were prepared. 1,000 mg of PLGA was dissolved in 100 ml acetone under stirring overnight, APTS-coated glass slides were dipped in the solution for 40 min and air dried at room temperature.

For films containing TEL-coated silver nanoparticles (PLGA/TEL-Ag), the 10 mg/ml PLGA/acetone solution was used and 1 ml (~1m molar) of the suspension of TEL-coated silver nanoparticles was added and the same dipping and drying steps were followed as previous. The same procedure was run for PLGA/NF/TEL-Ag film preparation and the same concentrations of PLGA and TEL-Ag were used and the only modification is the addition of 100 or 200 mg of norfloxacin to the dipping solution. The coated slides were stored at -20 °C under light exclusion.

Film Characterization

Water contact angle measurement

Surface wettability was evaluated by water contact angle measurement using the sessile drop method and Laplace-approach (OCA20, DataPhysics Instruments GmbH, Filderstadt/ Germany). Contact angle of distilled water was determined by dropping 3µl of water onto the surface followed by measuring the angle within the first 10 s after dropping. The contact angle was the mean of fifteen readings from three different parts of the surface (± the standard division). All measurements were performed at ambient conditions.

Atomic force microscopy

Atomic force microscopy was performed on a NanoWizard (JPK instruments, Berlin, Germany) as described elsewhere [40]. Commercial pyramidal silicon tips (NSC16AlBS, Micromasch, Estonia) mounted to cantilevers (length 230 µm, resonance frequency 170 kHz and nominal force constant ~40 N/m) were used. AFM was used to measure surface topography of the films and all measurements were performed in intermittent contact mode to avoid damaging of the surfaces. The scan speed was proportional to the scan size where the scan frequency was between 0.5 and 1 Hz. Images were captured by displaying the height, phase and amplitude signals in the trace direction (512 x 512 pixel).

Film Stability

The stability of the films upon exposing to PBS was investigated. All prepared Polymer films were incubated in PBS with 0.01% sodium azide under gentle shaking at 37 °C for 60 days. Surface morphology of the films was imaged by AFM before and after PBS incubation and the effects of PBS incubation were noticed.

Norfloxacin Release

For measuring the release of norfloxacin, the norfloxacin loaded PLGA films were incubated in PBS (pH 7.4) with 0.01% sodium azide under gentle shaking (20 rpm) (Rothaterm®, Gebr. Liebisch, Bielefeld, Germany) at 37 °C.

At predetermined time points, 3ml samples were taken and replaced with 3 ml fresh PBS. The samples were then stored at 4°C under light exclusion. To determine the Norfloxacin concentration in the probes, fluorescence intensity was measured using a fluorescent plate reader (Saphire II; Tecan, Austria) at wavelength 330 nm excitation/440 nm emission. Cumulative release amount and percentage were calculated at each time point.

Artificial Urine

The synthesized urine was based on a proposal by Griffith et al. [60]; two aqueous solutions A and B were prepared and added to the bioreactor device to avoid the precipitation of brushite ($CaHPO_4.2H_2O$) [61]. Solution A was composed of $CaCl_2.H_2O$, $MgCl_2.6H_2O$, NaCl, Na_2SO_4, Na_2Oxalate, Na_3Citrate·$2H_2O$, KCl and urease. Solution B was composed of K_2PO_4, $Na_2C_2O_4$,NH_4Cl and urea. Creatinine was also added to the urine. A volume of 1.5 l of artificial urine solution were sterilized by filtration and then used for the *in vitro* encrustation model.

In vitro Encrustation Model

For encrustation assays, bioreactor devices (reaction vessels) coupled with temperature and pH measurement system were employed as described by Jones *et al.* [61]. A laboratory bioreactor (Rettberg, Germany) was filled with 1.5 l artificial urine and sterilized prior to the experiments. The temperature was adjusted to 37 °C and the samples were placed vertically and fixed inside the vessels. During the experiments, the urine inside the vessels was gently stirred (150 rpm). This model allows a simultaneous testing of up to sixteen samples. Both uncoated and PLGA coated glass substrate were analyzed. It is known, that the urinary tract infection is induced above all by urease-producing bacteria. Consequently, in the *in vitro* – crystallization model the pH increase was triggered by addition of urease to the artificial urine. During a following period of 14 days the pH was enhanced slowly from 5.7 to 8.8, this allowed salt formation over an incubation time of up to 14 days. After the incubation, the samples were imaged by Scanning Electron Microscopy (SEM). The samples were treated with 1N HCl to dissolve the crystalline deposits. The encrustation of Ca, Mg, Phosphate and Oxalate on the sample surfaces was investigated by quantitative and qualitative analysis. The

amount of Na^+, K^+ and Ca^{+2} was quantified by means of atomic adsorption spectroscopy while photochemical detection was employed to analyze Phosphate, Oxalate and Ureate. All experiments were done in triplicate.

Bacterial Adhesion

*E.coli*was used for the initial adhesion experiments. The bacteria were grown in Trypic Soy Broth (TSB) over night at 37 °C under gentle stirring. The suspension was centrifuged and the bacteria were collected and washed with PBS followed by the next centrifugation step. The bacteria were then resuspended in artificial urine and their concentration was adjusted to 10^8 cells/ml. A 24-well multiwell culture plate was filled with bacterial suspension and the samples were incubated in the suspension for 24 h at 37 °C. The samples were then removed and extensively washed with PBS and treated in ultrasonic path to remove the non-adherent bacteria. Cell viability assay was applied to quantify both dead and live bacterial by the use of LIVE/DEAD *Bac*Light kits. Imaged were captured by confocal laser scanning microscopy (CLSM). Evaluation of adhered bacteria was confirmed by SEM.

Investigations of bacterial adhesion were done on unmodified glass and PLGA coated glass. Four different kind of PLGA coating were also tested: unloaded PLGA coating, 10% NF loaded PLGA coating, 20% NF loaded PLGA coating and PLGA films loaded with NF (20%) and TEL-Ag (1mmolar/1g).

Additionally, *in vitro*–bioadhesion experiments based on a new microbiological model of urinary tract infection were performed. In this model the antibacterial and antiadhesive effectiveness of unmodified Glass vs. PLGA films loaded with NF (20%) and TEL-Ag (1mmolar/1g) was tested. This infection model comprised five bacteria strains: *Staphylococcus aureus, Staphylococcus epidermides, Escherichia coli, Enterococcus faecalis*

and *Pseudomonas aeruginosa* cultivated in artificial urine. The experimental procedure of this adhesion experiment corresponds to the method for the *E.coli* monoculture described above.

Results and Discussion

TEL coated Silver Nanoparticles

In our previous work [38] we described the method to prepare TEL coated silver nanoparticles. Chemical reduction method was used to synthesize of silver nanoparticles; the particles had a size of 19.2±2.5 nm. After particle preparation, a thin layer of silver oxide is formed on the particle surface and the surface becomes –OH rich in aqueous solution.

The TEL were activated with cyanuric chloride and the covalent coupling process were confirmed by FTIR spectroscopy where new peaks at 1509 cm^{-1} and 1541 cm^{-1} were visible which corresponds to the C=N valence oscillation of cyanuric chloride.

Thin film of the activated TEL was formed on the bottom of the flask after evaporation of the solvent. After adding the silver nanoparticles and the aqueous solution of SDS to the film, the mixture was ultrasound treated. The energy gained from ultrasound treatment leads to the formation of TEL incorporated SDS micelles.

The activated TEL are covalently bonded to hydroxyl groups on the surface of silver nanoparticles and a TEL film is formed on the surface.

Polymer Film Preparation and Characterization

PLGA was used as coating matrix for controlled release of both norfloxacin and silver ions and for improved anti-encrustation properties. Dipping method was chosen for the coating process. This method enables the fabrication of films with thicknesses ranging from a couple of nanometres up to millimetres. The ease and simplicity of the employed method makes it applicable for coating of several catheter materials. After immersion of the samples in the polymer solution, a polymer film is formed on the surface. The film thickness depends on various parameters like polymer concentration and incubation time. After film drying, a thin

layer of the polymer is created. The formed film is only adsorbed to the sample surface and different kinds of polymer-surface interactions are responsible for this adhesion. These interactions depend on chemical and physical properties of the sample surface and on the polymer nature.

It is evident that PLGA with free carboxylic acid possesses a good affinity to surfaces with –OH groups (like glass) due to hydrogen bonds that are formed between the hydroxyl groups and the –COOH groups of PLGA [62]. Nevertheless when it comes in contact with body fluids these bonds are weak and they fail to keep the polymer attached to the surface over the whole catheterization time.

PLGA chains contain carboxyl groups and therefore modification of glass with amino-terminated layer can upgrade the stability of the PLGA film in aqueous milieu. Modifying of surfaces is widely used to enhance the polymer-surface interactions and amino-terminated layer was constructed on the surface when polymers with negatively charged groups were used to coat these surfaces [37, 59, 63].

In this work, APTES was used to produce amino-terminated layer on the glass surface. The electrostatic interactions between the negatively-charged carboxyl groups on the polymer and the positively-charged amine groups on glass surface are essential for film stability.

Fig 2shows AFM images of cleaned and APTES-coated glass. Unmodified glass shows an unstructured surface, its roughness average (Ra) was 0.19±0.11 nm and the root mean square value (RMS) of its roughness was 0.24±0.11 nm. After APTES coating, both Ra and RMS increased to reach the values of 1.05±0.24 nmand 1.28±0.26 nm respectively.

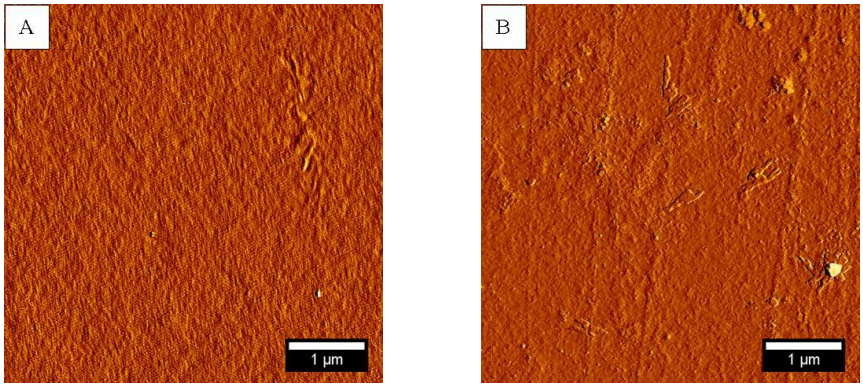

Fig. 2AFM imaging of unmodified glass surface (A) and APTES modified surface (B).

By immersion of the APTES-coated glass in PLGA/acetone solution, a homogenous and smooth film of PLGA was formed (Fig 3). When the aqueous suspension of TEL-coated silver nanoparticles was added to the PLGA/acetone solution, the yielded films were less homogenous (Fig 4). It is unlikely that the silver nanoparticles affected significantly the homogeneity of the polymer films as a very low amount of the particles was added. Our explanation is based on the fact that PLGA is water-insoluble polymer. When the aqueous suspension of silver nanoparticles was added to thePLGA/acetone solution, the water was dissolved in the acetone and a mixture of the two components was formed. The solubility of PLGA was not affected as the ratio water/acetone was too low (about 1% (v/v)). Using this mixture, films were prepared and then air dried at room temperature. During the drying process, acetone evaporates more rapidly than water as it has a much lower boiling point (56 °C). This leads to an increasing water/acetone ratio and the polymer solubility decreases. Then a continuing evaporation of acetone could lead to phase separation.

Silver nanoparticles were distributed inside the film and only some particles could be seen on the top of the film surface. Fig 4 presents low density of the particles on the surface. The upper-right side of the image (A) shows a phase image of the surface where silver nanoparticles appear like black spots spreaded on the film surface without having aggregated.

Adding norfloxacin to the mixture didn't considerably change the film topography (Fig 5).

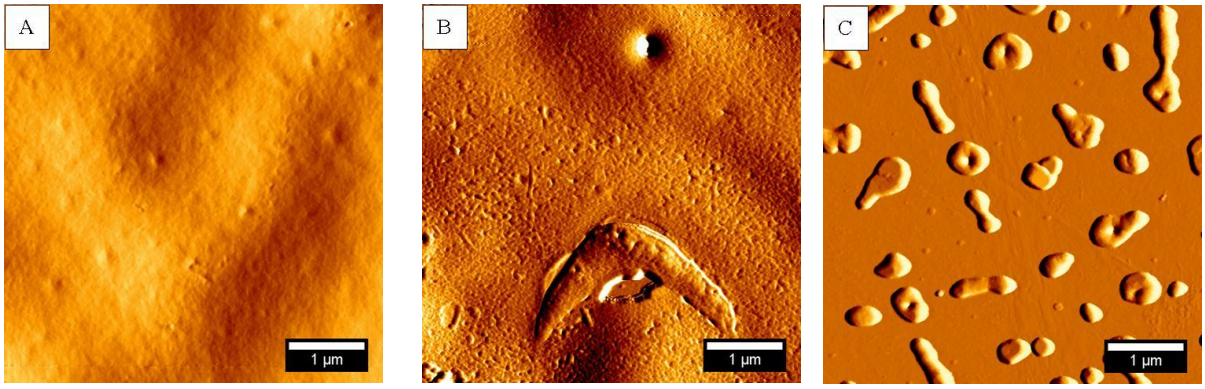

Fig. 3AFM images of PLGA coating, (A) film prepared on ATPES modified glass (B) film prepared on ATPES modified glass after 53 days of incubation in PBS and (C) film prepared on unmodified glass after 53 days of incubation in PBS.

Surface wettability of the film was investigated. Fig6 shows that surface wettability was determined by the type of the anti-bacterial loaded in the film which suggested that the films were successfully loaded with these agents. As expected the glass surface had the lowest contact angle (14.3±1.3°) due to its high hydrophilicity. After deposition of PLGA film, the surface became more hydrophobic because of the hydrophobic nature of the polymer and the contact angel was 80.4±0.7°. In Fig 6, it can be seen that PLGA/TEL-Ag surface shows the highest value of water contact angle (106.1±2.1°). In our previous work, we suggested that coating of cellulose membrane with TEL-Ag enhances the surface hydrophobicity and the contact angle raises significantly (27° to 93°) [38]. The presence of particles on the polymer surface provides a good explanation of the increasing contact angel. In addition to surface chemistry, surface topography must also be considered. Li *et al* [64] introduced micropatterns on Thermanox surfaces by laser-pattering. Both patterned and not patterned Thermanox were coated with collagen. Contact angle of the patterned surface differed from that of not patterned surface. Despite of the fact that both surfaces were collagen-coated and had the same chemical nature, their microstructure resulted in a change of surface wettability.

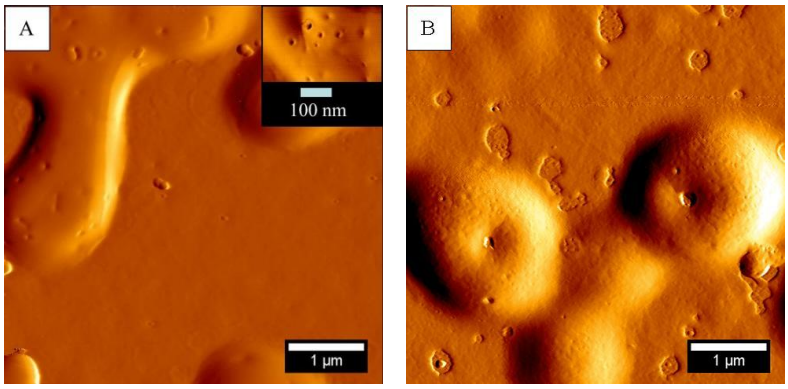

Fig. 4AFM images of PLGA/TEL-Ag on APTES modified glass, (A) after the preparation and (B) after 53 days of incubation in PBS.

Adding of norfloxacin to the PLGA reduced the contact angle value (62.9±2.0°). Norfloxacin has very low water solubility and one can expect that its adding can increase the contact angel. The possible explanation is based on the chemical properties of norfloxacin. Norfloxacin hydrates have higher water solubility than the anhydrates [65] and norfloxacin molecules on the film surface can be hydrated with water molecules from ambient air. Thus hydration effect can be detected through enhancement of surface wettability.

Film stability and Norfloxacin release

To demonstrate the utility of the coating for urinary catheter, the films were incubated in PBS at 37 °C and the surface morphology was examined before and after the incubation. The effectiveness of catheter coating depends highly on the film stability in body fluids during the indwelling time and a complete or partial detachment of the film from the surface is one of the most common reasons of coating failure.

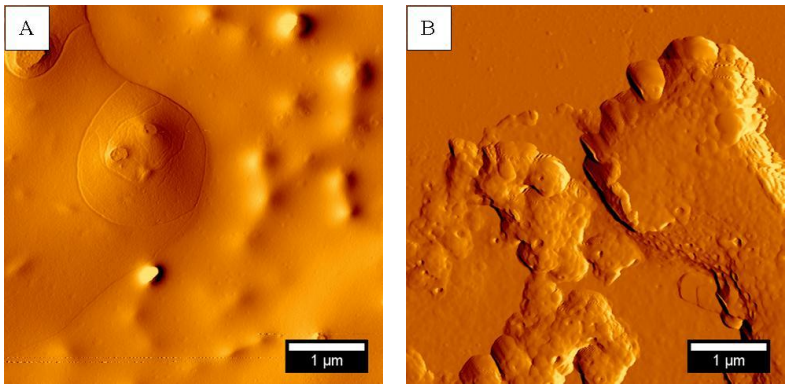

Fig. 5 AFM imaging of PLGA/TEL-Ag/NF film on APTES modified glass surface, (A) after the preparation and (B) after 53 days of incubation in PBS.

In our study, APTES was tested and found to be essential for coating stability. PLGA film, attached on unmodified glass surface, was partially detached from the surface after 4 days exposure to buffer solution and the surface coverage with the film reduced to only 30% (Fig 3). The hydrogen bonds between carboxyl groups on PLGA and hydroxyl groups on glass surface are not strong enough to keep the film attached to the surface as described previously. APTES modification of glass leads to better attachment of PLGA. This modification produces amine groups providing a positive charge of glass surface in moderate medium. When PLGA film is formed on this surface, carboxyl-group/amine-group electrostatic interaction insures a better attachment of the film to the surface. Fig 3, 4 and 5represent AFM imaging of the films prepared on modified glass revealing morphology changes before and after incubation in buffer. Despite the long incubation period (˜ 2months) and the shear forces induced by shaking, the films remained attached to the surface.

AFM images show little effect of polymer degradation on the film after incubation of the samples in buffer solution, the surfaces became rougher and a limited “bulk erosion” was detectable.

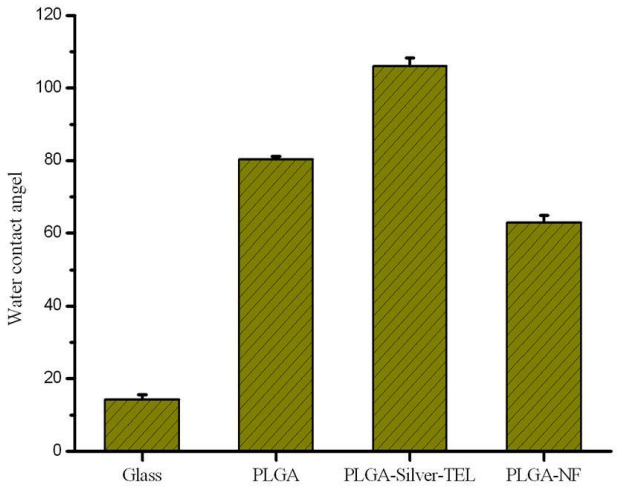

Fig. 6 Water contact angel of Glass, unloaded PLGA film, PLGA/TEL-Ag film and PLGA/NF film.

In order to investigate the feasibility of employment of PLGA as polymer film matrix for norfloxacin controlled release, *in vitro* release study was performed in PBS (pH 7.4) at 37 °C. Fig 7 shows cumulative release profiles of norfloxacin from the film. A fast release rate of about 60% was observed in the first few days (burst-release) followed by slow release in the next 50 days (Fig. 7B). Fig. 7A shows that the burst release amount in the first day was 103.59 ng/cm² followed by slow release of 70.39 ng/cm² in the next 52 days. The film must release a daily amount of norfloxacin in the aqueous environment surrounding the catheter that is equal to or exceed the overkill dose (400µg/l). The dipping method used for the surface coating enables the film to get controlled thickness as well as desired antibiotic loading level to reach the overkill dose. In this work the loading and film thickness provided potential protection against bacterial adhesion.

Norfloxacin is a fluoroquinolone with hydrophobic nature which was used as anti-bacterial agent for long-term catheterization [66]. The fast release in the first few days might have been

due to the drug diffusion from the film, the release rate decreased in the next days up to the day 10 because of the hydrophobic interaction between the drug and the polymer chain. Increasing of release rate was noticed after the 10 day, this might be due to the drop of pH value within the film. Degradation of PLGA ester bond results in oligomers with carboxyl end groups or lactic and glycolic acids, this phenomenon is called autocatalysis and it seems to be responsible for the faster internal degradation of the film when the acids within the film cannot be set free [67]. Norfloxacin is more soluble in acidic milieu than in mediated one [68]. The low pH value within the film enhanced the drug solubility in water and decreased the drug/polymer hydrophobic interaction which resulted in faster release from the film.

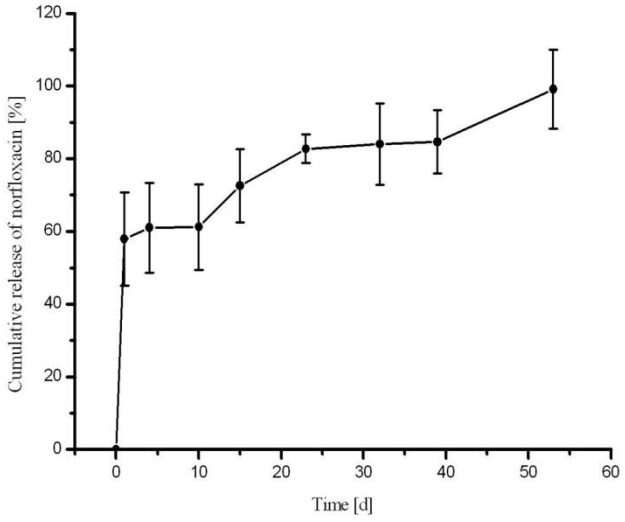

Fig. 7. Cumulative percentage release of norfloxacin from PLGA film in PBS at 37 °C.

Bacterial Adhesion and Encrustation

The adhesion of *E.coli* on unmodified and coated glass was investigated in artificial urine during 24 h at 37° C. *E.coli* showed more potential to adhere to the uncoated glass than hydrophobic surface of PLGA (Fig 8). The hydrophlilc nature of E.coli [69,70] and the physiochemical properties of the surface influence the adhesion process. Bacterial adhesion to

biomaterials is a complex process and depends on chemical compositions of the material used, hydrophobicity and surface roughness and other factors [63, 69-73].

Four different types of PLGA coating were also tested: unloaded PLGA, 10% norfloxacin loaded PLGA, 20% norfloxacin loaded PLGA and PLGA loaded with norfloxacin (10%) and TEL-Ag (1 m molar/1 g Ag/PLGA). Copper discs were used as standard test to be able to reference the anti-bacterial properties of the different coatings. The anti-bacterial effectiveness of copper is exploited centuries ago and its broad-spectrum anti-microbial capacity was intensively investigated in the last decades.

Loading of PLGA with norfloxacin enhanced the anti-adhesive and anti-bacterial properties of the films. The number of adhered bacteria was significantly decreased after the loading (Fig. 9). It can also be seen that most of the bacteria adhered to unloaded PLGA were still alive while significantly higher ratio of dead/live bacteria (~50%) was observed on norfloxacin loaded PLGA coating. Rising of norfloxacin concentration from 10% to 20% resulted in drop of bacterial adhesion. Adding of TEL coated silver nanoparticles to the coating enhanced the anti-adhesive property while the ratio of dead/live bacteria was still constant. A comparison between the four coatings led to the conclusion, that the copper wafer showed a high anti-bacterial activity where most of the bacteria attached to copper surface were dead and a negligible number of live bacteria was detectable. Nevertheless, our polymer coating loaded with silver and norfloxacin showed a higher potential to prevent bacteria adhesion than copper wafer.

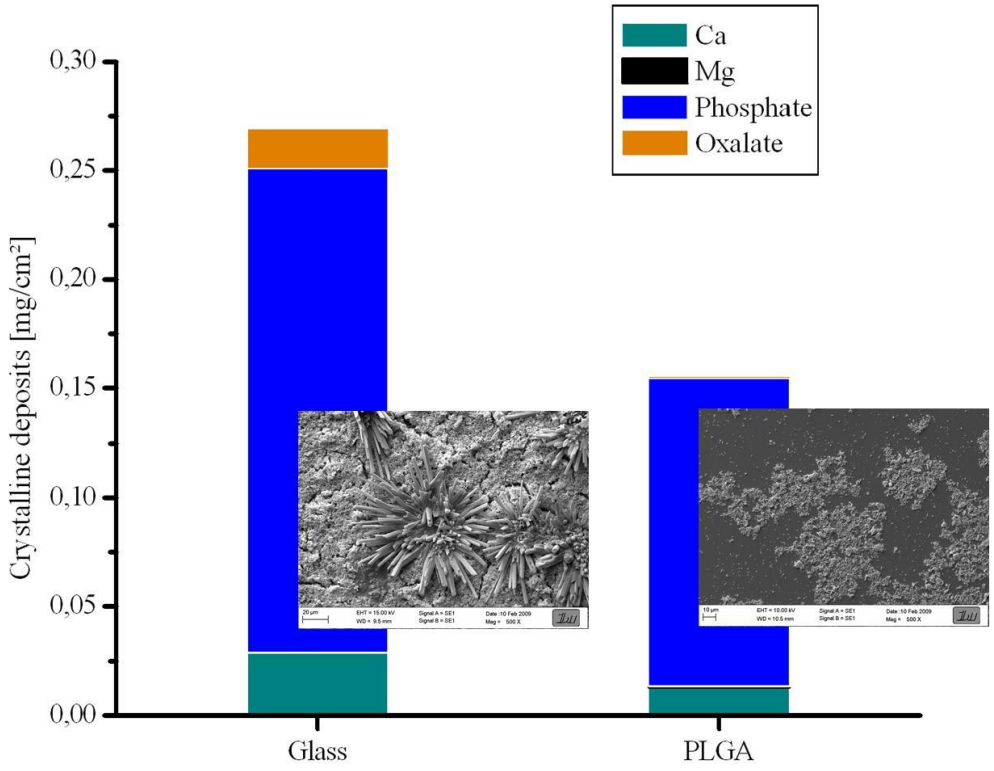

Fig. 8 Masse and of Ca, Mg, Phosphate and Oxalate in the crystalline deposits formed on unmodified glass and PLGA film after 14 days of incubation in artificial urine. The figure shows also Scanning Electron microscopy images of the crystalline deposits.

Fig 10 represents the results of *in vitro*-bioadhesion experiments in urinary tract infection model using five strains of bacteria. A successful validation of further statements for simple infection culture was reached. In contrast to the uncoated glass surface, a strongly reduced number of adhered cells (decrease of 45%) was shown on the PLGA/NF/TEL-Ag film. Scanning microscopic images confirmed the successful anti-adhesive effect.

PLGA was widely used as polymer matrix coating for controlled release of drugs and biomolecules. The function of PLGA in our system was not limited to control the release but it also neutralized the alkali products on the coating surface.

Fig 8 shows a considerable reduce of encrustation on PLGA coated glass compared to uncoated glass after 2 weeks of sample incubation in synthesized urine. The total mass of crystalline deposition was reduced by approximately 40%.

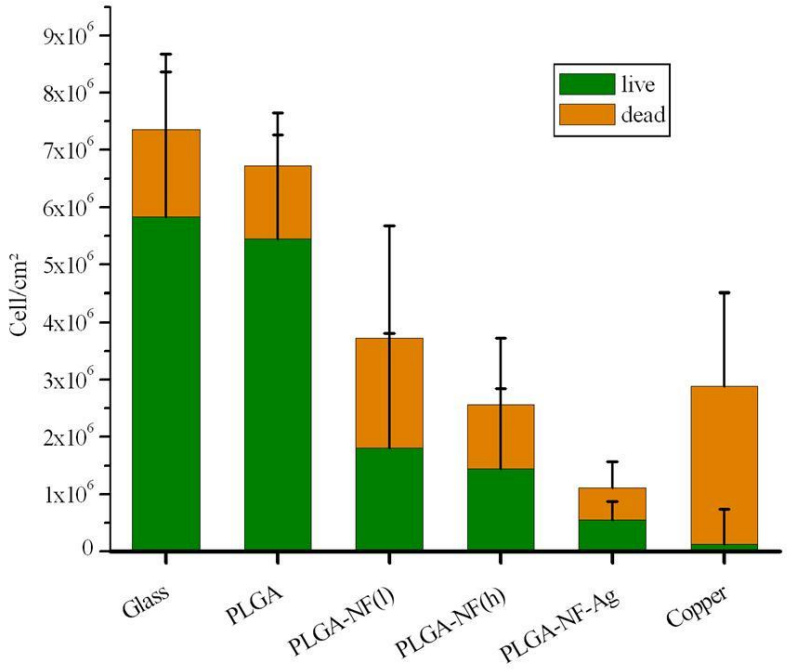

Fig. 9 Adhesion of both live and dead *E.coli* on unmodified glass, PLGA film, PLGA film loaded with 10% norfloxacin (PLGA-NF(l)), PLGA film loaded with 20% norfloxacin (PLGA-NF(h)), PLGA film loaded with both 20% norfloxacin and TEL-Ag and copper. All samples were incubated in *E.coli* suspension for 24 h at 37 ℃.

The urease catalyzed the urea hydrolysis producing ammonia which increased the pH value of urine. The pH value of urine was 8.8 and when uncoated glass was incubated in the urine, the alkalic milieu leaded to the precipitation of crystalline deposits onto the glass. When glass samples were coated with PLGA, the free carboxylic acid groups on the surface of polymer coating reduced amount of crystalline deposited on the surface. PLGA undergoes degradationby hydrolysis of its ester bond in water resulting in acidic monomers and

oligomers. It is evident that increasing the pH of the environment promotes the polymer degradation

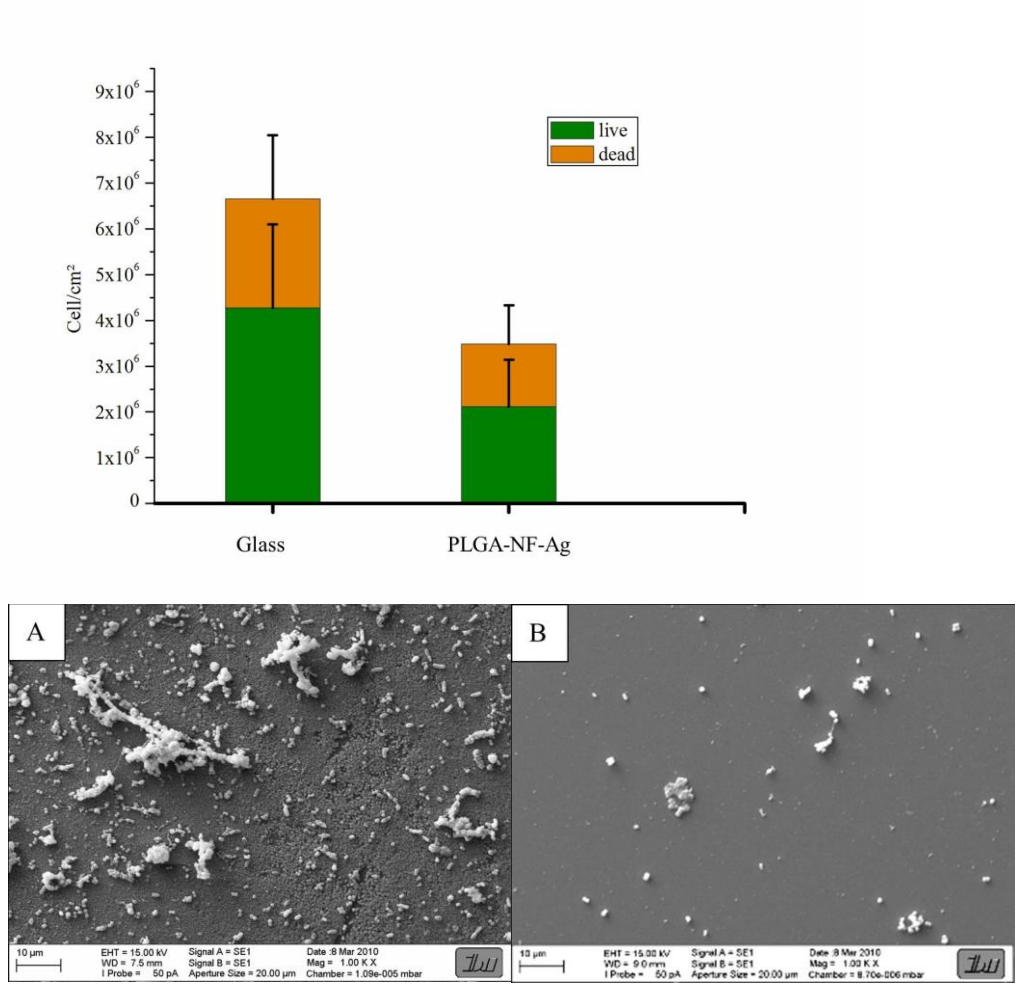

Fig. 10 Adhesion of both live and dead bacteria (five bacteria strains) on unmodified glass and PLGA film loaded with both 20% norfloxacin and TEL-Ag after 24h in synthesized urine and Scanning electron microscopy images of the two films showing the adhered bacteria.

producing more acids [74]. On the other hand, hydrolysis of urea, which is catalyzed by urease, produces ammonia and carbon dioxide. Ammonia is a base which dissolves in water producing hydroxide ions [75]. These hydroxide ions can neutralize the acidic products of PLGA degradation. When the number of the available hydroxide ions is higher than that of H+, the urine becomes more alkali and this promotes the polymer degradation producing

more acids and neutralizing more hydroxide ions. This process protects the coating surface from the increasing deposition of crystals during the contact with human urine.

Conclusion

In this work, we have introduced a newly developed PLGA film with anti-bacterial and anti-encrustation functionalities to be used as coating for urinary catheters. Two anti-bacterial agents, norfloxacin and tetraether lipid coated silver nanoparticles were successfully incorporated in the film.

Film was deposited on aminated glass by means of dipping-method. The modification of glass surface with amino-terminated layer supported the film stability in aqueous environment. From the atomic force microscopy images, it was demonstrated that surface homogeneity of the films was depended on the antibacterial agent loaded in the film; the silver nanoparticles were uniformly distributed within the film when they were coated with TEL.

The films released the loaded norfloxacin in about two months through diffusion of the drug in aqueous milieu. The films effectively inhibited the *in vitro* adhesion of bacteria compared to glass and copper surface and unloaded polymer films. It is of value to point out, that the films did not only reduce the number of adhered bacteria but also decreased the bacterial viability on the surface.

The results obtained from encrustation experiments in artificial urine demonstrated that the polymer coating could efficiently reduce the crystalline formation on the surface as the alkali products of urea hydrolysis were neutralized by acidic products of polymer degradation. This phenomenon resulted in resistance of the coating against encrustation compared to uncoated glass. The *in vitro* bacteria and encrustation tests suggest promising use of these coating to promote the biocompatibility and biofunctionality of urethral catheters.

Acknowledgement

The authors would like to thank Novoplast Schlauchtechnik GmbH (Halberstadt, Germany), Primed Halberstadt Medizintechnik GmbH (Halberstadt, Germany), MAT PlasMATec GmbH (Dresden Germany), TRUMPF Medizin Systeme GmbH Deutschland, (Saalfeld Germany), JPK Instruments Berlin (Germany) and BMWI/AiF (AZ IGF-05/05-AiF-Nr. 15090 BG/2) for the support. Christian Hobler (research group M. Keusgen) is gratefully acknowledged for performing the spectrophotometry measurements and Maria Solovey for the helpful discussion.

References

[1]Ramakrishnan K, Mold J.W. Urinary Catheters: A Review. The Internet Journal of family Practice 2005;3.

[2] Park HJ, Cho YW, Kwon IC, Jeong SY, Bae YH. Assessment of PEO/PTMO multiblockcopolymer/segmented polyurethane blends as coating materials for urinary catheters: in vitro bacterial adhesion and encrustation behaviour. Biomaterials 2002;23:3991–4000.

[3] Jarvis WR. Selected aspects of the socioeconomic impact of nosocomial infection: morbidity, mortality, cost, and prevention. Infect Control Hosp Epidemiol 1996;17:552-7.

[4] Cho YW, Park JH, Kim SH, Cho Y-H, Choi JM, Shin HJ et al. Gentamicin-releasing urethral catheter for short-term catheterization. J Biomater Sci Polym Ed 2003;14:963–72.

[5] Kunin CM. Urinary Tract Infections: Detection, Prevention and management. 4th ed. Philadelphia: Lea & Febiger, 1987. P. 248-51.

[6] Barford JMT, Coates ARM.The pathogenesis of catheter-associated urinary tract infection.Journal of Infection Prevention2009;10:50-6.

[7] Daifuku R , Stamm WE. Bacterial adherence to bladder uroepithelial cells in catheter-associated urinary tract infection. New England Journal of Medicine 1986;314:1208–13.

[8] Thomas WE , Nilsson LM , Forero M , Sokurenko EV , Vogel V. Shear-dependent ‘stick-and-roll’ adhesion of type 1 fimbriated *Escherichia coli* . Molecular Microbiology2004;53:1545–57 .

[9] Kulik E, Ikada Y. In vitro platelet adhesion to non-ionic and ionic hydrogels with different water contents. J Biomed Mater Res 1996;30:295-304.

[10] Talja M, Korpela A, J.arvi K. Comparison of urethral reaction to full silicone, hydrogel-coated and siliconised latex catheters. Br J Urol 1990;66:652–7.

[11] Denstedt JD, Wollin TA, Reid G. Biomaterials used in urology: current issues of biocompatibility, infection, and encrustation. J Endourol 1998;12:493–500.

[12]Liedl B. Catheter-associated urinary tract infections. Curr Opin Urol 2001;11:75-9.

[13] Mobley HLT, Warren JW. Urease-positive bacteriuria and obstruction of long-term catheters. J Clin Microbiol 1987;25:2216–17.

[14] Kunin CM. Blockage of urinary catheters: role of microorganisms and the constituents of the urine on formation of encrustations. J Clin Epidemiol 1989;42:835–42.

[15] Cox AJ, Hukins DWL. Morphology of mineral deposits on encrusted urinary catheters investigated by scanning electron microscopy. J Urol 1989;142:1347–50.

[16] Morris NS, Stickler DJ, McLean RJC. The development of bacterial biofilms on indwelling catheters. World J Urol 1999;17:345–50.

[17] Stickler DJ, Feneley RCL. The encrustation and blockage of long-term indwelling bladder catheters: a way forward in prevention and control. Spinal Cord 2010;48:784–90.

[18] Kunin CM. Nosocomial urinary tract infections and the indwelling catheter: what is new and what is true?. Chest 2001;120:10-2.

[19] Wu P, Grainger DW. Drug/device combinations for local drug therapies and infection prophylaxis. Biomaterials 2006;27:2450–67.

[20] Cormio L, La Forgia P, Siitonen A, Ruutu M, Tormala P, Talja M. Immersion in antibiotic solution prevents bacterial adhesion onto biodegradable prostatic stents. Br J Urol 1997;79:409–13.

[21] Cormio L, La Forgia P, La Forgia D, Siitonen A, Ruutu M. Bacterial adhesion to urethral catheters: role of coating materials and immersion in antibiotic solution. Eur Urol 2001;40:354–9.

[22] Cormio L, La Forgia P, La Forgia D, Sittonen A, Ruutu M. is it possible to prevent bacterial adhesion onto ureteric stents?. Urol Res 1997;25:213-6.

[23]Cormio L, La Forgia P, La Forgia D, Sittonen A, Ruutu M. Bacterial Adhesion to Urethral Catheters: Role of Coating Materials and Immersion in Antibiotic Solution. Eur Urol 2001;40:354–9.

[24] Ahearn DG, Grace DT, Jennings MJ, Borazjani RN, Boles KJ, Rose LJ et al. Effects of Hydrogel/Silver Coatings on In Vitro Adhesion to Catheters of Bacteria Associated with Urinary Tract Infection. Curr Microbiol 2000;41:120-5.

[25] Liedberg H, Lundeberg T. Silver coating of urinary catheters prevents adherence and growth of Pseudomonas aeruginosa. Urol Res 1989;17:357-8.

[26] Roe D, Karandikar B, Bonn-Savage N, Gibbins B, Roullet JB. Antimicrobial surface functionalization of plastic catheters by silver nanoparticles.Journal of Antimicrobial Chemotherapy 2008;61:869–76.

[27] Stobie N, Duffy B, McCormackDE , Colreavy J, Hidalgo M, McHaleP et al. Prevention of *Staphylococcus epidermidis*biofilm formation using a low-temperature processed silver-doped phenyltriethoxysilanesol–gel coating. Biomaterials 2008;29:963-9.

[28] Melaiye A, Youngs WJ. Silver and its application as an antimicrobial agent.Expert Opin.Ther. Patents 2005;15:125–30.

[29] Johnson JR, Kuskowski MA, Wilt TJ. Systematic Review: Antimicrobial Urinary Catheters To Prevent Catheter-Associated Urinary Tract Infection in Hospitalized Patients Annals of Internal Medicine, Ann Intern Med 2006;144:116-26.

[30] Melaiye A, Youngs WJ. Silver and its application as an antimicrobial agent.Expert Opin.Ther. Patents 2005;15:125–30.

[31]Rai M , Yadav A, Gade A. Silver nanoparticles as a new generation of antimicrobials. Biotechnology Advances 2009;27:76–83.

[32] Furno F, Morley KS, Wong B, Sharp BL, Arnold PL, Howdle SM et al. Silver nanoparticles and polymeric medical devices: a new approach to prevention of infection?. J Antimicrob Chemother 2004;54:1019–24.

[33] Mohan YM, Lee K, Premkumar T, Geckeler KE.Hydrogel networks as nanoreactors: A novel approach to silver nanoparticles for antibacterial applications. Polymer 2007;48:158-64.

[34] Vimala K, Sivudu KS, Mohan YM, Sreedhar B, K. Raju KM. Controlled silver nanoparticles synthesis in semi-hydrogel networks of poly(acrylamide) and carbohydrates: A rational methodology for antibacterial application. Carbohydrate Polymers 2009;75:463–71.

[35] Thomas V, Yallapu MM, Sreedhar B, Bajpai SK.A versatile strategy to fabricate hydrogel–silver nanocomposites and investigation of their antimicrobial activity.Journal of Colloid and Interface Science 2007;315:389–95.

[36]Yu DG, Lin WC, Yang MC. Surface Modification of Poly(l-lactic acid) Membrane via Layer-by-Layer Assembly of Silver Nanoparticle-Embedded Polyelectrolyte Multilayer. Bioconjugate Chem 2007;18:1521–9.

[37] FuJ, JiJ, FanD, ShenJ. Construction of antibacterial multilayer films containing nanosilver via layer-by-layer assembly of heparin and chitosan-silverions complex. J Biomed Mater Res A 2006;79:665-74.

[38] Dayyoub E, Sitterberg J, Rothe U, Bakowsky U. New antibacterial, antiadhesive films based on self assemblies ofmodified Tetraetherlipids. Advances in Science and Technology 2008;57:188-94.

[39] E. Antonopoulos, U. Bakowsky, H. J. Freisleben, U. Rothe. Tetraether lipids and liposomes containing said lipids, and use of the same. European Patent No.EP19970905135, 2002.

[40] Ozcetin A, Mutlu S, Bakowsky U. Methods Mol. Biol 2010;605:87–96.

[41] Frant M, Stenstad P, Johnsen H, Dölling K, Rothe U, Schmid R et al. Anti-infective surfaces based on tetraether lipids for peritoneal dialysis catheter systems. Mat.-wiss. u. Werkstofftech 2006;37:538-45.

[42] VidawatiS, SitterbergJ, BakowskyB, RotheU. AFM and ellipsometric studies on LB films of natural asymmetric and symmetric bolaamphiphilic archaebacterial tetraether lipids on silicon wafers. Colloids and Surfaces B: Biointerfaces 2010;78:303–9.

[43]OzcetinA, Dayyoub E, HoblerC, KeusgenM, Bakowsky U. Selective interactions of concanavalin A-modified tetraether lipid liposomes. Phys. Status Solidi 2011;8:1985–9.

[44] Appelbaum PC, Hunter PA. The fluoroquinolone antibacterials: past, present and future perspectives. Int. J. Antimicrob. Agents2000;16:5-15.

[45] Hooton TM.2003. The current management strategies for community-acquired urinary tract infection. Infect. Dis. Clin. N. Am 2003;17:303–32.

[46] Oliphant CM, Green GM. Quinolones: A Comprehensive Review. Am. Fam. Physician2002;65:455-65.

[47] Nickel JC, Olson ME, Costerton JW. In vivo coefficient of kinetic friction: study of urinary catheter biocompatibility. Urology 1987;29:501–03.

[48] Nacey JN, Delahunt B. Toxicity study of first and second generation hydrogel-coated latex urinary catheters. Br J Urol 1991;67:314–6.

[49] Stensballe J, Looms D, Nielsen PN, Tvede M. Hydrophilic-coated catheters for intermittent catheterisation reduce urethral micro trauma: a prospective, randomised, participant-blinded, crossover study of three different types of catheters. Eur Urol 2005;48:978–83.

[50] Cox AJ, Millington RS, Hukins DWL, Sutton TM. Resistance of catheters coated with a modified hydrogel to encrustation during an in vitro test. Urol Res 1989;17:353–6.

[51] Cox AJ, Hukins DWL, Sutton TM. Comparison of in vitro encrustation on silicone and hydrogel-coated latex catheters. Br J Urol 1988;61:156–61.

[52] Tunney MM, Keane PF, Jones DS, Gorman SP. Comparative assessment of ureteral stent biomaterial encrustation. Biomaterials 1996;17:1541–6.

[53] Anderson JM, Shive MS. Biodegradation and biocompatibility of PLA and PLGA microspheres. Adv Drug Deliv Rev 1997;28:5–24.

[54] Athanasiou KA, Niederauer GG, Agrawal CM. Sterilization, toxicity, biocompatibility and clinical applications of polylactic acid polyglycolic acid copolymers.Biomaterials 1996;17:93–102.

[55] Emerich DF, Tracy MA, Ward KL, Figueiredo M, Qian RL, Henschel C et al. Biocompatibility of poly (DL-lactide-co-glycolide) microspheres implanted into the brain. Cell Transplant 1999;8:47–58.

[56] Kitchell JP, Wise DL. Poly(lactic/glycolic acid) biodegradable drug-polymer matrix systems. Meth Enzymol 1985;112:436-48.

[57] Xie S, Zhu Q, Wang B, Gu H, Liu W, Cui L et al. Incorporation of tripolyphosphate nanoparticles into fibrous poly(lactide-co-glycolide) scaffolds for tissue engineering. Biomaterials 2010;31:5100-9.

[58] Abid Jean-Pierre. Laser induced synthesis and nonlinear optical properties of metal nanoparticles, PHD. Thesis S. 117ff 2003.

[59] Emoto K, Nagasaki Y, Kataoka K. Coating of Surfaces with Stabilized Reactive Micelles from Poly(ethylene glycol)-Poly(DL-lactic acid) Block Copolymer**.** Langmuir1999;15:5212-8.

[60] Griffith DP, Musher DM, Itin C. Urease: the preliminary cause of infection-induced urinary stones. Invest Urol 1976;13:346-50.

[61] Jones DS, Djokic J, Gorman SP. Characterization and optimization of experimental variables within a reproducible bladder encrustation model and in vitro evaluation of the efficacy of urease inhibitors for the prevention of medical device-related encrustation. Biomed Mater Res B Appl Biomater 2006;76:1-7.

[62] Li DX, Yamamoto H, Takeuchi H, Kawashima Y. A novel method for modifying AFM probe to investigate the interaction between biomaterial polymers (Chitosan-coated PLGA) and mucin film. Eur J Pharm Biopharm 2010;75:277–83.

[63] Fu J, Ji J, Yuan W, Shen J. Construction of anti-adhesive and antibacterial multilayer films via layer-by-layer assembly of heparin and chitosan. Biomaterials 2005;26: 6684–92.

[64] Li P, Bakowsky U, Yu F, Loehbach C, Muecklich F, Lehr CM. Laser Ablation Patterning by Interference Induces Directional Cell Growth. IEEE Trans Nanobiosceince 2003;2:138-45.

[65] Roy S, Goud NR, Babu NJ, Iqbal J, Kruthiventi A. Crystal structures of norfloxacin hydrates. Cryst Growth Des 2008;8:4343-6.

[66] Park JH, Cho YW, Cho YH, Choi JM, Shin HJ, Bae YH et al. Norfloxacin-releasing urethral catheter for long-term Catheterization. J. Biomater. Sci. Polymer Edn 2003;14:951-62.

[67] Li S. Hydrolytic degradation characteristics of aliphatic polyesters derived from lactic and glycolic acids. J Biomed Mater Res 1999;48:342-53.

[68]ReddyJS, GaneshSV, NagalapalliR, DandelaR, SolomonKA, KumarKA et al. Fluoroquinolone salts with carboxylic acids. J Pharm Sci 2011;100:3160-76.

[69]Ong YL, Razatos A, Georgiou G, Sharma MM. Adhesion Forces between *E. coli* Bacteria and Biomaterial Surfaces**.** Langmuir1999;15:2719-25.

[70] Li B, Logan BE. Bacterial adhesion to glass and metal-oxide surfaces. Colloids and Surfaces B: Biointerfaces 2004;36:81–90.

[71]Dayyoub E, Belz E, Dassinger N, Keusgen M, Bakowsky U. A novel method for designing nanostructured polymer surfaces for reduced bacteria adhesion.Phys. Status Solid 2011;208:1279-83.

[72] Truong VK, Lapovok R, Estrin YS, Rundell S, Wang JY, Fluke CJ et al.The influence of nano-scale surface roughness on bacterial adhesion to ultrafine-grained titanium. Biomaterials 2010;31:3674–83.

[73] Ploux L, Anselme K, Dirani A, Ponche A, Soppera O, Roucoules V. Opposite Responses of Cells and Bacteria to Micro/Nanopatterned Surfaces Prepared by Pulsed Plasma Polymerization and UV-Irradiation. Langmuir 2009;25:8161–9.

[74] Burkersroda FV, Schedl L, Göpferich A.Why degradable polymers undergo surface erosion or bulk erosion. Biomaterials 2002;23:4221–31.

[75] Bibby JM, Hukins DW. Acidification of Urine is not a Feasible Method for Preventing Encrustation of Indwelling Urinary Catheters. Scand J Urol Nephrol 1993;27:63-5.

3 Highly Ordered Self-Organized Polymer Coatings for Reduced Bacteria Adhesion

In preparation for Acta Biomaterialia

Abstract

Nanostructuring of implant surfaces has emerged as promising way to control biological responses especially bacterial adhesion. Here, poly(lactic-co-glycolic acid) (PLGA) was used to create nanostrtuctured films consisting of polymer features on polyurethane (PUR) surface. For this purpose, dipping method was employed by using acetone solution of PLGA as dipping solution and adding non-solvent (water) to this solution. The yielded polymer nanofeatures were half-sphere shaped and their size was tunable by changing manufacturing parameters. Film stability under shear forces was investigated and it was found that the polymer films were still attached to PUR surface after 30 days of phosphate buffered saline (PBS) incubation. *Invitro* bacterial adhesion tests showed different potential of the nanostructured films to reduce bacteria attachment. Features with spacing smaller than bacteria width inhibited the bacterial adhesion in comparison to flat spin-coated PLGA film, reverse relationship was found between feature spacing and the number of the adhered bacteria. In contrast, rising of features spacing over the bacterial width decreased their capacity to reduce bacterial adhesion. These results highlight the importance of designing nanofeature with accurate size and shaping when reduction of bacterial adhesion is aimed.

This study also pointed the significance of development of new implant coating that show nanostructured topography and have the ability to be loaded with active agents by choosing the suitable method for film preparation and the appropriate polymer.

Introduction

Textured surfaces of nanoscale topography are of growing importance for several fields such as medicine and biology. The use of nanostructured materials in these Fields is innovative [1]. It is well-recognized that surface topography at the macro- and microscale has strong effect on 1.Cell orientation and grow direction [2-7] 2.Cell proliferation [8] and 3.Cell functions [9] and also on bacteria behavior [10-11]. However, in recent years the bacteria-nanostructured man-made substrate interactions gained more attention and were studied intensively. These interactions are of high importance for implant applications, since the biological performance of biomedical implants strongly depends on the first interaction happening when implant surfaces come into contact with a biological environment [12]. Microbial cells can foul implant surface and form biofilm after the body implantation. This biofilm consists of microorganisms attaching irreversibly to the surfaces and they form a congregate of single or multiple populations [13], this biofilm become resistant against the immune system and conventional treatments with antibiotic, therefore new approaches are needed for the inhibition of biofilm growth during its development [14]. The formation and development of the biofilm follows steps that may differ depending on the biological characteristics of the bacteria present. However, four common steps are generally distinguished. In the first step, a bacterium is brought into contact with the surface by the gravitational forces, Brownian motion or hydrodynamic forces, in some bacterial species flagella can also induce motion. The second step of biofilm is the adhesion of the bacteria to the surface. Usually this adhesion is described as two separate stages: reversible adhesion and irreversible adhesion. These two stages involve different physio-chemical and chemical bacteria-surface interactions. These interactions are significantly dependent on the properties of the surface on which the biofilm is forming [15]. Many researchers found that the second step is the step most influenced by topographical and chemical properties of the surface [16] and it is a crucial step in the process

of biofilm development [17].In principle, it should be possible to retard, if not prevent, the formation of biofilms on substrates by using materials to which bacteria cannot attach initially [18]. Recently many approaches were used to arrange nanostructured surfaces by structural pattering of the surfaces at nanometre scale to control or prevent the initial bacteria adhesion [19, 20]. Many techniques were employed for topographical pattering of surfaces at nanoscale like photolithography [21], self-assembled polymers [22], polymer demixing [23, 24], colloidal lithography [21], surface roughening [25] metal oxidation [26] and electrospinning [27]. A variety of these methods were used to improve the biocompatibility of implants, but most of these methods are limited to very small area [28,29] or the shape of the resulted features and the space between them is hard to control and in some cases the method depended on chemical modification of the implant surface which changes the surface chemical nature and this may negatively alter the biological response [30]. The main advantage of our presented method is the ease to construct nanostructured coating using dipping method which can be applied on unlimited area. In this study, we used PLGA to design the films. PLGA is FDA-approved polymer, it degrades by hydrolysis of its ester bonds to lactic and glycolic acid, these acids are removed from human body through metabolic pathways and therefore it is biocompatible [31,32]. It is widely used for tissue engineering scaffolds and pharmaceutical products like drug delivery and targeting [28,29,33-38]. It is also used as coating matrix to control the release of drugs and active agents from implant surfaces [39,40]. Coating of implant surface with drug-loaded PLGA films can inhibit the undesired implant-human body interactions by releasing therapeutic agents that reduce the negative reaction of the body after the implantation. However these interactions are not the only factors that influence the effectiveness of implants. Bacteria colonization and biofilm formation on implant surface are counted as serious problems which can lead to implant failure and/or implant removal. An Ideal coating must have the potential to release drugs in

effective concentration during implantation time and to reduce or prevent implant-associated biofilm and infections. Nanostructuring of the coating is an innovative choice to inhibit bacterial biofilm. Since the local or systematical administration of antibiotics can lead to antibiotic resistant strains, surface structuring with nanofeatures introduces a safe and effective way to avoid the side-effects of antibiotics and appearance of resistant bacteria strains. In this work, PLGA nanostructured films were prepared on polyurethane surface by simple dipping method. This method is a useful technique to produce drug-loaded polymer films by dissolving the drug and the polymer in a the same solvents and incubation the substratum in the polymer/drug solution, the formed film can then be dried to be used as drug release coating. Drying parameters like temperature and air humidity in addition to solvent and polymer nature influence the structure and the shape of the yielded film. To produce nanostructured films we added non-solvent(water) to PLGA/acetone solution and the resulted films were nanostructured. Our method doesn't differ from the known dipping method where drug-loaded polymer film can be constructed and the only modification was adding of PLGA-insoluble solvent (water) to change surface structuring. The new morphology of the films increased their ability to reduce bacterial adhesion compared to flat and unstructured PLGA film.

Materials and methods

Materials

Poly($_{D,L}$-lactide-co-glycolide) (PLGA), lactide/glycolide ratio 53:47 was a gift from Purac Biochem (Purac, Netherlands). Safranin was purchased from Sigma-Aldrich (Sigma-Aldrich chemie GmbH, Germany). PUR wafers were a gift from Primed Halberstadt Medizintechnik GmbH (Halberstadt, Germany).

All other chemicals and solvents were of high analytical grade and commercially available.

Nanostructured Film preparation

PUR wafers were washed with Acetone, 2-propanol and double distilled water and then dried in nitrogen flow. 100 mg PLGA was dissolved in 100 ml acetone under gentle stirring at room temperature overnight. The solution was then slowly injected in desired amount of double distilled water at constant rate of 10 ml/min by the use of injection needle (Neopoint® 0.90 × 70 mm; Servopharma GmbH, Wesel, Germany) under magnetic stirring (300 rpm). Cleaned PUR wafers were then directly incubated in the Acetone-PLGA/water mixture for different times. After the incubation, the wafers were then allowed to dry at ambient conditions (23 °C and 55% relative humidity) and then stored at -20 °C. All the films were prepared at the same ambient condition.

Spin-coated PLGA films were prepared on glass slides. Glass slides (round, 20mm in diameter) were cleaned as previously and dried by exposing to nitrogen flow. The slides were then spin-coated from 5% (w/v) PLGA/Ethyl acetate solution by using spin coater (Novocontrol Technologies, Germany) at rate of 2000 rpm for 60 s at ambient condition. The coated slides were then stored at -20 °C to use later for AFM and bacterial adhesion measurements.

Surface morphology

Morphology of the PUR wafers before and after the coating was analyzed by atomic force microscopy (AFM). The measurements were performed on a JPK NanoWizard™ (JPK Instruments, Berlin). Commercially available silicon cantilevers (NSC 16 AIBS, Micromasch, Estonia) with ultra-sharp pyramidal tips (radius of the tip curvature <10 nm), resonance frequency between 150-200 kHz and a nominal force constant of ~40 N/m were used for the AFM imaging. To avoid damaging of the surfaces, intermittent contact (air) mode was chosen. The scan speeds were proportional to the scan sizes. Images were taken by displaying the amplitude, height and phase reflection signals of the cantilever in the trace direction. For each surface the Root-Mean-Squared roughness (RMS) and the arithmetic average roughness (Ra) were calculated by jpk software. The software was also used to calculate the height of polymer features and the distance between them.

Film stability

The coated PUR wafers were incubated in PBS with 1% sodium azid at 37 °C in a rotary shaker for 60 days. Surface morphology of the films was examined before and after the incubation by the use of AFM. Feature density onto the surface was calculated by the use of image j software. Changes of feature size and number before and after the incubation were investigated.

Bactrial adhesion

For bacterial measurement, spin-coated film and nanostructured PLGA films were employed. *E.coli* (BL21 strain) was grown overnight in lysogeny broth agar plates (10 g/l Bacto-Trypton, 5 g/l Bacto-Yeast Extract, 5 g/l NaCl, 1,5 (w/v) Bacto-Agar) at 37 C° in CO2-inkubator. One colony was used to inoculate a 3ml of lysogeny broth medium (LB, 10 g/l Bacto-Trypton; 5

g/l Bacto-Yeast Extract; 5 g/l NaCl), the medium with bacteria was then incubated under constant shaking (250 rpm) for 10 hours at 37 C°. To harvest the bacteria, the suspension was centrifuged (3000 rpm, 10 min) and the bacteria were washed three times with PBS to remove the bacteria nutrition, finally the bacteria were resuspended in phosphate buffered saline (PBS)to reach a concentration of. Bacteria concentration in the suspension was adjusted to 5 x 10^9 cell/ml. All experiments were done by taking the desired volume from the same bacteria suspension to avoid variation of cell density.

Each film was incubated in 1 ml of the bacteria suspension at room temperature for 6, 18 and 30 h. The loosely adhered bacteria were eliminated from the surface by washing with large amount of PBS and distilled water.

Bacteria were stained with Safranin. One drop of the stain was placed on the surface for 3 min and then washed extensively with distilled water. Surfaces were the imaged by camera (1.3 M pixel) mounted to light microscopy (Müller, Germany). The pictures were then analyzed by image j software to calculate the surface coverage with the *E.coli* and determine bacterial colonization.

Results

Film characterization

The uncoated PUR surface as purchased possessed ununiformed nanometer features as shown in Fig 1. After incubation in the dipping mixture, half-sphere polymer nanofeatures were formed on the surface. The topography as a function of water/acetone ratio and incubation times was measured using AFM. After coating with PLGA (1mg/ml concentration, 10 min dipping time, 1/1 water/acetone ratio) the surface possessed half-sphered nanofeatures with diameter of 155± 23 nm. Raising the water/acetone ration to 5/4 resulted in increasing of the nanofeatures to 270 ± 55 nm in diameter while employment of 6/4 ratio leaded to increasing the size up to 370 ± 73 nm. Amplitude images of the prepared nanostructured PLGA films are presented in Fig 1.

Fig 2 represented the films when different incubation times were used. Images show uniform structures of PLGA, the size of the features increased by increasing the incubation time. 250 ± 48 nm features were obtained when the wafters were incubated for 15 min and increasing of size was noticed when incubation time was increased to 30 min and feature of 275 ± 50 nm size were obtained. For incubation times above 30 min the films were random and rising the incubation times resulted in increasing the feature sizes. RMS and Ra of all surfaces were also calculated by JPK software from five images (each 10x10 μm), the averages are presented in table 1.

water/acetone ratio	Incubation time (min)	Ra (nm)	RMS (nm)	Feature size(nm)
4/4	10	6.66±1.15	8.85±1.51	155± 23
5/4	10	19.70±2.79	23.70±3.59	270 ± 55
6/4	10	35.35±4.04	42.14±5.78	370 ± 73
1/1	15	23.28±1.68	27.56±1.93	250 ± 48
1/1	30	20.38±2.29	24.64±2.43	275 ± 50
1/1	60	31.00±4.36	37.14±4.88	___
1/1	120	37.90±8.21	45.18±10.62	___

Table 1. Feature sizes and roughness values of the nanostructured surfaces prepared with different incubation times and water/acetone ratios.

Film stability

The stability of the nanostructured films were investigated by examination the films morphology before and after PBS exposure for 30 days. The PLGA features were still attached to the surface and insignificant change of their sizes were observed. Fig 4 shows feature surface before and after the incubation. Features exhibited negligible changes of their surface roughness, this expected results are due to the degradation of PLGA in water. Since the bulk erosion of the used PLGA begins first after two months of PBS incubation, little changes of surface roughness after PBS incubation can be expected.

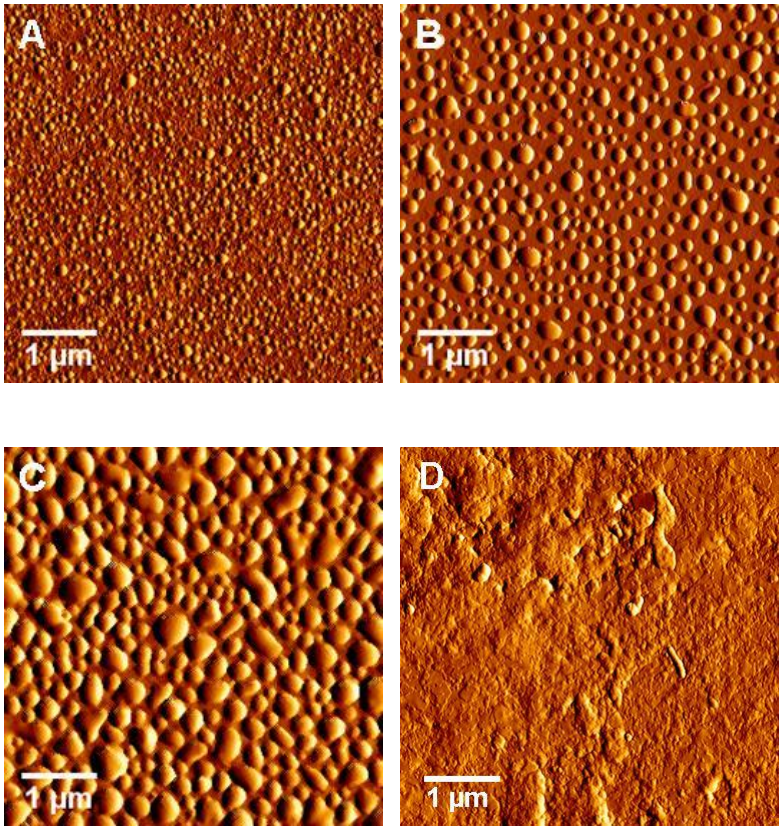

Fig. 1. Surface morphology of coated and uncoated PUR: (A) (1/1) water/acetone mixture was used, (B) (5/4), (C) (6/4) and (D) the uncoated PUR. Particle sizes increase with the increasing of acetone ratio (PLGA amount) in the mixture.

Bacterial Adhesion

Light microscope was used to estimate the bacterial adhesion on nanostructured PLGA surface the spin-coated glass surface. After staining with safranin, surface coverage with the bacteria was calculated with image J software. Bacteria attachment to spin-coated surface, surfaces with different PLGA feature sizes and is represented in Fig 5.

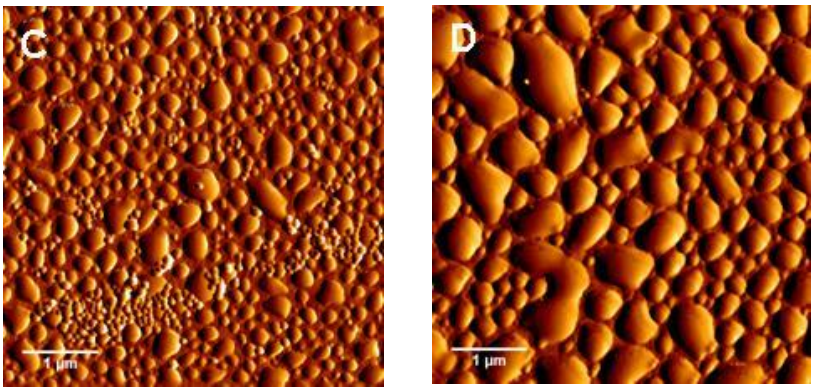

Fig. 2.PUR nanostructured coating. 1mg/ml PLGA concentration was used: (A) PUR was incubated for 15 min, (B) 30 min, (C) for 60 min and (D) for 120 min. Films were examined under AFM.

No significant increase of bacterial adhesion onto 100 nm diameter features was seen in comparison to spin-coated surface. The 250 nm features had the ability to inhibit bacterial attachment and their efficiency was up to four times higher than the 250 nm features and spin-coated surface. Bacterial response to other feature sizes varied due to the size of the features. 350 nm features were able to reduce bacteria attachment and the surface coverage was 2.0±0.8% after 30 h of incubation. These features had the highest potential to reduce the bacterial adhesion whereas bigger and smaller features had lower ability.

Discussion

AFM investigation of the polymer features showed that increasing the incubation times and water/acetone ratios leaded to increase of the polymer features. These features were uniform up to size 450 nm and they had half-sphere shape while bigger features were ununiformed and not half-sphere shaped. One explanation of the features formation on PUR surface is the forming of PLGA films when PUR chips were incubated in the PLGA-Acetone/water mixture. The thickness of these films depends on the incubation time so that more polymer chains are able to stick to the surface when incubation times are increased. Exposure of these films to air can change the shape of the films due to the phase separation and leads to the forming of polymer features. Acetone has a boiling point of about 56 °C. When the film is exposed to air, acetone evaporates faster than water due to its low boiling point, this leads to decrease the acetone/water ratio in the film and only little amount of acetone is available in the film. The process continues until the complete evaporation of acetone. Decreasing of acetone amount in the film reduces the polymer solubility in the acetone/water mixture and at this point the film changes its shape from continues to intermittierend film and when acetone completely evaporated, the polymerforms nanofeatures on PUR surface.

Similar effect of water/acetone-polymer ratio was found and increasing of the ratio leaded to increase of the feature sizes (Table 1).

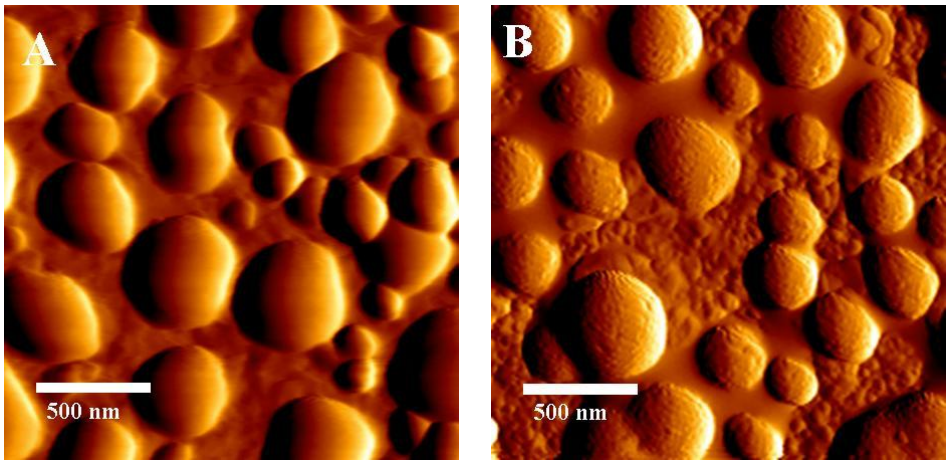

Fig. 3. Nanostructured film stability. (A) before PBS incubation, (B) after 30 days of PBS incubation.

Analysing the uniform features (up to 450 nm) with JPK software showed that the spacing between the features (the distance between the centres of two neighbour features) depends on the feature size and it was about the 3/2 of the feature diameter. The features with sizes higher than 450 nm were uniform and there was no relationship between their sizes and the spacing. Employment of the uniform features provides the ability to investigate bacterial adhesion on high-ordered surface with spacing of good regularity and to study the influence of features spacing on bacterial adhesion and therefore the features with sizes over than 450 nm were precluded from bacterial adhesion studies. Edwards et al [41] constructed microfeatures on metal sulphide surfaces by scratching the surface and studied the influence of the pit depth and cross-sectional shape on bacterial adhesion. They found that bacteria prefer to adhere to the bottom of the pits, they attach in such a manner as to maximize bacteria-surface contact area. They found also that 500 nm pits hada low contact area for bacteria, which may be less energetically favourable for bacterial adhesion than the other pit sizes which explain the poor bacteria adhesion.

These results are in agreement with our results. The 350 nm features had the highest potential to reduce bacteria adhesion where the 450 nm and 250 nm features were more preferred for bacterial adhesion. The width of the used *E.coli* cells is about 500-600 nm which is higher than the features spacing (~ 525 nm). Bacteria have a characteristic shape and they are also greatly less deformable than eukaryotic cells, they maintain their shape upon attachment to the surface [16]. Therefore it is not expected that the bacteria can attach to the grooves

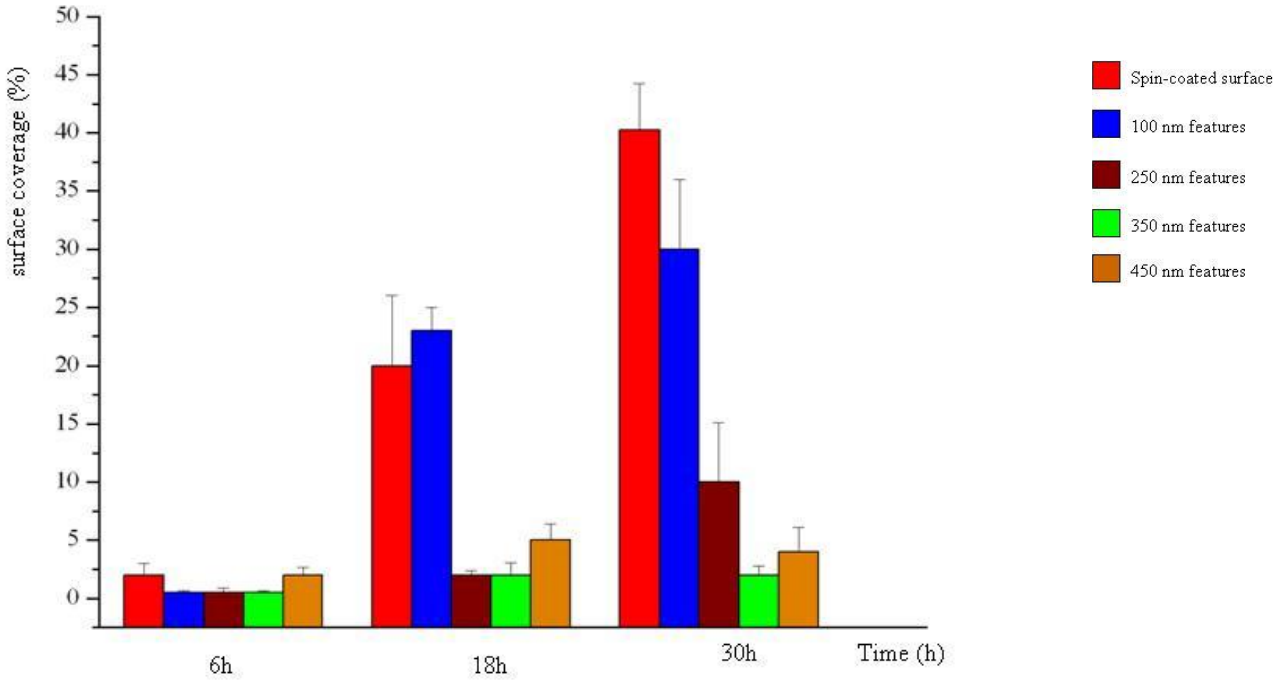

Fig. 5.*E.coli* adhesion to different nanostructured PLGA coatings after 6, 18 and 30 hour of incubation. The features with 350 nm size average show the highest potential to reduce the bacterial adhesion.

Between the features when the spacing is smaller than bacterial width. Features with spacing which are little smaller than bacteria width prevent bacterial attachment to the bottom of the features and at the same time minimize bacteria-surface contact area resulting in decreasing

bacterial adhesion such as in the case of 350 nm features while features with sizes which are much smaller than bacteria width like in the case of 100 and 250 nm features prevent bacterial attachment to the bottom of the surface but they provide more contact surface area to the bacteria and therefore they have lower capability to reduce the adhesion than the 350 nm features.

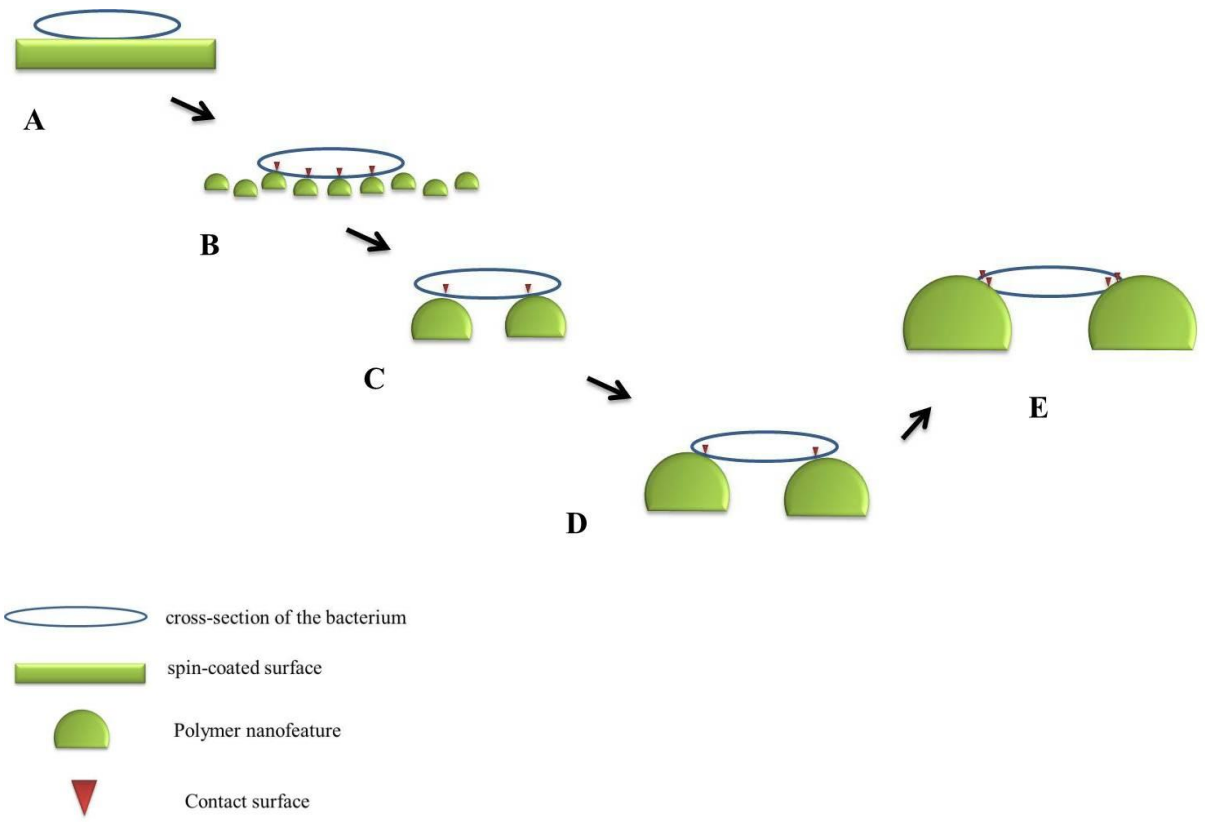

Fig. 6.Schematic representation of the contact surface between bacteria and nanostructured surfaces and the comparison with spin-coated surface.Bacteria-surface contact area decreases (B > C > D) when nanofeature spacing increases.Increasing the spacing to 525 nm (higher than bacteria width) increases the contact area (E > D). Unstructured spin-coated surface (A) provides the highest contact area.

When the spacing value is a littlehigher than bacteria width like in the case of 450 nm features, little more contact area is available for the attachment and the anti-adhesive properties of the film decreases again. Fig 6 shows schematic representation of the bacteria-surface contact area, the differences between the features and the comparison with flat spin-coated surface.

The spin-coated surface has theoretically the highest bacteria-surface contact area and therefore the lowest potential to inhibit bacteria attachment. After exposing the nanostructured films to PBS, the features were still attached to the surface. The hydrophobic nature to the used PLGA may is responsible to the high stability of the films for at least 30 days. The use of such films as anti-adhesion implants coating are highly depended on the stability of the film after exposing to blood or body fluids. After 30 days of incubation in PBS, no significantly differences of surface coverage with polymer and feature shapes were found. Slightly changes of feature surface roughness were noticed because of the degradation of PLGA in water as result of ester bond splitting.

Conclusion

High-ordered polymer nanofeatures with different sizes were successfully prepared on PUR surface. It has been found that adding nonsolvent (water) to PLGA/acetone solution is a useful way to design nanostructured film on PUR wafer. Dipping method was used to achieve this goal and altering of incubation time and water/acetone ratio resulted in varying sizes of the yielded features. The thickness of the adsorbed polymer film after the incubation depended on the incubation time which explain the direct proportion between feature size and incubation time. The hydrophobic interactions between the features and PUR were the dominant forces which kept the features attached to the surface after 30 days of PBS incubation. When bacterial adhesion testes on the different sized polymer features and spin-coated polymer films were done, the films were found to have resistance properties against adhesion of *E.coli* in comparison to the spin-coated films. Analysing of surface roughness, feature size and spacing leaded to the final conclusion that the available surface contact area for bacterial attachment influences the bacteria favourability to attach to the surface and that, in our study, no significant correlation between the number of the adhered bacteria and surface roughness were found.

Acknowledgement

The authors would like to thank Novoplast Schlauchtechnik GmbH (Halberstadt, Germany), Primed Halberstadt Medizintechnik GmbH (Halberstadt, Germany), MAT PlasMATec GmbH (Dresden Germany), TRUMPF Medizin Systeme GmbH Deutschland, (Saalfeld Germany), JPK Instruments Berlin (Germany) and BMWI/AiF (AZ IGF-05/05-AiF-Nr. 15090 BG/2) for the support.

References

1.Ploux L, Anselme K, Dirani A, Ponche A, Soppera O, Roucoules V. Opposite Responses of Cells and Bacteria to Micro/Nanopatterned Surfaces. Langmuir 2009;25:8161-8169.

2. Li P, Bakowsky U, Yu F, Loehbach C, Muecklich F, and Lehr CM. Laser Ablation Patterning by Interference Induces Directional Cell Growth. IEEE Trans Nanobioscience 2003;2:138-145.

3. Anselme K, Bigerelle M,Noël B,Iost A, Hardouin P. Effect of grooved titanium substratum on human osteoblastic cell growth 2002;60:529–540.

4. Y Fayou, Mücklicha F, Li P, Shenc H, Mathurc S, Lehr CM, Bakowsky U. In Vitro Cell Response to Polymer Surface Micropatterned by Laser Interference Lithography.Macromolecules 2005;6:1160-1167.

5. den Braber ET, de Ruijter JE, Ginsel LA, von Recum AF, Jansen JA. Quantitative analysis of fibroblast morphology on microgrooved surfaces with various groove and ridge dimensions. Biomaterials 1996;17:2037-2044.

6. Rajnicek AM, Britland S, McCaig CD. Contact guidance of CNS neurites on grooved quartz: Influence of groove dimensions, neuronal age and cell type. J. Cell Science 1997;110: 2905-2913.

7. Clark P, Connolly P, Curtis AS, Dow JA, Wilkinson CD. Topographical control of cell behavior: I. Simple step cues. Development 1987;99:439-448.

8. van Kooten T G, Whitesides JF, von Recum AF. Influence of Silicone (PDMS) Surface Texture on Human Skin Fibroblast Proliferation as Determined by Cell Cycle Analysis.JBiomed Mater Res B Appl Biomater 1998;43:1–14.

9. Ito Y. Surface micropatterning to regulate cell functions. Biomaterials 1999;20: 2333-2342.

10. Scheuerman TR, Camper AK, Hamilton MA. Effects of Substratum Topography on Bacterial Adhesion. J Colloid Interface Sci 1998;208:23–33.

11. Ploux L, Beckendorff S, Nardin M, Neunlist S. Colloids Surf., B 2007;57:174–181.

12.Cai K , Bossert J, Jandt KD. Does the nanometre scale topography of titanium influence protein adsorption and cell proliferation? Colloids Surf B Biointerfaces 2006;49:136–144.

13Tamilvanan S, Venkateshan N, Ludwig A. The potential of lipid- and polymer-based drug delivery carriers for eradicating biofilm consortia on device-related nosocomial infections. J. Control. Release 2008;128:2-22.

14. Annich GM, Meinhardt JP, Mowery KA, Ashton BA, Merz SI, Hirschal RB, Meyerhoff ME, Bartlett RH. Reduced platelet activation and thrombosis in extracorporeal circuits coated with NO-release polymers. Crit. Care Med 2000;28, 915.

15. Ploux L, Ponche A, Anselme K. Bacteria/material interfaces: role of the material and cell wall properties. J Adhesion Sci Technol 2010;24:2165-2201.

16. Anselme K, Davidson P, Popa A M, Giazzon M, Liley M, Ploux L. The interaction of cells and bacteria with surfaces structured at the nanometre scale. Acta Biomaterialia 2010;6:3824-3846.

17. Razatos A, Ong Y, Sharma MM, Georgious G. Molecular determinants of bacterial adhesion monitored by atomic force microscopy. PNAS 1998;15:11059–11064.

18. SateeshA, VogelJ, DayssE, FrickeB, DöllingK, RotheU. Surface modification of medical-grade polyurethane by cyanurchloride-activated tetraether lipid (a new approach for bacterial antiadhesion). J Biomed Mater Res A 2007;84A:672-681.

19. Ivanova EP, Truong VK, Wang JY, Berndt CC, Jones RT, Yusuf II, Peake I, W. Schmidt HW, Fluke C, Barnes D, Crawford RJ. Impact of Nanoscale Roughness of Titanium Thin Film Surfaces on Bacterial Retention.Langmuir 2010; 26:1973–1982.

20.Truong VK, Lapovok R, Estrin YS, Rundell S, Wang JY, Fluke CJ, Crawford RJ, Ivanova EP. The influence of nano-scale surface roughness on bacterial adhesion to ultrafine-grained titanium. Biomaterials 2010;31:3674–3683.

21. Blättler T, Huwiler C, Ochsner M, Städler B, Solak H, Vörös J, Michelle GH. Nanopatterns with biological function. J Nanosci Nanotechnol 2006;6:2237-2264.

22. Meli MV, Badia A, Grütter P, Lennox RB. Self-assembled masks for the transfer of nanometer-scale patterns into surfaces: characterization by AFM and LFM. Nano Lett 2002;2:131–5.

23. Dalby MJ, Riehle MO, Johnstone H, Affrossman S, Curtis AS. In vitro reaction of endothelial cells to polymer demixed nanotopography. Biomaterials 2002;23:2945–54.

24. Dalby MJ, Pasqui D, Affrossman S. Cell response to nano-islands produced by polymer demixing: a brief review. IEEE Proc Nanobiotechnol 2004;151:53–61.

25. Zinger O, Anselme K, Denzer A, Habersetzer P, Wieland M, Jeanfils J, Hardouin P, Landolt D. Time-dependent morphology and adhesion of osteoblastic cells on titaniummodel surfaces featuring scale dependant morphology. Biomaterials2004;25:2695–711.

26. Park J, Bauer S, Schlegel KA, Neukam FW, von der Mark K, Schmuki P. TiO2 Nanotube surfaces: 15 nm – an optimal length scale of surface topography for cell adhesion and differentiation. Small 2009;5:666–71.

27. Megelski S, Stephens JS, Chase DB, Rabolt JF. Micro- and Nanostructured Surface Morphology on Electrospun Polymer Fibers. Macromolecules 2002;35:8456–8466.

28.Xu LC, Siedlecki CA. Submicron-textured biomaterial surface reduces staphylococcal bacterial adhesion and biofilm formation. Acta Biomaterialia 2012;8:72–81.

29. Krsko P, Kaplan JB, Libera M. Spatially controlled bacterial adhesion using surface-patterned poly(ethylene glycol) hydrogels, , Acta Biomaterialia 2009;5:589–596.

30. Puckett SD, Taylor E, Raimondo T, Webster TJ. The relationship between the nanostructure of titanium surfaces and bacterial attachment. Biomaterials 2010;31:706–713.

31. Jain R, Shah NH, Malick AW, Rhodes CT. Controlled drug delivery by biodegradable poly(ester) devices: different preparative approaches. Drug Dev. Ind. Pharm1998;24:703-727.

32.Kunou N, Ogura Y, Yasukawa T, Kimura H, Miyamoto H, Honda Y, Ikada Y. Long-term sustained release of ganciclovir from biodegradable scleral implant for the treatment of cytomegalovirus retinitis. J. Control Rel 2000;68:263:271.

33. Jain RA. The manufacturing techniques of various drug loaded biodegradable poly (lactide-co-glycolide) (PLGA) devices. Biomaterials 2000;21:2475-2490.

34.Kim DH, Martin DC. Sustained release of dexamethasone from hydrophilic matrices using PLGA nanoparticles for neural drug delivery. Biomaterials 2006;27:3031-3037.

35. Brigger I, Dubernet C, Couvreur P. Nanoparticles in cancer therapy and diagnosis. Adv Drug Deliv Rev 2002;54:631-651.

36.Anderson JM, Shive MS. Biodegradation and biocompatibility of PLA and PLGA microspheres. Adv Drug Deliv Rev 1997;28:5-24.

37. Cai C, Bakowsky U, Rytting E, Schaper AK, Kissel T. Charged nanoparticles as protein delivery systems: A feasibility study using lysozyme as model protein. Eur J Pharm Biopharm 2008;69:31–42.

38.Preparation and characterization of cationic PLGA nanospheres as DNA carriers. Kumar MNVR, Bakowsky U, Lehr CM. Biomaterials 2004;25:1771–1777.

39.Wang X, Venkatraman SS, Boey FYC, Loo JSC, Tan LP. Controlled release of sirolimus from a multilayered PLGA stent matrix. Biomaterials 2006;27:5588–5595.

40. Dorta MJ, Santoven˜a A, Llabre´s M, Farin˜a JB. Potential applications of PLGA film implants in modulating in vitro drugs release, Int J Pharm 2002;248:149-156.

41.Edwards KJ, Rutenberg AD, Microbial response to surface microtopography: the role of metabolism in localized mineral dissolution.Chemical Geology 2001;180:19–32.

4 A novel Method for Designing Nanostructured Polymer Surfaces for Reduced Bacteria Adhesion

Published in Physica Status Solidi (a)

Volume 208, issue 6, pages 1279-1283, June 2011

Abstract

Bacteria adhesion on implant surfaces is the major reason for local and systemic infections after implantation. In order to establish an anti-adhesion material, we constructed self-assembly nanostructured surfaces by wetting of poly(lactic-co-glycolic acid) (PLGA) films in ethyl acetate followed by a next step of dewetting under wet conditions. The resulting films had nanostructured surfaces with pores at nanoscale range between 200 and 500 nm. *E.coli* adhesion was examined on both flat spin coated and nanostructured PLGA films. The observations revealed that the bacterial adhesion onto the nanostructured surfaces was reduced in compared to the flat surfaces. Pore sizes affected the bacteria adhesion significantly. Due to its high biocompatibility and effectiveness against bacterial adhesion, these surfaces are ideal for biomedical device coatings.

Introduction

Bacterial infection on biomedical devices is a serious clinical problem; it is related to bacterial adhesion and biofilm formation [5]. Since the bacteria within the biofilm are highly resistant to antibiotics [6] and the elimination of the biofilm is hard to achieve, the prevention of initial bacterial adhesion has been mostly chosen as the optimal control strategy [7].

Surface topography at nanoscale range has strong effect on the bacteria adhesion. Several investigators have revealed that nanopattering of the surface can influence bacteria response to the surfaces [8-10]. In the last decades, many attempts have been made to manufacture ordered nanostructured surfaces and to evaluate the bacteria adhesion on it. Most of these attempts are based on designing nanopatterned surfaces using techniques which are limited to a very small area [8,9]. The aim of this study was to develop a new versatile technique to construct ordered PLGA films with nanoscale features and to investigate the adhesion of *E.coli* onto these films

Breath figure pattering of polymer surfaces, firstly reported by François et al [11] could be used to achieve surfaces of potential interest as model surface for biomedical application [4,9]. The overcoming of the limitation of this technique is of high importance. This work focused on creating new method which is based on the conventional breath figure pattering process and applicable for a wide area.

PLGA was used to construct new surfaces. It was chosen due to its biocompatibility which is an essential advantage for man-made biomedical devices and implants.

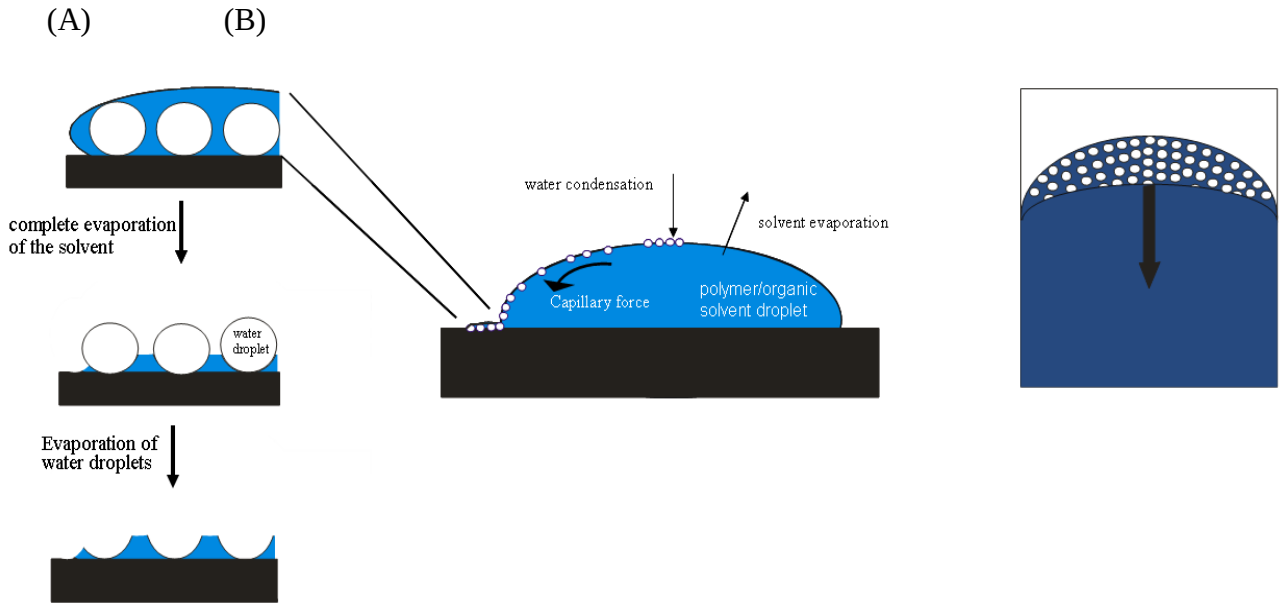

Fig. 1. Schematic representation of the process formation of the honeycomb-like structures (A) side sight, (B) top sight

Material and methods

Film preparation

Glass slides (76x26 mm) were washed with chloroform, isopropanol respectively and rinsed with a large amount of distilled water and then dried in nitrogen flow. Nanostructured films were prepared onto the cleaned glass slides using new technique. Briefly, 100 mg PLGA (57:43 lactide/glycolide) were dissolved in 100 ml ethyl acetate under gentle stirring overnight. Dipping method was used to arrange primary films on the glass slides by immersing the slides in the PLGA solution for 30 min, the consisting films were then dried in a vacuum and stored at 4 ºC for further modifications. In the next step, the primary films were wetted in ethyl acetate by dipping the coated slides in ethyl acetate for 1, 3, 6 and 9s (surfaces A, B, C and D respectively) and then pulled and allowed to dry under ambient conditions. To avoid different influences resulted from the use of different ambient parameters on the resulting films; all the films were constructed under the same ambient condition (relative humidity 45% and temperature 21 ºC). In the case of flat films, glass slides (round, 20mm in diameter) were cleaned as previously and dried in nitrogen flow. The flat films were prepared by spin coating from 1% PLGA/ethyl acetate (w/v) solution at rate of 2000 rpm for 60 s (spin coater: Novocontrol Technologies, Germany).

AFM Measurements

Atomic force microscopy (AFM) measurements were carried out on a JPK NanoWizard™ (JPK Instruments, Berlin), the instrument was used to measure the surface morphologyof the films. AFM cantilevers (NSC 16 AIBS, Micromasch, Estonia) with ultra-sharp tips, a length of about 125 µm, resonance frequency of 220 kHz and a nominal force constant of 36 N/m were chosen for all the measurement. To avoid the damage of the surfaces, intermittent contact (air) mode was preferred. The scan speed was proportional to the scan size.

Bacteria culture

E.coli (BL21 strain) was grown overnight in lysogeny broth agar plates (10 g/l Bacto-Trypton, 5 g/l Bacto-Yeast Extract, 5 g/l NaCl, 15 (w/v) Bacto-Agar) in CO_2-inkubator at 37 ºC. One colony was used to inoculate a 3ml of lysogeny broth medium (LB, 10 g/l Bacto-Trypton; 5 g/l Bacto-Yeast Extract; 5 g/l NaCl), which was incubated under constant shaking (250 rpm) at 37 ºC for 10 hours. The bacteria were then harvested by centrifugation (3000 rpm, 10 min) and then washed three times with distilled water. Finally the bacteria were resuspended in PBS (phosphate buffered saline pH 7.4) to reach a concentration of 5 x 10^9cell/ml.

Bacterial adhesion and quantification of biofilm

The adhesion of *E.coli* was evaluated under static conditions. Bacterial suspensions with a concentration of 5 x 10^9 cell/ml were used. Each coated sample was incubated in the bacteria suspension by dropping 100 µl onto the surface and the bacteria were allowed to adhere at 37 C°. After 8, 18 and 28 h of incubation, the samples were rinsed twice with fresh PBS to eliminate the nonadherent bacteria. Safranin was used for staining both live and dead bacteria and the adhering bacteria were observed with a Camera (1.3 M pixel) mounted on a microscope (Müller, Germany). Images were collected and then analyzed using Image J software to determine the surface coverage with bacteria. The surface coverage (%) was calculated by dividing the surface area covered with bacteria to the total area of the surface which imaged (time 100 to convert to %). The captured images were converted into black and white images by the use of Image J. In these images the bacteria appear like black spots while the uncovered surface looks white. The surface coverage (%) was calculated by dividing the number of black pixels to the number of the total pixels of the image (time 100). The adhesion experiments were carried out three times.

Results and Discussion

Formation mechanism of the honeycomb-like structures

Ordered honeycomb-like features of polymer assemblies formed by a similar mechanism were investigated by several researchers [1, 2, 4]. As shown in Fig 1, when a drop of highly diluted solution of water-insoluble polymer is allowed to dry under wet conditions (ambient conditions), the organic solvent (ethyl acetate) starts to evaporate. This leads to a cooling of the solution and water droplets condense onto the ethyl acetate-air interface. The droplets are transported to the three-phase line and are packed by capillary force produced at solution front. After complete evaporation of both the ethyl acetate and the water droplets, arranged holes are stamped in the place where the water droplets condensed. Our films have some differences compared to the honeycomb-like surfaces which were usually constructed using the so called ``breath figure`` methodology. In our work, primary films of PLGA were prepared on glass slides, and then wetted in ethyl acetate and allowed to dry under wet conditions. This differs from the ``classical `` methodology used to construct honeycomb-like polymer films in which a drop of highly diluted solution of water-insoluble polymer forms hexagonally porous film when the solvent evaporate. And thus some differences in pore sizes and film shape could be expected.

Nanostructured surface morphology

The uncoated glass showed smooth and unstructured surface when it was measured with AFM. It has a surface roughness (Ra) of 0.353 nm and RMS roughness (root-mean-squared) of 0.494 nm for a scan region of about 5x5 µm. The spin coated films demonstrate smooth surfaces (RMS 1.79 nm and Ra 1.35 nm). Regarding AFM measurement, the roughness of the surface Ra and RMS increased to 5.776 nm and 7.049 nm respectively when it was coated

with the first PLGA film (film A). Table I shows the surface roughness of the different prepared surfaces. Surfaces B and C showed slightly increasing in the RMS roughness from 3.006 nm for surface B to 3.090 nm for Surface C and in Ra values from 2.124 nm to 2.396 nm for the surfaces B, C respectively, where the surface D has the lowest Ra and RMS roughness.

Type of surface	RMS (nm)	Ra (nm)	Scanned area
Spin coated	1.79	1.35	5x5 µm
Surface (A)	7.04	5.77	5x5 µm
Surface (B)	3.00	2.12	5x5 µm
Surface (C)	3.09	2.39	5x5 µm
Surface (D)	1.13	0.78	5x5 µm

Table 1. RMS roughness (root-mean-squared), Ra roughness and scanned area of spin coated and the four surfaces A, B, C and D.

The thickness of the walls surrounding the holes was affected by the dipping time in ethyl acetate which is an agreement to the finding of Maruyama et al [1]. He described similar phenomenon when a drop of high diluted polyion complex evaporates. In his investigation he observed that polymer concentration in the drop is one of the most important parameters that influence the wall thickness and established that cell wall thickness decreases with the decreasing of the polymer concentration.

In our study, one can expect that the long dipping time of the film in ethyl acetate leads to reducing of the film thickness since a division of the PLGA could be dissolved in the organic solvent. Or in other words, long dipping time reduces the polymer concentration in the wet film and thus thinner cells will be formed. Analyzing of AFM images taken from our four

surfaces shows slimming down of the wall thickness from 20 nm for surface A to 15, 13 nm for the surfaces B and C respectively (Fig 2)

Solvent evaporation rate must be also considered. As described above, when the wetting times in ethyl acetate increase, the thickness of the wet film decrease and the ethyl acetate evaporates very fast from the wet film, while high PLGA concentration in the wet film leads to increasing of ethyl acetate evaporation temperature and slow evaporation rate takes a place. Slow evaporation of the solvent produces large holes because the condense water droplets have more time to coalesce and grow during the self-organization [2] this could provide a possible explanation of the growing sizes of the cells in our study. Surfaces A and B had pore sizes of 643±158 nm and 278±67 nm respectively, while surface C had smaller pore size (168±58 nm) and surface D had the smallest pore size (50±12 nm). As shown in fig. 2, the higher the size of the pores, the lower its density onto the surface.

The equilibrium contact angle of the nanostructured surfaces was measured as described elsewhere [13]: one drop of 1 µl water (MilliQ, pH 5.5) was dropped on each of the nanostructured surfaces and the equilibrium contact angles were determined by the use of contact angle goniometer (Erma, Tokyo, Japan).

Our nanostructured surfaces didn't exhibit superhyrophobicity. The contact angles of water were less than 90°.

Zhai et al prepared polyelectrolyte honeycomb-like structures and then coated them with silica particles [3]. Their surfaces were not superhydophobe due to the hydrophilic nature of the polyelectrolyte and the silica. Theyachieved superhydrophobic surfaces only when they coated the surfaces with semifluorinated silane. Since PLGA has low hydrophobicity, it is logically not expectant to get superhyrophobic surfaces as long as PLGA without further modification is used.

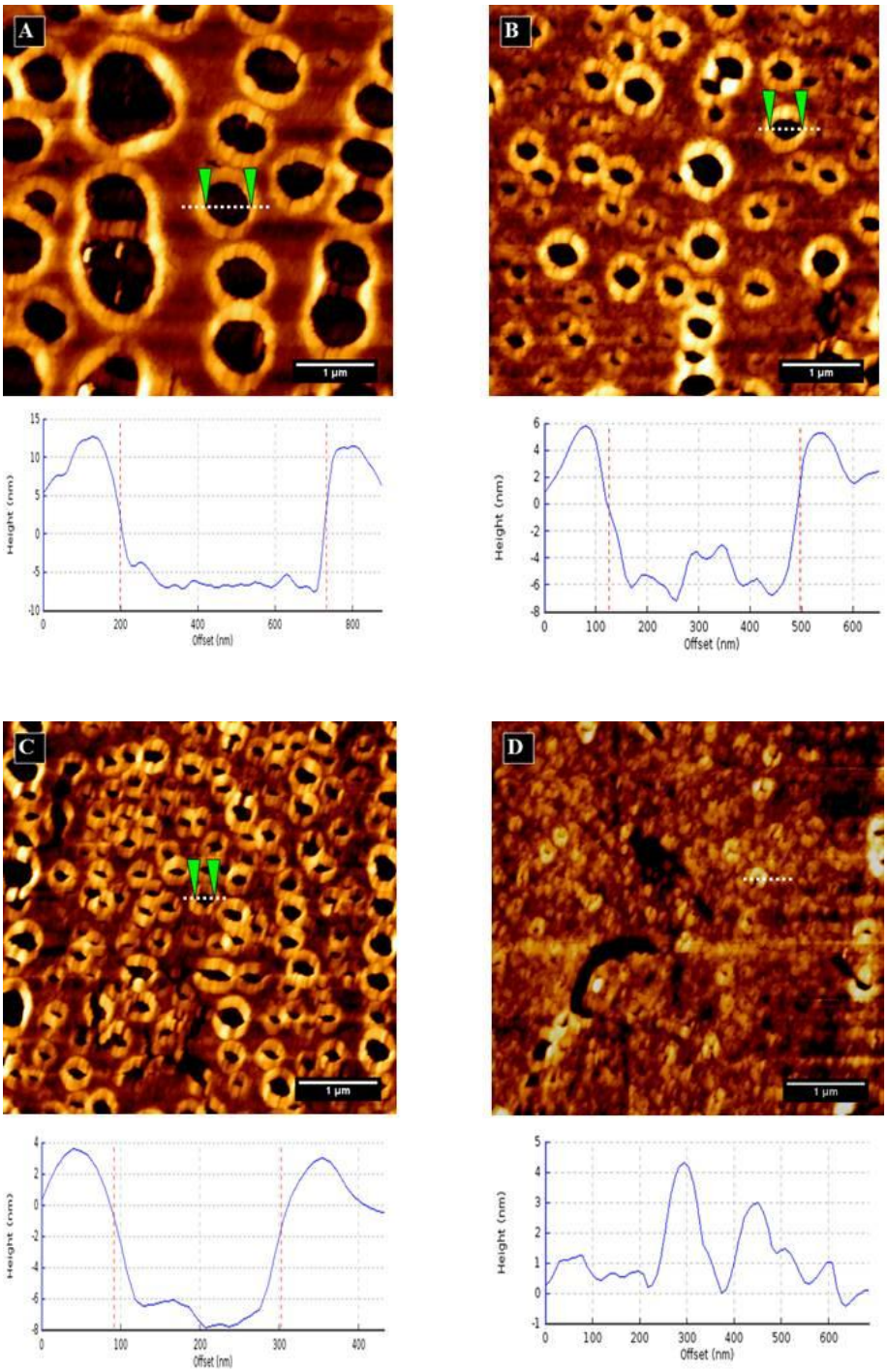

Figure. 2. AFM imaging and line profiles of surface topology of (A) surface A, (B) surface B, (C and D) for surfaces C and D respectively.

Bacterial adhesion

To determine the effect of the topology on the bacterial adhesion, bacteria suspensions were centrifuged to eliminate the LB medium which may cover the film surface and change its topography during the incubation time. The adhesion measurements aim to elucidate the relationship between the bacteria adhesion and the order and sizes of the pores. Also nonporous flat films of PLGA were employed to compare with the nanostructured films.

Surface roughness was widely determined as an important key for bacterial adhesion. In the present study, surface roughness of our films didn't play the major role which affected the adhesion (Table 1) whereas pore sizes and shape had the perceptible effect on the adhesion.

Fig 3 shows high potential of the surface A to reduce *E.coli* adhesion in compared to the flat and the other three surfaces. It has the largest pore size of 643±158 nm while the other three surfaces had decreasing pore sizes and they showed also decreasing anti-adhesive properties against *E.coli*.Nevertheless the flat surface reduced the adhesion weakly. Consequently, this finding confirms that surface features are the main factor responsible for the bacteria attachment which is an agreement with the investigations of Truong et al [12].

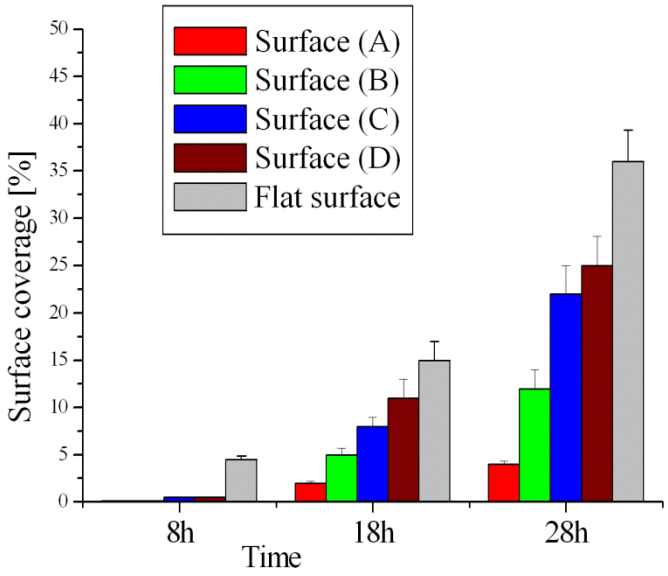

Figure. 3. Surface coverages (%) of adhered *E.coli* onto the flat and the other four nanostructured surfaces (A,B,C and D). Surface coverages were determined after 8,18 and 28 hour of *E.coli* incubation for each surface.

Conclusion

In this paper, we demonstrated the ability to construct PLGA nanostructured films applicable for a coating of wide surface area. The pore sizes of the films could be tuned to achieve the desired structures by adjustment the preparation parameters. The bacterial adhesion measurements show interest behavior of the bacteria on the five surfaces and point out the necessity of the surface features when antiadhesive coatings are designed. The ease of the preparation and the biocompatibility and the excellent anti-adhesion properties of the presented films are the significant advantages of this novel coating and this finding may allow the produce of anti-fouling coatings for medical implants.

Acknowledgements

The authors would like to thank JPK Instruments Berlin (Germany) and BMBF/AiF (AZ IGF-05/05-AiF-Nr. 15090 BG/2) for the support.

References

[1] N. Maruyama, O. Karthaus, K. Ijiro and M. Shimomura, Supramolecular Science **5**, 331(1999).

[2] P. Tang and J. Hao, J Colloid Interface Sci **333**, 1 (2009).

[3] L. Zhai, R. E Cebecci and M. F. Rubner, Nano Lett **4**, 1349 (2004).

[4] A. Munoz-Bonilla, E Ibarboure, V. Bordege, M. Fernandez-Garcia and J. Rodriguez-Hernandez, Langmuir.

[5] J.W. Costerton, K.J. Cheng, G.G. Geesey, T.I. Ladd, J.C. Nickel, M. Dasgupta and T.J. Marie, Ann. Rev. Microbiol **41**, 435 (1987).

[6] H. Anwar, J.L. Strap and J.W. Costerton, Antimicrob. Agents Chemother **36**, 1347 (1992).

[7] B. Gottenbos, H.C. Van Der Mei and H.J. Busscher, J. Biomed. Mater.Res **50**, 208 (2000).

[8] C. Satriano, G.M.L. Messina, S. Carnazza, S. Guglielmino and G. Marletta, Materials Science and Engineering C **26**, 942 (2006).

[9] E. Sohn, J. Kim, B. Gak Kim, J. Kang, J. Chung, J. Ahn, J. Yoon and J. Lee, Colloids and Surfaces B: Biointerfaces, (2010).

[10] L. Ploux, K. Anselme, A. Dirani, A. Ponche, O. Soppera and V. Roucoules, Langmuir **25,** 8161 (2009).

[11] G. Widawski, M. Rawisco and B. François, Nature **369**, 387 (1994).

[12] V. K. Truong, R. Lapovok, Y. S. Estrin, S. Rundell, J. Y. Wang ,C. J. Fluke, R. J. Crawford and E. P. Ivanova, Biomaterials **31**, 3674 (2010).

[13] P. Li, U. Bakowsky, F. Yu, C. Loehbach, F. Muecklich and CM. Lehr, IEEE TRANSACTIONS ON NANOBIOSCEINCE **2**, 138 (2003).

5 New antibacterial, Antiadhesive Films Based on Self-assemblies ofModified Tetraetherlipids

Published in Advances in Science and Technology

Volume 57, pages 188-184, September 2008

Abstract

We report the surface modification of a cellulose dialysis membrane by tetraether lipids and silver colloids to improve the antiadhesive and antibacterial properties of the biopolymer. The lipid was covalently attached to the membrane via the bivalent linker cyanuric chloride. The biologically evaluation show that the adhesion of serum components as well as bacteria, was decreased by this novel coating**.**

Introduction

The common medical therapy by use of hemodialysis and peritoneal catheters is still associated with infection problems. Infections of the catheter and peritonitis are serious complications, responsible for substantial morbidity and sometimes even mortality [1-3]. In addition, bacterial infections of catheters are one of the most frequent problems in applications of biomaterials to the urogenital system [3]. The bacterial germs originate from the intestinal flora as well as from the flora of the skin and the mucous [2, 4]. Recent operation techniques and hygienic standards can minimize the infections of the intracorporal parts of the catheter, but some problems remain unsolved. Especially fatal is the ability of some bacterial species to grow on a great variety of plastic materials and to metabolize those. Furthermore, most of the coagulase active bacteria species are resistant to antibiotics and represent a hazardous germ reservoir. One of the potential methods to protect biomaterials from bacterial adhesion is the surface modification with thin films of anti-microbial and anti-adhesive substances such as silver ions [3, 5], chlorhexidine [5] and phosphaditylcholines etc. The major innovation of the presented study is the development of a ultrathin but stable antiadhesive and anti-bacterial barrier of a thin composite film on different biomaterials based on tetraether lipids and silver colloids. The tetraether lipids are the major part of the cell - membrane of the archaeon Thermoplasma acidiphilum which is grown in an environmental milieu of sulfuric acid at pH 2 and 56°C [6, 7]. The absence of double bonds in the hydrocarbon chain and the ether bonds to the glycerols guarantee the resistance towards hydrolytic, oxidative and other (bio)chemical attack. Because of the high chemical and thermal stability of these membrane forming molecules, the tetraether lipids might be useful for the sealing of all types of vulnerable surfaces. It could be shown that stable, biological inert and compatible surface coatings can be produced on (bio)materials, such as dialysis membranes made of cellulose. The lipids could be attached covalently to the surface and are

constituted in a highly ordered impermeable and antiadhesive monolayer. The polymers as well as the colloids can additionally be applied to the medical device surface via self-assembly and dipping techniques. The physicochemical and biological properties of the supported film were examined.

Materials and methods

Tetraether Lipids Extraction and Activation

The tetraether lipids (TL, see Figure 1) were extracted and purified as described in [6], modified by a two-step chromatography with DEAE-cellulose and silica columns eluted with chloroform and methanol (2:1, v:v). The lipid was lyophilized at 10-2 torr and stored at –20°C under nitrogen. To activate the TL, equimolar amounts of cyanur chlorid and TL were allowed to react at 40°C overnight in chloroform with N,Ndiisopropylethylamineas catalyzer. The activated lipid was isolated with thin layer chromatography.

Silver Colloid Preparation

The silver colloids were prepared according to Abid [7]. 0.8ml ethylene diamine tetraacetic acid (EDTA) 0.1molar was added to 4 ml sodium hydroxide solution (0.1molar) and the mixture was diluted to a final volume of 100ml by distilled water under heating. Then, 1.3 ml silver nitrate (0.1molar) and 0.3ml HCL (0.1molar) were added to the solution. After 90 seconds of boiling the mixture was cooled down to room temperature. The resulting silver colloid dispersion was stored under light exclusion.

TL Coating of Silver Colloids

1 ml of the silver colloid dispersion (1.3mmolar Ag) was diluted to 15 ml with distilled water. The colloids were purified by centrifugation of the dispersion (2000rpm, 5 min) followed by washing and re-dispersion. 2mg of the activated TL were dissolved in 1ml chloroform. During the chloroform evaporation, a TL film was formed on the surface of a glass flask. The 15ml silver colloid dispersion were transferred to the flask, 100µl sodium dodecyl sulfate (SDS) 30% were added. After ultrasonic treatment, a TL film was formed surrounding the silver

colloids. The mixture was dialysed in water for 12h to remove the SDS. The colloid was collected and stored in dark container at 4C°.

Cellulose Surface Modification and Characterization

The supported TL monolayers were formed by self-assembly. The cellulose dialysis membranes were treated with NaOH solution(0.1molar) for 5 minutes at 20°C. The membranes were thoroughly washed with deionized water and dried. The hydrolysed cellulose was then incubated with cyanuric chloride activated TL (1mmolar in chloroform). The covalentely coupled TL monofilm was formed within 6 hours. The cyanuric chloride as bivalent linker facilitated the lipid coupling to the surface. After washing the biomaterials with chloroform/methanol 2:1 (v:v, 25°C) the membrane was dried in a dry nitrogen stream. For the silver colloid adsorption, the TL modified cellulose membrane was further incubated with the silver colloid dispersion (1mmolar, chloroform). In dependence on time, the density of colloids on the surface could be adjusted. The membranes were characterized by the use of the equilibrium contact angle, atomic force microscopy (Bioscope IV, Veeco Instruments Darmstadt,Germany), FTIR and light microscopy measurements.

Biological Evaluation

To determine the antiadhesive properties of the lipid and silver colloid modified cellulose membrane, different adhesion models were used: i) the modified surfaces were immersed with human serum over a period of 72 hours and ii) the adhesion of a suspension of *E. coli* under static conditions (72 h) was detected. The content of adhesion was evaluated byvisualization the biomaterial surface by AFM or light microscopy.

Results and Discussion

The present study shows that antiadhesive and antibacterial coatings consisting of monolayers of modified TL could be prepared on cellulose membrane surfaces.

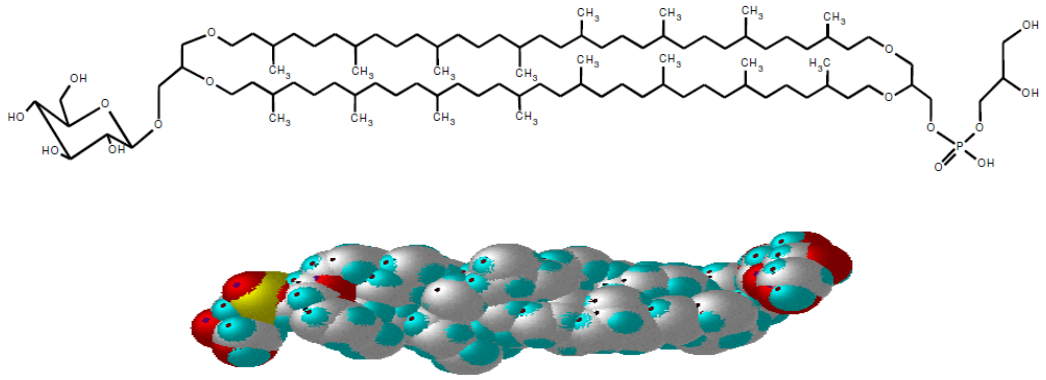

Figure. 1. The scheme shows the chemical structure of the used TL. The activation with cyanuric acid, in which one of the primary hydroxyl groups was substituted by the bivalent linker, allows the chemical coupling of the lipid to various surfaces with free hydroxyl or amino groups such as cellulose or polyurethane. The total thickness of the TL layer is about 4-5nm, depending on the molecular orientation.

A new process for coating of cellulose monolayers has been developed with special emphasis on applicability for the coating of other medical devices. Figure 2 shows the modification of a cellulose membrane surface with TL. The surface morphology changed from a relatively rough surface to a smoother one after modification. The lipid formed a highly ordered monomolecular film without visible inhomogenities or gaps. The film thickness was determined by AFM to 3.2nm ± 0.8nm. From the molecular structure of the TL [8,9], it can be concluded that the lipid is organised mainly in an uprightstanding conformation. The covalent coupling process could be confirmed by fourier transform infrared spectroscopy(FTIR), where new peaks at 1509 $cm^{-1}$and 1541 cm^{-1}, which corresponds to the C=N valence oscillations of cyanuric chloride, became visible. Contact angle measurements (water) have demonstrated an

increase of hydrophobicity caused by lipid coating on the cellulose membrane. The contact angle Θeq increased from 27° to 79°. The monomolecular lipid film is densely coated over the whole surface and is relatively impermeable for water, which explains the higher hydrophobicity. The uprightstanding conformation with the second hydrophilic headgroup orientated outside, limited the increase of hydrophobicity.

The silver colloids adsorbed spontaneously from the chloroformic dispersion onto the TL modified cellulose membrane (Figure 3). The silver colloids have a size of 19.2 ± 2.5nm and were of uniform round shape. After 10 min, 414 ± 68 silver nanoparticles (1x1µm) adsorbed onto the surface. The density of nanoparticles increased with time and reached a maximum after three hours (1589 ± 215 nanoparticle's respectively).The contact angle increased from 79° (TL coating), 87° (silver nanoparticle low density) to 93° (silver nanoparticle high density).

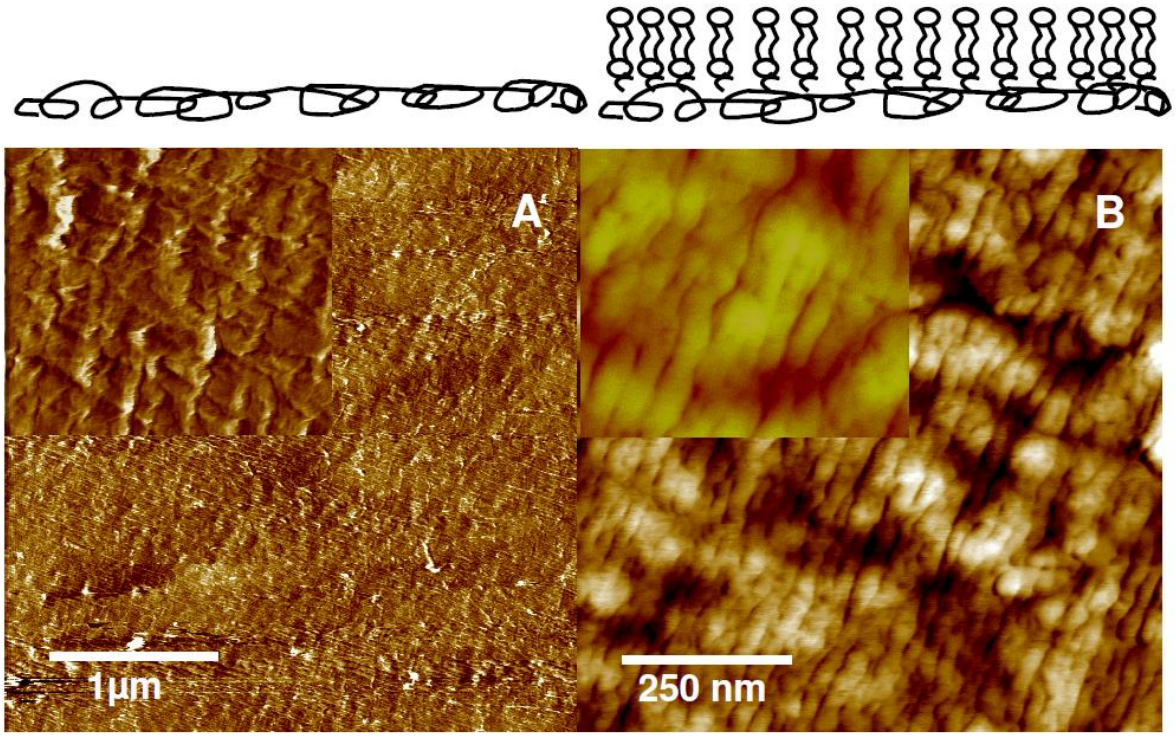

Figure. 2.AFM images of the surface modification of dialysis membranes. A) unmodified membrane, insert 125 x 125nm B) modified with TL, insert 125 x 125nm. The typical TL morphology on the cellulose surface could be visualized.

The results of adhesion studies with human serum are shown in Figure 4. After the adsorption time of 12 h, the unmodified cellulose membranes were completely covered by serum components. The underlying morphology could not be visualized after adsorption any more. The thickness of the formed biofilm is about 200 nm (AFM). The surface became more hydrophilic which was indicated by a decreased contact angle (45°). For lipid modified membranes, the adhesion of serum components was decreased. Some lymphocytes and proteins were adhered onto the surface, but still free areas were visible. The basic membrane structure could still be seen (Figure 4).The addition of TL coated silver colloids leads to a further improvement of the antiadhesive surface properties. As shown in Figure 3, the nanoparticles are organized in a nanostructure on the celluluse surface.

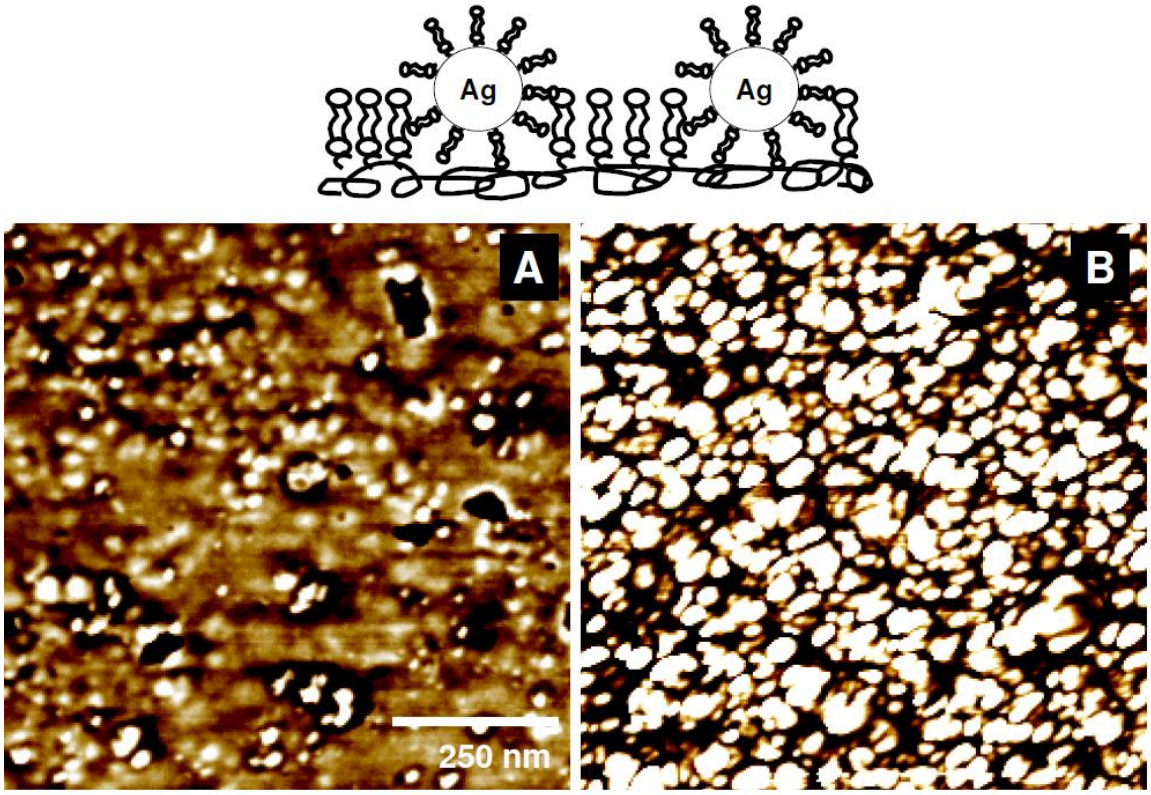

Figure. 3.AFM images of the surface modification of the dialysis membrane with silver colloids after TL pre-activation. A) low density, B) high density.

The nano roughness increased, whereas the microscopically visible roughness decreased. These structures can be discussed as the important key for the better antiadhesivity of the surface. Figure 5 shows the time dependence of the serum adhesion.

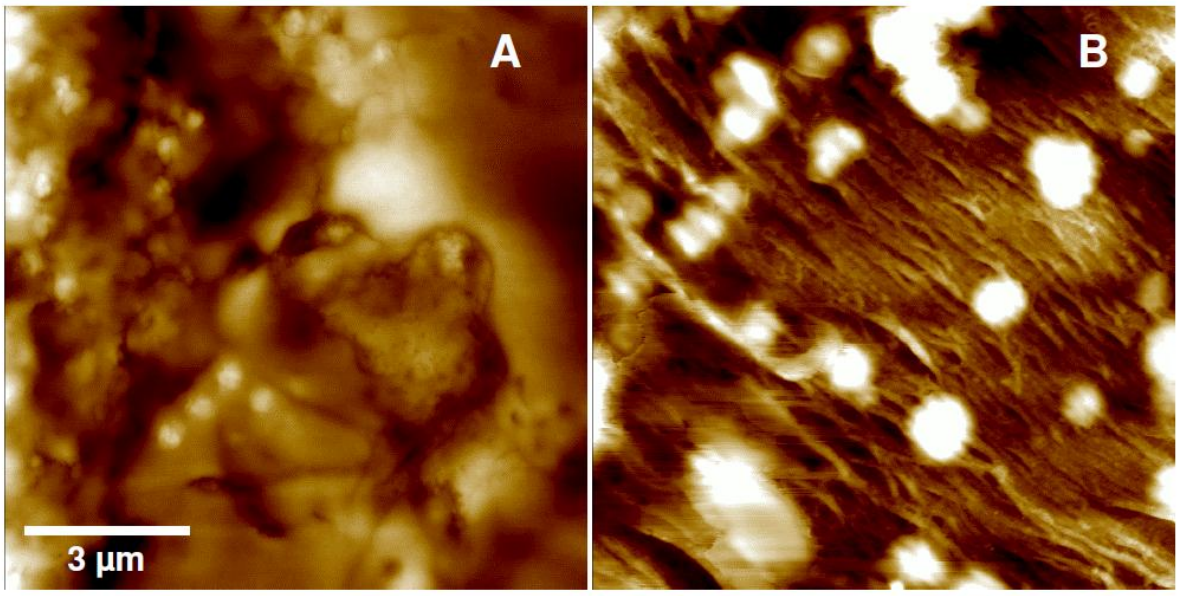

Figure. 4. AFM images of A) unmodified and B) TL modified dialysis membrane after serum adhesion.

The same effect of a decreased adhesion in the case of TL coated membranes was found by the use of suspensions of E.coli. Especially, the beginning of the biofilm formation in the first 24 h is slowed down (data not shown). This is in agreement to previous investigations by Frant et al. [10]. When the silver colloids were attached, the surface was protected against E.coli growth for more than 14 days.

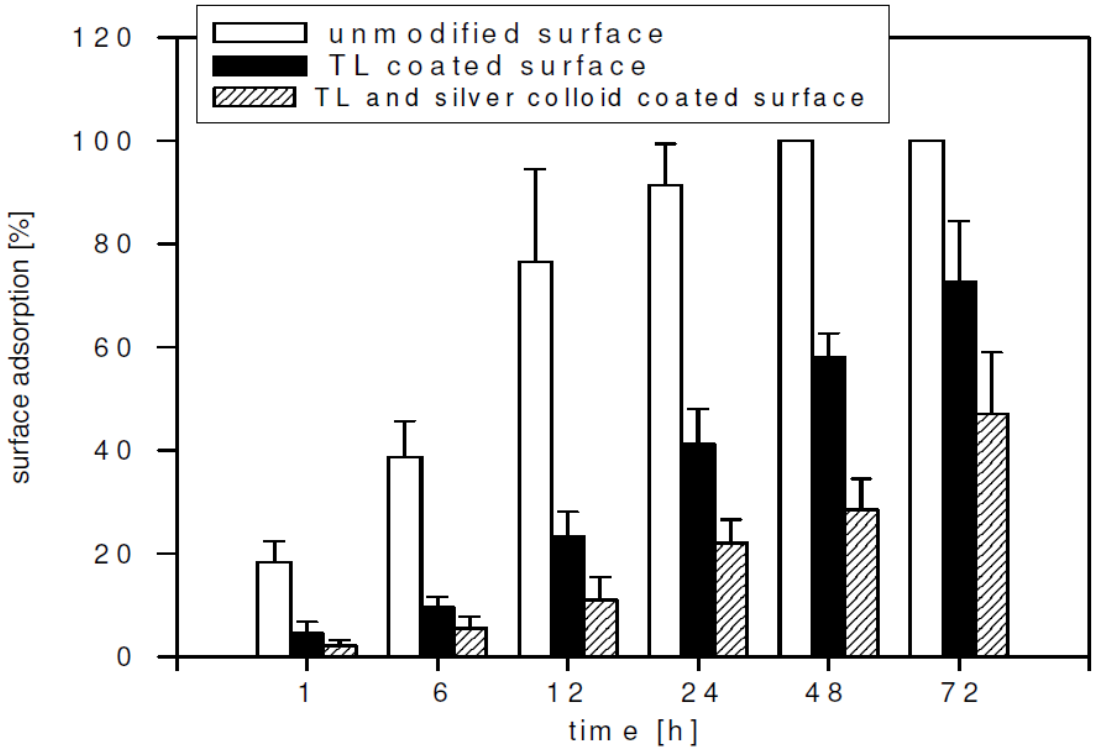

Figure. 5. The diagram shows the quantification of the serum adhesion. Covered surface area vs. adsorption time.

Conclusion

It could be shown that a highly ordered monomolecular and covalently coupled tetraether lipid film is formed by the chemical modification of a commercial available cellulose dialysis membrane. The film is resistant against oxidative or enzymatic degradation and prevents the membrane surface for protein adhesion and biofilm formation. It was found that it is possible to control the surface morphology in the nanometer scale by choice of the process parameters. The further modification of the surface by adsorption of tetraether lipid coated silver colloids leads to an improvement of the antadhesive and antibacterial properties of the biomedical membrane. The developed method may be adapted to other polymers than cellulose (e.g. polyurethane, silicon) and even to the coupling of other biomolecules, e.g. sugars, proteins, peptides and nucleic acids, and also non-biological coatings, such as hydrogels and dendrimers. Compared to the state-of-the-art, the new process has the advantage to produce a stable, covalent linkage of the lipid.

Acknowledgement

This work was supported by DFG Forschergruppe Nanohale 627, DFG Forschergruppe Biohybride 495, JPK Instruments Berlin (Germany) and SIT Surface and Interface Technologies GmbH, Heiligenstadt (Germany).

References

[1] B. R. Di Iorio, V. Bellizzi, N. Cillo, M. Cirillo, F. Avella, V. E. Andreucci, N. G. De Santo: JNephrol Vol. 17 (2004), p. 19

[2] R. P. Wenzel, M. B. Edmond: N Engl J Med Vol. 340 (1999), p. 48

[3] J. Brosnahan, A. Jull, C. Tracy: Cochrane Database Syst Rev CD004013 (2004).

[4] Danese: Chemistry & Biology Vol. 9(2002), p. 873

[5] R. O. Darouiche, Raad, II, S. O. Heard, J. I. Thornby, O. C. Wenker, A. Gabrielli, J. Berg, N. Khardori, H. Hanna, R. Hachem, R. L. Harris, G. Mayhall: N Engl J Med Vol. 340(1999), p. 1

[6] a.PCT/EP97/01011, 1997, E. Antonopoulos, U. Bakowsky, H. J. Freisleben, U. Rothe, b. PCT/DE2005/001162, 2006, U. Bakowsky, C. Kneuer, U. Rothe, K. Liefeith, M. Frant, K. Dölling, R. Schmid, H. Johnsen, P. Stenstad.

[7] Abid, Jean-Pierre 2003; PHD. Thesis S. 117ff, Laser induced synthesis and nonlinear optical properties of metal nanoparticles,

[8] Bakowsky U, Rothe U, Antonopoulos E, Martini T, Henkel L, Freisleben HJ: Chem Phys Lipids Vol. 105, Mar 2000, p. 31

[9] Mirghani Z, Bertoia D, Gliozzi A, De Rosa M, Gambacorta: Chem Phys Lipids Vol. 55, Aug 1990, p. 85

[10]M. Frant, P. Stenstad, H. Johnsen, K. Doelling U. Rothe, R. Schmid, K. Liefeith: Mat.-wiss. u. Werkstofftech Vol. 37, No. 6 (2006), p. 538

6 Self-assembled *N*-succinyl-chitosan Nanofibers for Reduced Protein Adhesion

Published in Advances in Science and Technology

Volume 76, pages 36-41, October 2010

Abstract

Protein adhesion on biomaterial surfaces plays a major role in determining their biocompatibility and cell responses. The goal of this study was to produce chitosan-based coatings of implant material polyurethane (PUR) for reduced human serum albumin (HSA) adhesion. Succinic anhydride was employed for modifying chitosan and synthesis *N*-succinyl-chitosan (NSCS) which was used as a matrix coating of PUR. NSCS showed self-assembly behaviour as nanofiber structures onto PUR surface. Atomic force Microscopy (AFM) has emerged as useful instrument for the molecular force measurements and thus it has chosen to investigate the adhesion properties of Human serum albumin (HSA) on the new matrix coatings and other three implant materials PUR, Silicon and Titanium.

HSA molecules were covalently bound to the AFM tip by the use of cyanuric chloride as bivalent linker. Analyzing of the force curves demonstrated the anti-adhesive properties of the NSCS films in comparison with the uncoated PUR, Silicon and Titanium.

Introduction

Protein adsorption on implant surfaces occurs when they are inserted into the human body. As a layer of the protein is formed, biological response like cellular interaction [2,3], bacterial adhesion [5] and platelet adhesion and thrombus formation [4] will be influenced by the produced layer. Many attempts to develop new biomaterials have focused on designing adhesion-resistant interfaces to promote the biocompatibility of these biomaterials by finding a solution to protein adsorption on the interfaces [8].

Human blood plasma comprises abundance of Human serum albumin (HSA), it consists of about 50% of HSA [6] and therefore it has to be carefully considered when the man-made implants/protein adsorption is studied [7].

Chitosan is a biocompatible and biodegradable polymer [9] it is derived from chitin by deacetylation process [1]. It is a versatile bio-polysaccharide commonly used in medical and pharmaceutical fields and widely used as coatings for surface modification of biomedical devices [11,12]. The aim of this study was to manufacture a chitosan derivate *N*-succinyl-chitosan as biomedical coating matrix and to investigate its effectiveness to reduce HSA adhesion in comparison with implants materials.

Materials and Methods

N-Succinyl-chitosan (NSCS) Synthesis

The NSCS was synthesized according to the method of Aiping et al [1]. Briefly, one gram of chitosan was dissolved in 1 wt % HAc solution under gentle stirring overnight. 0.2 gram succinic anhydride was dissolved in 20 ml acetone and then added to the chitosan solution by drop-wise for 30 min at room temperature. The components were then allowed to react for 4h at 40°C. Finally, the reaction mixture was cooled down to room temperature and then stored at 4°C.

N-Succinyl-chitosan Nanofibers Coating

Polyurethane (PUR) slides were washed with acetone and isopropanol, then rinsed with distilled water and dried in nitrogen flow. The slides were incubated in the previous NSCS solution for 30 min and then rinsed with distilled water and dried by exposing the samples for nitrogen flow for 3 min and then stored at 4 C°.

AFM Imaging

Atomic force microscopy (AFM) measurements were performed on a JPK NanoWizard™ (JPK Instruments, Berlin). The instrument was used for the visualisation as well as to measure the nanoindentation of the films. Silicon nitride AFM cantilevers (NSC 16 AIBS, Micromasch, Estonia) with ultra-sharp pyramidal tips (radius of the tip curvature less than 10 nm), resonance frequency of ~172 kHz and a nominal force constant of ~45 N/m were used for the topography measurement. To avoid damaging of the surfaces, intermittent contact (air) mode was chosen. The scan speeds were proportional and so the scan sizes. Images were taken by displaying the amplitude and height reflection signals of the cantilever in the trace direction.

Tip Functionalization

For force measurements, AFM triangular cantilevers (CSC21/NoAl) with a length of about 290 µm and spring constant of 0.086 ± 0.01N/m were functionalized. The Tips were treated with Piranha solution [1:2, H_2O_2 (30%, v/v):H_2SO_4 (98%, v/v)] for 20 min to remove the organic contamination and increase the number of –OH groups onto the surface and then rinsed extensively with distilled water and dried under nitrogen. The clean tips were incubated in 0.1 mol cyanuric chloride/chloroform overnight and N,N-diisopropylethylamine was used as catalyzer for the reaction. Human serum albumin (HSA) was immobilized on the cantilevers by dipping the cyanuric chloride activated tips in 1% w/v solution of HSA in borate buffer (pH 8) for 1h. The functionalized tips were then washed with distilled water and dried in nitrogen flow to use for force measurements. To demonstrate the protein coating, force curves of tip adhesion to cleaned glass surface, were captured before and after the tip modification.

Force Spectroscopy

Adhesion measurements of HAS modified AFM tips were carried out on PUR coated with NSCS nanofibers, PUR, and commercially available silicon and titanium chips. The force curves were recorded by moving the cantilever down from a starting point to reach the surface and allow the tip to interact with it and then retracing to the start position. The spring constant and the sensitivity of the cantilever had to be determined first. The spring constant was defined from the tracing force curve as the slope of section of the force curve captured through the tip-inelastic surface contact. Mica surface was used for this purpose. For each measured surface 192 force curves taken from three 5x5 µm force scan maps were recorded under ambient conditions (relative humidity 56% temperature 21 C°) and the distorted curves were not quantified. The adhesion force was determined from the retracing curve as the

difference between cantilever signal in equilibrium position and the lowest force (Fig. 2B). The extending and retracing times were adjusted on 0.6 s and the JPK image processing software was utilized for analyzing the force curves and calculating the adhesion forces. The average of adhesion values and the standard deviations were also estimated.

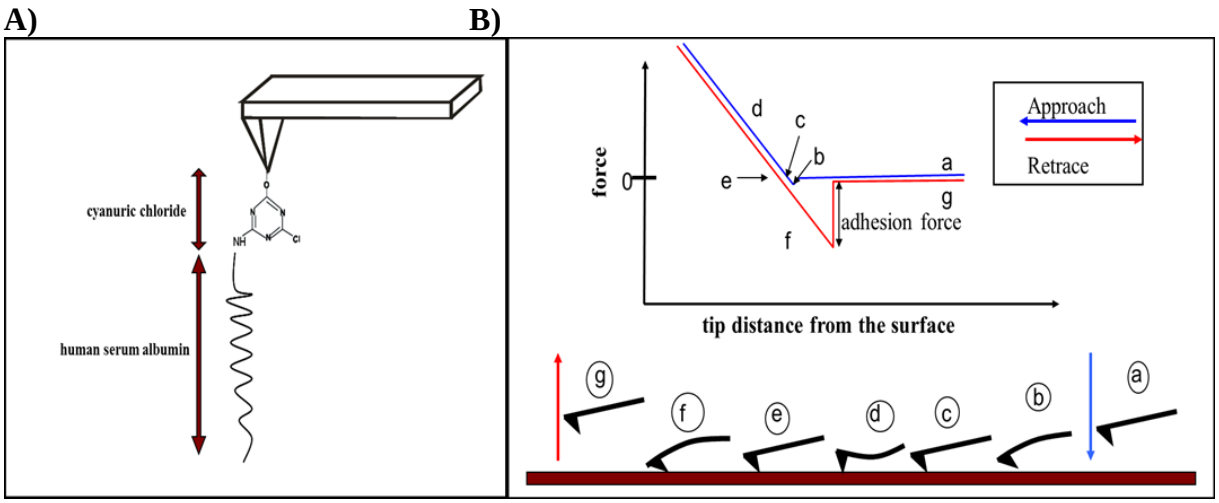

Fig. 1.(A)Representation of the chemistry used for covalent binding of HSA to AFM tip. HSA is shown attached to the surface through the bivalent linker cyanuric chloride. (B)Representation of a scheme of force-distance curve. The blue line shows the force as the tip approach the surface, C is the contact point and the red line shows the force recorded as the tip is retraced.

Results and Discussion

Synthesis and Self-assembly of NSCS

Succinic anhydride was used to synthesis NSCS from chitosan. Aiping et al [1]. reported on the chemical structure of NSCS. They demonstrated the formation of -NH-CO- bond structures when NSCS was synthesized and exhibited that the intramolecular hydrogen bonds (H-bonds) of chitosan were greatly reduced after the modification.

It is well-known that the intramolecular hydrogen bonds are responsible for the low water solubility of chitosan with high *N*-deacetylation degree because of the amine ($-NH_2$) and hydroxyl (-OH) groups along the chitosan chains. Nevertheless the weak intramolecular hydrogen bonds within the NSCS promote its water solubility due to the transformation of the amine ($–NH_2$) group into –NH-CO- bonds and enable the formation of NSCS nanoparticles when NSCS is dispersed in water. When PUR chips are dipped in the NSCS/HAc solution, a NSCS films on PUR surface will be formed by the attraction forces between the polymer and PUR surface.

After the film formation, the coated PUR chips were washed extensively with water and self-assembled NCSC nanofibers were constructed. These nanostructured films showed high stability onto the PUR surfaces after more than 14 days of incubation in Phosphate buffered saline (PBS) as no differences in the shape and sizes of the nanofibers could be noticed before and after the incubation. This leads to a possible explanation of the self-assembly of NSCS on PUR and its high stability onto the surface in neutral medium. Since the amino groups of chitosan were transformed into -NH-CO-, very little groups can be protonated and so the electrostatic interactions are not the expected forces which induce the formation of nanofibers and maybe are not responsible for its adsorption on PUR surfaces.

The alternative elucidation could depend on the hydrophobic domains within the NSCS and its amphiphlicity.

After cross linking of chitosan with succinic anhydride, moieties of (-CH_2 CH_2-) are formed. The hydrophobic nature of theses moieties as well as the acetyl groups helps NSCS to attach to the hydrophobic surface of PUR because of the hydrophobic forces while the H bonds and hydrophobic interaction within NSCS nanofibers are accountable for the assembly as nanofibers.

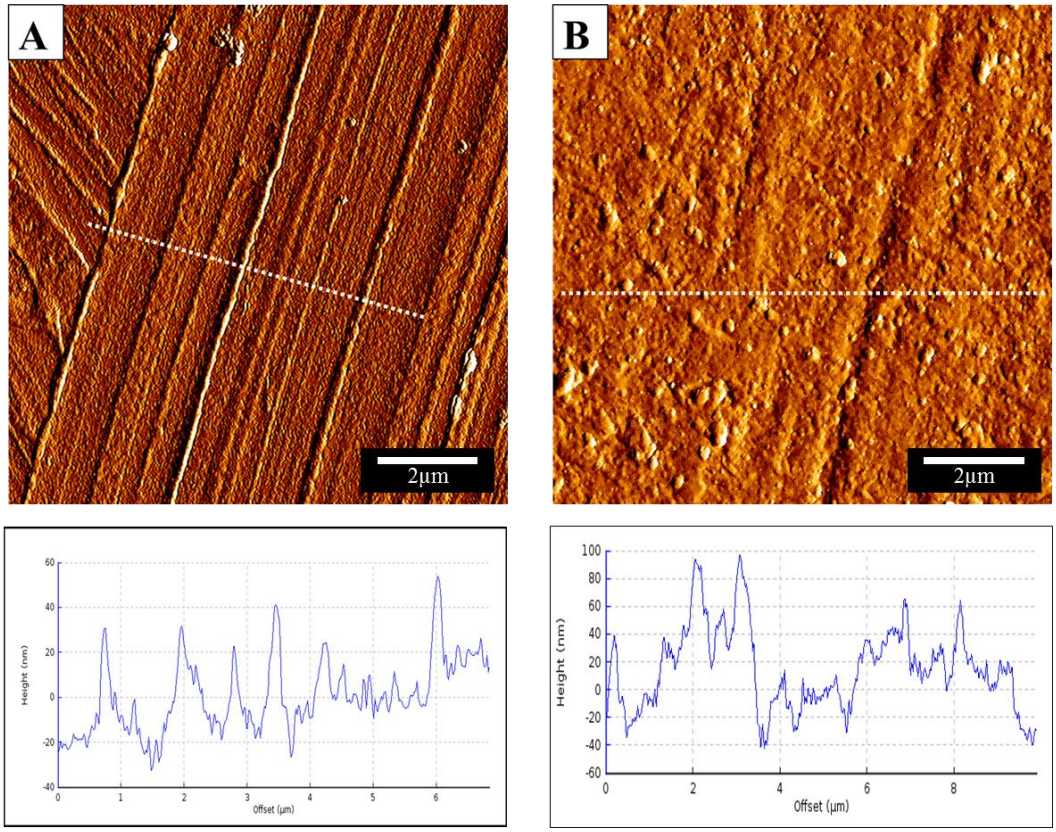

Fig. 3. AFM imaging and line profile of surface topography of (A) NSCS nanofiber coated PUR, (B) uncoated PUR.

Nanostructured Surface Morphology

Fig. 3.compares AFM image of the bare surface of PUR with the image of the surface after NSCS coating. The uncoated PUR shows rough and irregular surface while the film obtained

by NSCS coating presents regular nanofiber structure. This structure consists of assemblies of nanofibers and each assembly contains some nanofibers which are parallel to each other. The fiber width varied between 50 and 200 nm while they were between 25 and 75 nm in height. Line profile of the measured surface is shown in Fig. 3.

Tip Functionalization

Schematic representation of the tip modification chemistry is shown in Fig. 1. HSA immobilization on AFM tip was achieved by the use of cyanuric chloride as bivalent linker. Briefly, cyanuric chloride reacted with the free hydroxyl (-OH) group produced after Piranha treatment on the tip surface which resulted in a covalent bond. HSA was tethered to the tip through the reaction of cyanuric chloride with one of the free amine groups of the protein.

To confirm the presence of HSA molecules on the tip, the adhesions of blank and HSA modified tip to cleaned glass surface were examined. The force curves show significant differences of the adhesion forces of the unmodified tip (5.2 ± 0.4) compared to the modified one (7.41 ± 0.8 nN) which assures the existence of HSA on the tip.

HSA-Surface Interactions

AFM is a useful tool to measure forces between the tip and sample surfaces, these forces include van der Waals forces, electrostatic forces, specific forces and many other forces.

During the AFM measurements, the cantilever is approached to the surface, and after the tip-surface contact it is retraced. The retraction curve represents the force needed to separate the tip from the surface or to overcome the adhesion forces between the tip and the surface (Fig. 2B)

In this study, AFM was used to measure the adhesion forces between HSA and nanostructured NSCS films. These forces describe the affinity of HSA for the surface of NSCS film after

contact. Adhesion measurements were also done on uncoated PUR and commercially available silicon and titanium surfaces to compare the anti-adhesion effectiveness of NSCS nanofibers to the other implant materials.

The quantifications of HSA adhesion force to the different surfaces are shown in Fig. 4. It shows that NSCS has the lowest affinity to HSA. Protein adhesion at the interfaces is a complex process. It is regulated by many factors like chemical composition, surface roughness, hydrophobicity, etc [13].

The results presented in Fig .4 indicate that NSCS nanofibers have the highest effectiveness to reduce HSA adhesion (adhesion force 4.2 ± 0.4 nN) in comparison with PUR, Silicon and Titanium. This may due to the physicochemical and structural properties of the NSCS nanofibers.

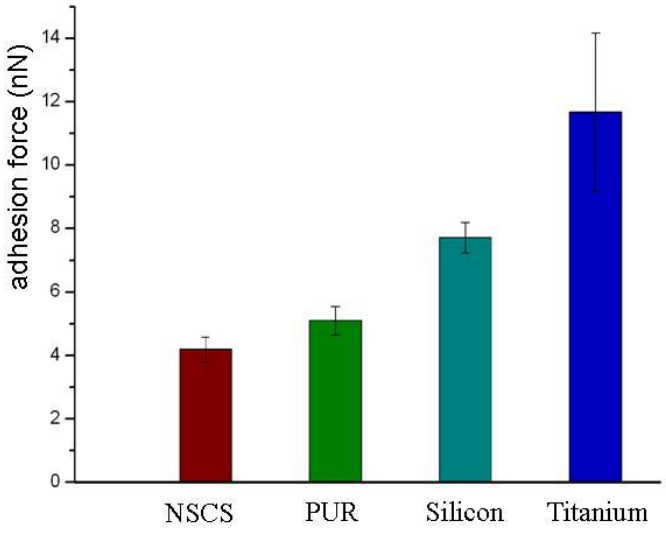

Fig. 4.HSA adhesion forces on NSCS film, PUR, Silicon and Titanium measured by modified AFM tips. NSCS films had the lowest protein affinity.

Summary

In this work, we demonstrated the ability to construct NSCS nanofibers films applicable for a coating of implant material PUR. The fibers are highly ordered and are at the nanoscale.

AFM was utilized to investigate the HSA-NSCS interaction by functionalizing the tip with HSA which was covalently bond to the tip surface.

The HSA adhesion measurements showed interest reduced adhesion properties of the NSCS compared to the other implant materials which make NSCS an important candidate when anti-adhesive coatings are designed.

Acknowledgement

The authors would like to thank JPK Instruments Berlin (Germany) for the support. This work was also partially supported by the AiF/EFDS 15090BG.

References

[1] Z. Aiping, C. Tian, Y. Lanhua, W. Hao, L. Ping: Carbohydrate Polymers Vol. 66 (2006), p. 274

[2] B.P. Swain: Appl. Surf. Sci Vol. 253 (2006), p. 2310

[3] P. Ying, Y. Yu, G. Jin, Z. Tao: Colloids Surf Vol. B 32 (2003), p. 1

[4] A. Zhu, T. Chen: Colloids Surf Vol. B 50 (2006), p. 120

[5] J. Strauss, Y. Liuand T.A. Camesano: Journal of minerals, metals, and materials society Vol. 61 (2009), p. 1543

[6] W. Faser, J.C. Chamberlain,*Blood and Transport Proteins*, in: J. Baynes, M.H. Dominiczak (Eds.), Medical Biochemistry, Mosby, Philadelphia, 1999, pp.21–29

[7] T. Indesta, J. Laine, K.S. Kleinschek, L.F. Zemlji: Colloids and Surfaces A. (2010)

[8]M.S. Wang, L.B. Palmer, J.D. Schwartz, A. Razatos: Langmuir Vol. 20 (2004), p. 7753

[9] Z. Orhan, E. Cevher, L. Mülazimoglu, D. Gürcan, M. Alper, A. Araman, Y. Özsoy: J Bone Joint Surg Vol. 88 (2006), p. 270

[10]B. Fei, H. Lu, J. H. Xin: PolymerVol. 47 (2006), p. 947

[11] J Fu, J. Ji, W. Yuan, J. Shen: BiomaterialsVol. 26 (2005), p. 6684

[12] J. Fu, J. Ji, D. Fan, J. Shen: Journal of Biomedical Materials Research part A Vol. 79A (2006), p. 665

[13] K. Mitsakakis, S. Lousinian, S. Logothetidis: Biomol. Eng Vol. 24 (2007), p.119

7 Nanostructured Medical Device Coatings Based on Self-assembled Poly(lactic-co-glycolic acid) Nanoparticles

Submitted to Colloids and Surfaces B: Biointerfaces

Abstract

Biological responses to implanted biomaterials often determine the biocompatibility and effectiveness of the implant. The physiochemical properties and drug loading of implant surface are the main factors which influence these responses. Here we present a new method for providing nanostructured drug-loaded polymer films which enable controlling the surface morphology and deliver therapeutic agents.

Silicon wafers were employed as model for implanted biomaterials and poly(lactic-co-glycolic acid) (PLGA) nanoparticles were assembled to silicon surface by electrostatic interaction. For the assembly process, modifying of silicon surface with amino-terminated layer was essential to produce positive charge on the surface. The prepared particles were negative charged due to the carboxyl end-group of PLGA. Mono layer of these particles attached to silicon surface when it was incubated in aqueous particle suspension. Particle density and surface coverage of silicon wafers were varied by altering particle concentration, incubation time in particle suspension and ionic strength of the suspension. Dye loaded nanoparticles were prepared and assembled to silicon surface to form nanoparticle films. After two weeks of incubation of these particle films in phosphate buffered saline (PBS), fluorescence intensity measurements showed diffusion-controlled release of the dye over 2 weeks and atomic force microscopy (AFM) observation revealed that these particles remained attached to the surface during the incubation time. Our work suggests that these nanoparticle coatings are versatile technique towards drug releasing from implant surface and modulation of surface morphology.

Introduction

Coating of biomedical devices is among the popular and efficient strategies to enhance biocompatibility and effectiveness of these devices and deliver therapeutic cargos. The films can act as reservoir for local or systemic drug delivery from the implant surface. Various studies focused on designing of drug-loaded polymer films, the used polymers varied between PLA, PLGA and their derivate [1-5], Chitosan and its blends [6-10] and other synthesized polymers.

The films can also be specifically designed to modulate surface properties in order to regulate biological responses. Numerous of studies showed that physiochemical properties of medical devices at interfaces influence the biological responses. Upon this fact, modification of device surfaces with biocompatible films can potentially reduce the undesired interactions associated with the implantation. For example, surface topography can be controlled through fabrication of micro- and nanostructured films, such surfaces potentially influenced protein adsorption, cell adhesion [11-14] and bacterial adhesion [14-17].

Colloidal lithography, based on self-assembly of colloidal particles onto surface, is a versatile method for surface pattering. This method has many advantages over the other methods which are used for producing patterned surfaces. i) It enables the fabrication of well-defined pattered surface over large surface area [18] ii) particle size and surface coverage can be varied and so the surface morphology [19] iii) the method provides low coast and high throughput producing process for designing structured surfaces. This technique can be applied to coat surfaces with 2D polymer particle and therefore it presents the advantages of being suitable for both i) modulate of surface morphology by controlling the particle size and organization and surface coverage ii) release biomolecules from the particles on the surface.

Some reports described the behaviour of cells on particles deposited on surfaces.

Kunzler et al. [20] demonstrated on the fabrication of gradient of negatively charged silica nanoparticles which were electrostatically adsorbed onto positively charged poly(ethylene imine) (PEI)-coated silicon wafers. After particle sintering, cell experiments with rat calvarial osteoblasts (RCO) showed that surface coverage with the particles considerably influenced cell proliferation and spreading and after seven days of seeding, the number of cells was eight times higher on the particle-free surface compared to the position with maximum particle coverage.

Gradients of microparticles were also investigated by Li et al. [21] in their work they used electrospray technique to construct density gradient of PLGA microparticles onto glass slides. After the deposition, the coated slide has varying surface roughness which enabled studying the effect of physical cues on neurite outgrowth from dorsal root ganglia. By optimising the surface roughness, the neuron adhesion and neurite extension were promoted.

Release of biomolecules from surface is another application of particles deposited on surfaces of medical devices. Lo et al. [22,23] presented in their works new method for coating of neural devices based on electrostatically attachment of negatively charged PLGA nanoparticles onto poly($_L$-lysine) (PLL) coated silicon surface. This particle coating showed high potential to release multiple agents simultaneously in addition to the high efficiency to deliver therapeutic agents and plasmid DNA.

Since Implantation process is associated with several of complexities resulted from undesired human body/implant-surface interactions, an ideal implant should be carefully designed to overcome these reactions. Tow strategies have shown promising results in this field: surface pattering at nanoscale and implant coating with drug loaded polymer. The combination of these two strategies can provide more advantages and promote the implant compatibility.

To the best of our knowledge, until now, no work focused on construction of highly ordered nanostructured polymer coating which controls the release of drugs or biomolecules.

Chapter 7

This work aim to present novel coating based on polymer nanoparticles assembled onto silicon surface for surface topography modulation and active agent release. Therefore, we investigated surfactant-free PLGA nanoparticles attached electrostatically to silicon surface. For this purpose, we prepared negative charged PLGA nanoparticles and fabricated films made of nanoparticles electrostatically assembled to negative charged silicon surface.

To control surface coverage with the particles, ionic strength and particle concentration in the aqueous suspension were tuned. To demonstrate the effectiveness of this coating for implants which are in contact with body fluids, morphological characterization of the films was investigated after PBS incubation. Fluorescence dye as model drug was also loaded into the particles to test the dye release from the films.

Materials and methods

Materials

Poly($_{D,L}$-lactide-co-glycolide) (PLGA), Type Resomer® RG 752H, lactide/glycolide ratio 75:25 was purchased from Boehringer Ingelheim , Ingelheim, Germany. 5-Aminofluorescein (AF) and (3-Aminopropyl)triethoxysilane (APTES), ≥ 98% and Phenylthrimethoxysilane (PTMS) were obtained from Sigma-Aldrich (Sigma-Aldrich chemie GmbH, Germany). All other chemicals and solvents used in this study were of high analytical grade and commercially available.

Nanoparticle preparation

AF loaded nanoparticles were formed according to the method described elsewhere [24]. Briefly, 160 mg PLGA were dissolved in 20 ml acetone at 25 °C under continuous stirring. Desired amount of AF was dissolved in 5 ml acetone and the solution was mixed vigorously with the polymer solution. The resulting solution was slowly added to 50 ml of filtered and double distilled water at constant flow rate of 10 ml/min and under magnetic stirring (360 rpm). For this purpose a syringe with injection needle (Neopoint® 0.90 × 70 mm; Servopharma GmbH, Wesel, Germany) was used. The resulting colloidal suspension was stirred for 4h under reduced pressure to evaporate off the organic solvent. The PLGA nanoparticles suspension was centrifuged at 10,000 rpm, resuspended in 50 ml double distilled water and then centrifuged a second time. The nanoparticles were collected and used for coating and release experiments.

Nanoparticles of 1% and 2% AF theoretical loading were prepared as described above by adding 1.6 mg and 3.2 mg to the polymer/acetone solution and the same steps were followed to make blank nanoparticles but without adding AF.

Nanoparticle characterization

Particle size measurement

The mean size and the size distribution of the particles were determined by photon correlation spectroscopy (PCS) using a Zetasizer NanoZS/ZEN3600 (Malvern Instruments, Herrenberg, Germany) at 25°C. To avoid multiscattering, the particles were suspended in filtrated and double distilled water to yield a concentration of (32µg/ml). Particle mean diameter (Z-Ave) and also the width of the fitted Gaussian distribution, which is displayed as the polydispersity index (PDI) were calculated using the DTS V. 5. 02 software. Each size measurement was carried out with at least 10 runs for more accuracy.

ζ -Potential measurement

The ζ -potential was measured by the use of NanoZS/ZEN3600 (Malvern Instruments, Herrenberg, Germany) at 25°C. Each sample was diluted in 1molar (1m) and 0.3molar (0.3m) Phosphat buffered saline (PBS) solutions and the ζ –potential was measured in these solutions of different ionic strength .The DTS V. 5.02 software was used to calculate the average ζ -potential values obtained from the data of 100 runs. All ζ –potential measurements were carried out in triplicate.

Encapsulation efficiency

The encapsulation efficiency is defined as the percentage of drug associated with the nanoparticles relative to the total amount of drug added during the nanoparticle preparation [25], while the theoretical drug loading is defined as the mass of drug added during the particle preparation relative to the total mass of the nanoparticles (polymer + drug).

$$\text{Encapsulation efficiency} = \frac{\text{drug associated with nanoparticles}}{\text{total amount of the added drug}} \times 100$$

$$\text{Theoretical drug loading} = \frac{\text{total amount of the added drug}}{\text{mass of nanoparticles (polymer + drug)}} \times 100$$

The encapsulation efficiency of the model drug AF was determined by calculating the mass of drug associated with 5 mg nanoparticles (experimental loading) by dissolving 5 mg of the AF in 5 ml DMSO at room temperature and diluting the solution in DMSO and then measuring the fluorescence absorbance. Plate reader (Saphire II; Tecan, Austria) was employed to determine the fluorescence intensities of the AF in the DMSO solutions at the wavelengths: 353 nm excitation/426 nm emission and glass plate was used for this purpose. The concentration of AF in the diluted solution and the mass of AF in 5 mg AF loaded nanoparticles were calculated. The theoretical load of the particles used in this study was 2% (w/w) (high dose-loaded nanoparticles) and 1 % (w/w) (low dose-loaded nanoparticles).

Silicon surface modification

Silicon wafers were washed with acetone, isopropanol and large amount of double distilled water and dried in nitrogen flow and then surface modified. Two kinds of surface modifications were prepared and examined regarding their effectiveness to produce self-assembly coating of PLGA nanoparticles. Surface modification with APTES was achieved by incubation the clean silicon wafers in 2µl/ml APTES/chloroform solution for 1h at room temperature. The wafers were washed with chloroform to remove loosely physisorbed APTES and then heated at 110 °C for 1h and stored at 4 °C for the coating experiments. Surface modification with PTMS was done by using 2µl/ml PTMS/chloroform by following the same steps. These two modifications were examined regarding their effectiveness to produce self-assembly coating of PLGA nanoparticles.

Nanoparticle self-assembly on modified silicon surface

APTES modified silicon wafers were incubated in blank nanoparticle suspensions in PBS at room temperature. After particle assembly, the wafer surfaces were extensively washed with distilled water to eliminate the unattached particle and then dried under vacuum overnight. Density of the particles and surface coverage on modified silicon surface was compared when different ionic strength, particle concentrations and incubation times were applied. Particle density was counted using ImageJ software. Each image was adjusted on 8-bit type and the particles were calculated by choosing the option "analyze particles". The software was able to give accurate count of the nanoparticles onto the surface. Five AFM images of each sample were taken and the average and standard deviation were calculated for each sample. Particle density was defined as the number of the nanoparticles attached to the surface relative the surface area. The surface coverage (%) was estimated from AFM images of phase contrast where nanoparticles appear like bright spots and the background as dark surface. ImageJ analysis was used to count the pixels of different colours. Surface coverage was calculated as percentage of pixels of the bright colour divided the pixels of the dark colour.

To determine the influence of nanoparticle concentrations on the assembly process, 0.32mg/ml, 0.16 mg/ml or 0.08 mg/ml suspensions of blank nanoparticle in 1m PBS were employed to construct nanoparticle coatings and the results of the different concentrations were examined. The wafers were incubated in particle suspensions for 5 min at room temperature.

To define the best ionic strength conditions for nanoparticle attachment, blank nanoparticles were suspended in PBS (1m) to yield a concentration of 0.32 mg/ml and then allowed to attach to the probe surface. The same experiments were repeated by the use of 0.3 m of PBS to reduce the ionic strength.

Keeping particle concentration and ionic strength constant (0.32 mg/ml particles in 0.3m PBS), the incubation time was increased from 2 to 20 min and both surface coverage and particle density on the surface were calculated.

For release studies, APTES modified silicon probes were incubated with 0.32mg/ml AF-loaded PLGA nanoparticle in 1m PBS for 5 min, followed by intensive washing with PBS and then dried in vacuum overnight. The release studies from nanoparticle coating were performed with coatings containing nanoparticles with 1% and 2 % (w/w) theoretical AF loading.

In vitro release studies

Nanoparticles for release experiments had a theoretical AF load of 1% and 2% (w/w).

The release of AF from the nanoparticle attached to silicon surface was carried out in 1m PBS at 37 °C for two weeks. The silicon probes were incubated in 40 ml PBS on a rotary shaker (20 rpm) (Rothaterm®, Gebr. Liebisch, Bielefeld, Germany). Samples of 3 ml were taken at predetermined time points and replaced with fresh medium of equivalent volume. The samples were then stored at 4 °C under light exclusion. AF concentrations in the samples were quantified by measuring the fluorescence intensity at the wavelengths 493 nm excitation/516 nm emission using plate reader and the cumulative release percentage was calculated at each time point.

In parallel, 5 mg AF loaded nanoparticles in 5 ml of PBS were incubated under the same conditions to compare the release profile from free particles with that of the nanoparticles attached to silicon surface. At predetermined time points the nanoparticle suspensions were centrifuged, the supernatants were collected and replaced with fresh medium. The particles were then resuspended in the fresh buffer for the next time point. Fluorescence intensities of

the supernatants were quantified and the cumulative release percentage was calculated at each time point.

Surface morphology of coatings

Morphology of the coatings was analyzed by AFM. The measurements were performed on a JPK NanoWizard™ (JPK Instruments, Berlin). Commercially available silicon cantilevers (NSC 16 AIBS, Micromasch, Estonia) with ultra-sharp pyramidal tips (radius of the tip curvature <10 nm), resonance frequency between 150-200 kHz and a nominal force constant of ~40 N/m were used for the AFM imaging. To avoid damaging of the surfaces, intermittent contact (air) mode was chosen. The scan speeds were proportional to the scan sizes. Images were taken by displaying the amplitude, height and phase reflection signals of the cantilever in the trace direction.

Nanoparticle coatings were visualized by AFM before and after the release studies and the effects of PBS incubation on both particle size and density were tested.

The JPK software was used to calculate the particle sizes and ImageJ software was used to estimate the particle density and surface coverage as described above. Five images of 5x5 µm size were captured of each sample.

Results and discussion

Nanoparticle characterization

The solvent displacement method was chosen to prepare the PLGA nanoparticles. This method is based on the Marangoni-effect phenomenon caused by the difference in the interfacial tension [26,27]. This technique provides many advantages over the commonly used methods such as the ease of scale up, good reproducibility and no requirement for homogenization during the preparation process. It is also suitable for the preparation of stabilizer-free PLGA nanoparticles.

The measured physiochemical properties of the nanoparticles are summarized in table 1. No significant changes of particles sizes before and after AF encapsulation were observed and the mean particle size ranged between 136 and 166 nm as confirmed by PCS. This indicates that AF encapsulation had no considerable effect on the particle size. The distribution of size was not wide and the polydispersity index was between 0.19 and 0.23.

Zeta potential of both blank and AF-loaded particles was measured in PBS (1 m and 0.3 m). Zeta potential measurements are shown in table 2.

Surface chemical properties of nanoparticles play a major role in the measured zeta potential.

The prepared nanoparticles were strongly negatively charged due to the PLGA chains which contain carboxyl-end groups. This negative charge of the particle was desired for the attachment to the amino-terminated films on silicon surface by electrostatic attractions .Since the used PLGA leaded to negatively charged nanoparticles, surface modification of the particles or the use of surfactants of negative charged polymers were unnecessary for particle assembly on silicon surface.

Zeta potential of particle suspended in aqueous solution is a function of surface charge density, shear plane location and surface structure. When the ion concentrations in this

solution are changed, the location of the shear plane changes, this leads to change of the zeta potential value [28]. For both blank and AF-Loaded nanoparticles, the absolute zeta potential increased when the buffer was diluted. This increasing was due to the reduction in ion concentrations in the buffer. PBS contains high concentration of cations like Na+ and K+ which can adsorb to the oppositely charged surface of the particle. When the PBS was diluted, less cations were available to adsorb to the surface and a shift in the shear plane took place.

The particles exhibited higher absolute values of zeta potential after AF loading (table 2)

The nanoparticles were loaded with AF. AF has low water solubility and relatively high solubility in acetone; it was used as model for hydrophobic drugs. The particles had high encapsulation efficiency varied between 87% and 97% for the 2% AF loaded nanoparticles and 1% AF loaded nanoparticles, respectively (table1). The encapsulation efficiency decreased as the amount of loaded AF increased. Higher loading resulted in lower encapsulation efficiency due to higher concentration gradients of the dye which promote the diffusion of the fluorescence dye out of the PLGA/acetone droplets to the water during the formation process of the nanoparticles.

Table 1

Properties of blank and AF loaded nanoparticles.

Nanoparticles	Size (nm)[a]	Polydispersity index	Experimental loading	Encapsulation efficiency (%)
Balnk PLGA	142 ± 23	0.23 ± 0.04	—	—
AF-Loaded nanoparticles	136 ± 60	0.19 ± 0.02	1%	97%
AF-Loaded nanoparticles	166 ± 21	0.23 ± 0.05	2%	87%

[a]n= 12

Nanoparticle self-assembly on modified silicon surface

Silicon probes were modified with APTES or PTMS. Nanoparticle coatings were prepared on APTES or PTMS modified silicon surfaces by immersing the silicon probe in 0.32 mg/ml nanoparticles suspension in 1m PBS at room temperature for 5 min and the effect of the used silane agent on nanoparticle coverage was investigated. The amino-terminated APTES surface was extensively covered with nanoparticles while the nanoparticle density on PMTS modified surface was extremely low. This indicates the role of the amino groups of APTES in self-assembly process compared to PTMS which has hydrophobic nature and no charged groups; this suggests that the electrostatic attraction is predominant for self-assembly of PLGA nanoparticles where hydrophobic interaction does not play a major role. The PMTS modified silicon wafers were therefore eliminated from further coating experimentations.

The effect of several parameters including the particles concentration, incubation time and buffer ionic strength on the nanoparticle coatings was tested by the use of blank nanoparticles. Surface coverage and particle density is considered to be associated with the particle concentration in the solution and therefore the relationship between particle concentration and surface coverage was investigated.

Fig 1 shows the AFM imaging of coatings obtained from 0.32 mg/ml, 0.16 mg/ml and 0.08 mg/ml nanoparticle suspensions in 1m PBS by 5 min incubation time.

Evaluation of particle density by image analysis showed increasing of surface coverage and particle density when particle concentration was increased. Particle density of images captured from coatings were found to be 16,200 ± 990 particles/mm2 (0.08 mg/ml), 22,080 ± 1800 particles/mm2 (0.16 mg/ml) and 38,720 ± 1550 particles/mm2 (0.32 mg/ml) and the surface coverage were estimated to be 13.44 ± 2%, 35.8 ± 4% and 66.5 ± 3% respectively

Similar effect of incubation time was observed. Keeping constant the other preparation parameters, the raise of incubation time yielded higher surfaces coverage and particle density.

Fig 1 shows nanoparticle coatings from 0.32 mg/ml suspension in two different incubation times: 5 and 30 min. The coating reached its maximal coverage after 30 min of incubation where the surface was almost completely covered with the nanoparticles. Since these nanoparticles have low zeta potential in magnitude, the hydrophobic effects dominates over the electrostatic repulsion which explains the closed packing of the particles.

Surface coverage with charged nanoparticles and the morphology of the resulted layer varied with the ionic strength of the medium [22,29]. Therefore we investigated the effect of ionic strength on the particle monolayer. The particles were negative charged in 1m PBS (ζ – Potential -15 ± 2 mV) whereas the magnitude of zeta potential raised up to -52 ± 7 mV in diluted PBS [table 2] which related to the difference in ionic concentration in the buffer as described above.

Table 2

ζ –Potentialmeasurements of Blank and AF loaded nanoparticles in 1 and 0.3 m PBS.

Nanoparticles	Buffer	ζ -Potential[a](mV)
Blank PLGA	1m PBS	-15 ± 2
Blank PLGA	0.3m PBS	-52 ± 7
1% AF-Loaded nanoparticles	1m PBS	-23 ± 2
1% AF-loaded nanoparticles	0.3m PBS	-53 ± 5
2% AF-loaded nanoparticles	1m PBS	-25 ± 4
2% AF-loaded nanoparticles	0.3m PBS	-54± 5

[a]n= 100

The electrostatic repulsion between particles with large zeta potential in magnitude limits surface coverage as the particles repel their neighbors preventing closed packing of the

particles [22,29,30]. This observation is consistent with the results in our study. Fig 1 shows very low density of nanoparticles onto the surface due to their high zeta potential value in 0.3m PBS (600 ± 90 particles/mm2 and surface coverage of 2 ± 1%) whereas the particles were densely attached to the surface when they were less charged in 1m PBS.

Depended on these results, the coating conditions were optimized to obtain required nanoparticle density and surface coverage for release studies. The nanoparticles exhibited increasing magnitude of zeta potential in PBS when AF was loaded [table 2]. Because of the high zeta potential value, suspensions of AF-loaded nanoparticle with high concentrations were used for the release experimentation. The concentration was set at 0.32 mg/ml to achieve high surface loading. The incubation time was kept on 5 min and all the coating experiments were done in undiluted PBS. Under these conditions the obtained particle density was 16,240 ± 900 nanoparticles/mm2 and 28,800 ± 2200 nanoparticles/mm2 for the 2% and 1% AF-loaded nanoparticles, respectively.

The effectiveness of coating can depend on the loading capability of the active agent in this coating. The coating must have the capacity to release the active agent in the desired level and poor loading my limit this capacity.

Lo et al [22]. demonstrated the fabrication of PLGA nanoparticle coating onto poly(L-lysine) (PLL) coated silicon oxide wafers. One limitation of this study is the low of the surface with particles where the maximum surface coverage was ~ 13%. When multilayering was attempted to improve the nanoparticle density, heavy aggregates of nanoparticles were observed on the surface. Attempt was also made by Jiao et al [31] to construct layer-by-layer assembly of poly(lactic acid) nanoparticles. Despite the higher number of the nanoparticle layers, the amount of the used model drug in the film was extremely low.

In comparison to Lo and Jiao studies, the unique advantage of our nanoparticle coating is the high loading capability of the surface with nanoparticles up to ~100% and the ability to

control the surface coverage by adjustment the coating parameters.

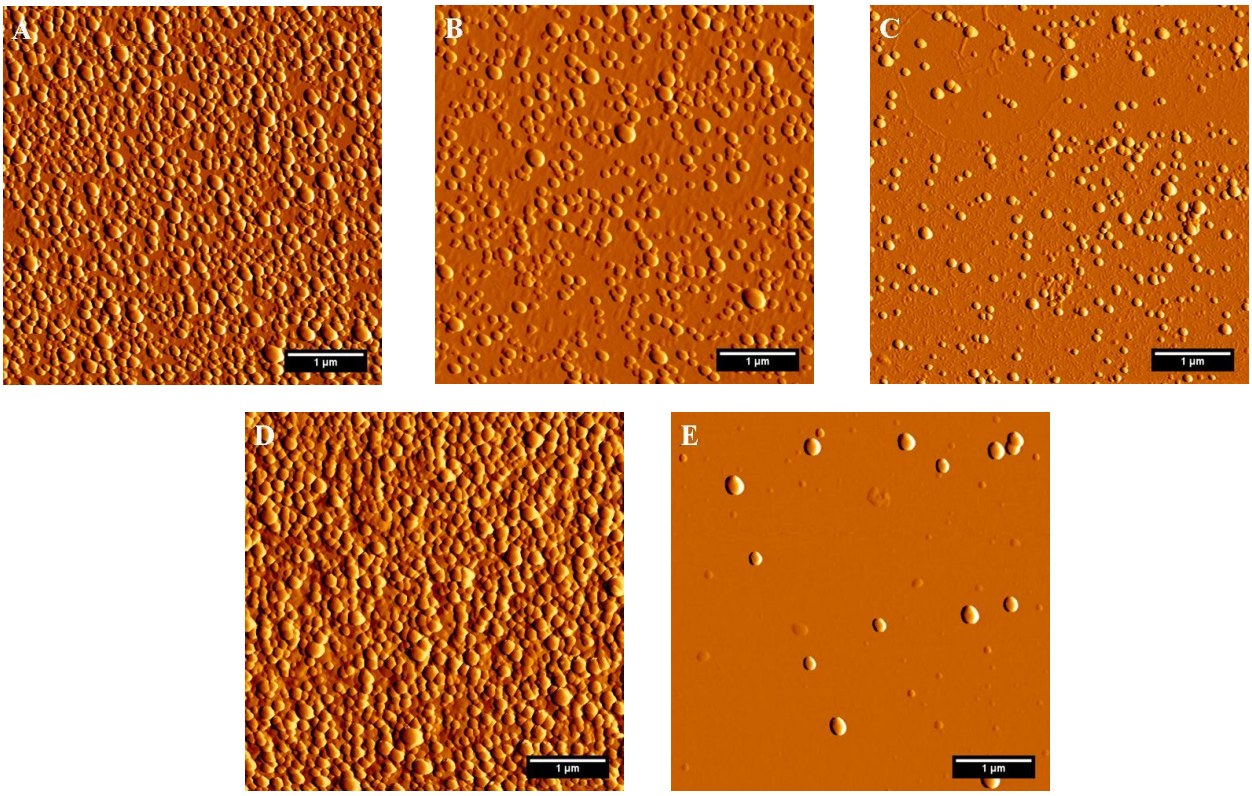

Fig. 1. Surface morphologies of nanoparticle coatings were observed under AFM. For self-assembly process, APTES modified silicon wafers were incubated in particle suspension in 1m PBS for 5 min and the particle concentration in the suspension was 0.32mg/ml (A), 0.16 mg/ml (B) and 0.08 mg/ml (C). Keeping the preparation parameters of surface (A) constant and raising the incubation time from 5 to 20 min resulted in higher surface coverage (D). Film

(E) was prepared using the same parameters like A but the ionic strength was reduced using 0.3m PBS.

In vitro release studies

For release studies AF was chosen as hydrophobic model drug. PLGA nanoparticles are suitable candidate for encapsulation of hydrophobic agents due to the hydrophobic nature of PLGA. Release kinetics of AF from our coatings was compared with the release profile from PLGA nanoparticles in PBS for 14 days at 37 °C. Fluorescence measurements of the released dye demonstrated typical release profile of PLGA nanoparticles. Fig 3 shows the release of AF from coated silicon and nanoparticles at different theoretical loading. An initial burst release in the first few days followed by sustained release at the next days was observed. The release efficiencies of the coatings were similar to that of the nanoparticles at the same theoretical loading. It can also be seen that the release rate at 1% theoretical loading was faster than that at 2% theoretical loading. The increased amount of loaded AF decreased the release rate. One possible explanation is the increasing dye-dye interaction when dye loading in the particle increases. Due to its hydrophobic nature, the dye may build small aggregates inside the polymer particle when acetone diffuse from the particle to water phase during particle formation process, these aggregates can slow the release rate.

The potential of these coating as drug delivery coatings depends strongly on the nanoparticle stability onto the surface after exposing to blood or other body fluids. Therefore, the nanoparticle coatings were examined in regards their stability on the surface before and after release studies. Surface morphology of the coating was imaged by AFM before and after PBS incubation. The particles were still attached to the surface after 14 days of incubation under mild stirring (20 rpm), the surface coverage remained almost the same and insignificant differences of particle size and shape were observed (Fig 2). PLGA degrades in water via

chemical hydrolysis of the ester bonds resulting in oligomers with carboxyl end groups or lactic and glycolic acids [32]. The initially yielded acids catalyze the further hydrolysis of other ester bonds. This phenomenon is called autocatalysis and it is responsible for the faster internal degradation of the nanoparticles when the acids within the particles cannot be freed

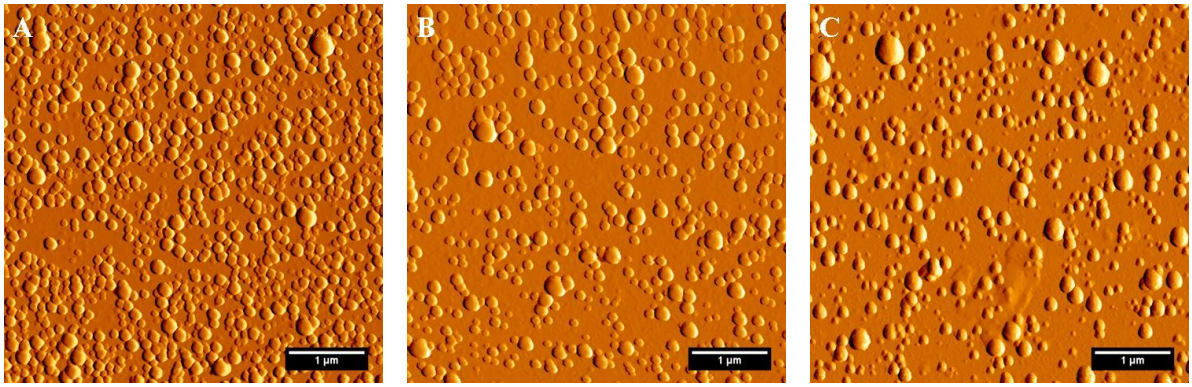

Fig. 2.AF loaded nanoparticles assembled to APTES modified silicon using 1% and 2% AF theoretical-loaded nanoparticles (A) and (B) respectively. Surface morphology after incubation of surface B in PBS for 2 weeks (C).

which induces internal morphological and compositional changes [33] were surface erosion of PLGA nanoparticles in not detectable in the first 2 weeks [22].

As expected Fig 2 shows no considerable changes of surface morphology of the particles whereas slightly increasing of particles sizes was noticed. This is because of the internal degradation of the particles leading to increase the hydrophilicity of the inner part and particle swelling in water. The assembly and release experiments suggest that the particles can be assembled to the surface with high density; they have also the ability to release active agents and remain attached to the surface.

Release from self-assembled nanoparticles

Release from free nanoparticles

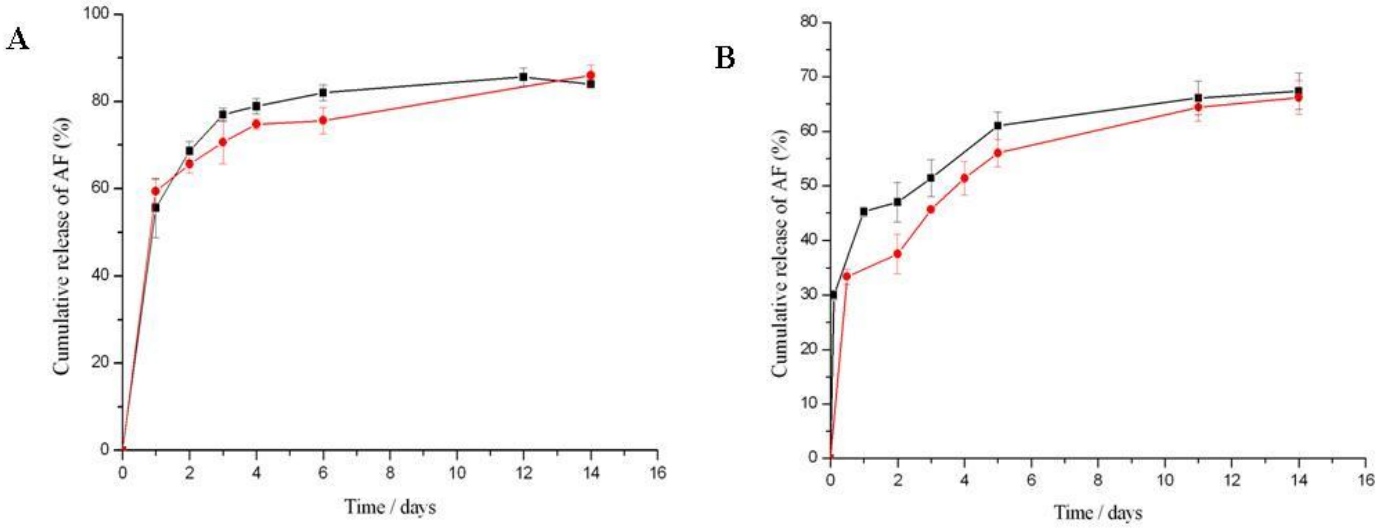

Fig. 3. Percentage cumulative release of AF from both free and surface-assembled nanoparticles. The AF theoretical loading was 1% (A) and 2% (B).

Conclusion

Herein, we demonstrated that mono layer of stabilizer-free PLGA nanoparticles can successfully construct onto silicon surface. The used particles were uniform and negative charged in PBS and the absolute value of their zeta potential depended on the ion concentration in the puffer. This negative charge enabled the attachment of the particle to silicon wafers by electrostatic interaction when the wafers were modified with amino-terminated layer. The particle attached in 1m PBS better than in 0.3m because diluting of PBS raises their absolute value of zeta potential and the attached particle repel their neighbour preventing further particle attachment. Increasing of particle concentration enhanced the attachment rate where more particles are available in the suspension and raising the incubation time provided higher surface coverage with the particles. These three factors enabled altering particle density and surface coverage of the coating. The coatings were proved regarding their effectiveness to release hydrophobic fluorescence dye (AF). The release profiles from attached particle were compared with that from free particles in 1m PBS. The two profiles were similar and the coatings were capable to release the dye over a period of two weeks. The particle/silicon-surface interactions were found to be strong enough to keep the particle attached to the surface after the two week of PBS incubation which makes these coating suitable for implants and biomaterials which are in contact with body fluids.

These results suggests that our technique for implant coating can be promising approach for eliciting desired biological responses by delivery of drugs and controlling surface morphology.

References

[1] M. Ravelingien, S. Mullens, J. Luyten, M. D'Hondt, J. Boonen c, B. D. Spiegeleer, T. Coenye, C. Vervaet, J. P. Remon, Eur J Pharm Biopharm, 76 (2010) 366.

[2] J. K. Jackson, J. Smith, K. Letchford, K. A. Babiuk, L.Machan, P. Signore, W. L. Hunter, K. Wang, H. M. Burt, Int J Pharm, 283 (2004) 97.

[3] U.Westedt, M. Wittmar, M. Hellwig, P. Hanefeld, A. Greiner, A. K. Schaper, T.Kissel, J Control Release, 111 (2006) 235.

[4] A. Finkelstein, D McClean, S. Kar, K. Takizawa, K. Varghese, N. Baek, K. Park, M. C. Fishbein, R. Makkar, F. Litvack, N. L. Eigler, Circulation, 107 (2003) 777.

[5] T. Xi, R. Gao, B. Xu, L. Chen, T. Luo, J. Liu, Y. Wei, S. Zhong, Biomaterials 31 (2010) 5151.

[6] N. Bhattarai, J. Gunn, M. Zhang, Adv Drug Deliv Rev, 62 (2010) 83.

[7] S. P. Noel, H. Courtney, J. D. Bumgardner, W. O. Haggard, Clin Orthop Relat Res 466 (2008) 1377.

[8] L. B. Rodrigues, H. F. Leite, M. I. Yoshida, J. B. Saliba, A. S. Cunha Junior, A.A.G. Faraco, Int J Pharm, 368 (2009) 1.

[9] J. Nunthanid, M. Luangtana-anan, P. Sriamornsak, S. Limmatvapirat, K. Huanbutta, S. Puttipipatkhachorn **;** Eur J Pharm Biopharm, 71 (2009 356.

[10] J. K. Smith, J. D. Bumgardner, H. S. Courtney, M. S. Smeltzer, W. O. Haggard, J Biomed Mater Res B Appl Biomater, 94B (2010) 203.

[11] KY. Suha, J. Seonga, A. Khademhosseinib, PE. Laibinisa, R. Langer, Biomaterials, 25 (2004) 557.

[12]R. Iwata, P. Suk-In, V. P. Hoven, A. Takahara, K. Akiyoshi, Y. Iwasaki, Biomacromolecules, 5 (2004) 2308.

[13] P. Kim, D. H. Kim, B. Kim, S. K. Choi, S. H. Lee, A. Khademhosseini, R. Langer, K. Y. Suh, Nanotechnology, 16(2005) 2420.

[14] L. Ploux, K. Anselme, A. Dirani, A. Ponche, O. Soppera, V. Roucoules, Langmuir, 25 (2009) 8161.

[15] E. Dayyoub, E. Belz, N. Dassinger, M. Keusgen, U. Bakowsky, Phys. Status Solidi A, 208 (2011) 1279.

[16] S. Hou, H. Gu, C. Smith, D. Ren, Langmuir, 27 (2011) 2686.

[17] C. Satriano, G.M.L. Messina, S. Carnazza, S. Guglielmino, G. Marletta, Mater Sci Eng C, 26 (2006) 942.

[18] P. Hanarp, D. Sutherland, J. Gold, B. Kasemo, Nanostruct. Mater.12 (1999) 429.

[19] P. Hanarp, D. Sutherland, J. Gold, B. Kasemo, Colloids SurfA,214 (2003) 23.

[20] T. P. Kunzlera, C. Huwiler, T. Drobek, J. Vörös, N. D. Spencer, Biomaterials, 28 (2007) 5000.

[21] X. Li, M. R. Macewan, J. Xie, D. Siewe, X. Yuan, Y. Xia, Adv. Funct. Mater. 20 (2010) 1632.

[22] C. T. Lo, P. R. Van Tassel, W. M. Saltzman, Biomaterials, 30 (2009) 4889.

[23] C. T. Lo, P. R. Van Tassel, W. M. Saltzman, Biomaterials, 31 (2010) 3631.

[24] C. Cai, U. Bakowsky, E. Rytting, A. K. Schaper, T. Kissel, Eur J Pharm Biopharm, 69 **(**2008) 31.

[25] E. Rytting, M. Bur , R. Cartier, T. Bouyssou, X. Wang, M. Krüger , CM. Lehr, T. Kissel, J Control Release, 141 **(**2010) 101.

[26] C.V Sternling, L.E Scriven, AIChE J, 5 (1959) 514.

[27] B. Dimitrova, I. Ivanov, E. Nakache, J. Dispers. Sci. Technol. 9 (1988) 321.

[28] M. D. Marco, C. Sadun, M. Port, I. Guilbert, P. Couvreur, C. Dubernet, Int J Nanomedicine, 2 (2007) 609.

[29] K. Yamaguchi, T. Taniguchi, S. Kawaguchi, K. Nagai, Colloid Polym Sci, 282 (2004) 684.

[30] IU. Vakarelski, CE. McNamee, K. Higashitani, Colloids Surf A Physicochem Eng Asp, 295 (2007) 16.

[31] YH. Jiao, Y. Li, S. Wang, K. Zhang, YG Jia, Y. Fu, Langmuir, 26 (2010) 8270.

[32]JP. Kitchell, DL. Wise, Meth Enzymol, 112 (1985) 436.

[33]S. Li, J Biomed Mater Res, 48 (1999) 342.

8 Summary and perspectives

Chapter 8

Summary

In this thesis, new coatings against bacterial adhesion and protein adsorptionwere developed, characterized and their effectiveness against bacterial adhesion and protein adsorption was investigated.

Two strategies were followed to resist the bacterial adhesion. The first one is based on designing of high-ordered nanostructured polymer features while the second one concern with construction of polymer loaded with anti-bacterial agents.

Reduction of protein adsorption is the second aim of this thesis. To achieve this goal, ultra-thin films with nano-scaled topography were manufactured.

Chapter 1 introduces the formation of biofilm. It describes detailed the formation steps and the factors that influence each phase during this process. Focusing on the biofilm associated with implant, risks of bacteria releasing from biofilm and the strategies to avoid bacterial adhesion were discussed. Since protein adsorption is mostly accompanying with biofilm formation, special concern was given to the driving factor that inhibit protein attachment on implant surfaces like nano-topography and surface chemistry.

Chapter 2 deals with thewell-known complications of urinary catheters, bacterial attachment to the surface and crystal encrustation. In this chapter, we suggested new way to solve these problems. In our developed method, antibiotic and silver ions-released film of biodegradable polymer (PLGA) was prepared and characterized to be deposited on catheter surface as anti-bacterial and anti-encrustation coating. The films had the ability to release the wide-spectrum antibiotic (norfloxacin) in an effective concentration over more than 50 days. In addition to norfloxacin, silver ions were released from silver nanoparticles incorporated in the films and the two showed high potential to inhibit the attachmentof four strains of urinary tract infection

bacteria in addition to *E.coli*. this due to the effect of the two antibacterial agents in addition to the anti-adhesive properties of tetraether lipids which were used to construct thin layer surrounding silver nanoparticles. Low viability of the adhered bacteria was noticed and so low number of the adhered bacteria has the capability to cause urinary tract infection. Crystal depositions resulted from increasing urine pH were reduced, this was achieved by choosing the suitable polymer for the films. The acidic products of PLGA degradation could neutralize the alkali resultant of urea hydrolysis on the film surface which can increase the biocompatibility of urinary catheter by reducing the complications and the pain associated with the encrustation.

Chapter 3 presents the development of nanostructured PLGA features using dipping method. The resulting films were characterized regarding their morphology using atomic force microscopy and their stability under flow conditions. It was shown that changing preparation parameters affect feature size and spacing. The half-sphere shaped features ranged between 100 and 450 nm in diameter, and this could be controlled by changing dipping time, and water/acetone content in the PLGA solution. The adhesion of *E.coli*on the coating surface for 30 h was investigated. Result analysing suggested significant relationship between both feature size and spacing and bacterial adhesion. It was concluded that features with spacing smaller than bacteria dimension inhibit bacterial attachment by reducing the available attachment area. Increasing of the spacing decreased the bacteria-surface contact area and bacterial attachment as expected and that was the case for spacing smaller than bacteria dimensions. When the spacing was raised up to values that are higher than bacteria dimension, surprising results showed decreased efficiency to prevent bacterial attachment. The results highlight the importance of feature size and spacing at nanoscale with respect to bacterial adhesion.

Chapter 4 includes explanation of new technique to construct polymer honeycomb-like films. Characterization of the topography of the yielded film was done via atomic force microscopy. The films were all similar in shape but variation of pore sizes were noticed when manufacturing parameters were changed, the size ranging was between 650 and 50 nm. Water contact angel of the film surfaces were investigated showing little differences between the films where no one of the nanostructured films showed superhydrophobic properties, this was discussed in the chapter. The bacterial adhesion results of this section also confirm that bacteria-surface contact area is key factor that influence bacterial adhesion and this was in agreement with the results of chapter 3. Rising of pore size reduced the contact area resulted in lower bacterial adhesion. Comparative experiments with smooth spin-coated PLGA films confirmed this hypothesis. The smooth film had the lowest anti-adhesive properties because provides the highest contact area.

Chapter 5 describes method for coating of cellulose dialysis membrane with tetraether lipid-coated silver nanoparticles. Fouling of this membrane with bacteria and proteins raises the risks of infection and membrane failure. Combination between silver nanoparticles as depot for silver ions and teteraether lipids was the aim of this study to present anti-bacterial and anti-adhesive film. Silver ions have wide popularity as antibacterial agent. Coating of silver nanoparticles with tetraether lipids provide extra anti-adhesive properties to the particles as described in this chapter. The lipid coated silver nanoparticles were self-assembled to cellulose dialysis membrane. Variation of particle concentration in the coating solution and incubation times resulted in different surface coverage with the particles. The different films were examined regarding their sufficiency to reduce protein adsorption.

Chapter 6presents the construction of N-succinyl-chitosan and its assembly as nanofibres on implant material, polyurethane. The topography of the assembled film was characterized by atomic force microscopy which showed fiber-shaped nanostructured surface. The same tool, atomic force microscopy, was utilized to estimate protein adhesion on the prepared surface. Cyanuric chloride was used as bilinker for covalently binding of human serum albumin to the tip of atomic force microscopy cantilever. The chapter includes Schematic presentation of the chemistry we used for the covalent binding. Force measurements with the modified tips were applied on the N-succinyl-chitosan surface and the results were compared with the adhesion values of the protein on uncoated polyurethane and commercially available implant materials (silicon and titanium). Calculation of the adhesion forces showed anti-adhesive properties of the N-succinyl-chitosan film.

Chapter 7 describes colloidal lithography-based technique to alter surface topography of silicon by deposition of drug-loaded PLGA nanoparticles. The negative charged particles were allowed to attach to modified positively charged silicon. Manufacturing parameters were optimized to obtain high surface coverage with the particle up to about 100%. Low surface coverage was also possible to achieve. The results gained from chapter 6 confirmed that feature spacing play major roll in bacterial adhesion and therefor this study aimed to design films with different spacing between the particles which was achieved by changing manufacturing parametes. This technique provides more adavantages since the deposited particles can be loaded with active agents or drugs and allowed to attach to the surface to release their cargo. The combination of the two mechanisms (nanostructuring of the surface and release therapeutic molecules) is a promising way to reduce bacterial adhesion by controlling surface topography and releasing antibacterial agents from the particle to decrease bacterial viability on the surface.

Perspectives

Development of medicine and medical technology leaded to the invention of implants. In last decades, new types of implant with more functions and improved biocompatibility appeared on the market. In spite of the fast development of implant material, functions and performance, the biofilm and protein adsorption are still the unsolved problems associated with implantation process. In this thesis, one step towards solving this problem was done. We present here varieties of method to reduce the bacterial adhesion and protein adsorption. Bacterial adhesion were inhibited by three ways: using of materials that resist bacterial adhesion like tetraether lipids, construction of nanostructured polymer films, and designing of polymer films loaded with antibacterial agents. The efficiency of each method was investigated separately and showed promosing results. Here, it must be considered that this war against bacterial adhesion and the associated infection is endless. Bacteria success to develop new strains and speices with higher virulence and capacity to adhere to wide range of surfaces and therefore a combination of the three strategies we used in one active method is more likely to inhibit bacterial adhesion than each method alone.

Reduction of protein adsorption was achieved by construction of nanostructured films and materials which repel the proteins and reduce the adhesion.The phenomenon of reduced protein adsorption of nanostructured surfaces was widely investigated but the reason is still not completely known. More focus on the adhesion process of proteins at molecular scale can improve our knowledge and lead to more understanding of this phenomenon towards producing new biomaterials with advanced properties against protein adsorption.

.

Zusammenfassung und Ausblick

.

Zusammenfassung

Im Rahmen der vorliegenden Dissertation wurden neuartige Beschichtungen von Kathetersystemen entwickelt, charakterisiert und ihre Effektivität gegenüber bakterieller Adhäsion und Proteinadsorption getestet.

Als erstes Ziel wurden zwei Strategien zur Verhinderung bakterieller Adhäsion verfolgt. Die Erste basiert auf der Entwicklung hochorganisierter nanostrukturierter Polymerfilme, während bei der zweiten Methode antibakterielle Wirkstoffe in die Polymerfilme eingebettet werden.

Das zweite Ziel dieser Arbeit setzte sich mit der Reduzierung der Proteinadsorption auseinander. Um dies zu erreichen, wurden ultra-dünne Filme mit nanostrukturierter Oberfläche entwickelt.

Kapitel 1 beschreibt die Grundlagen der Bildung und des Aufbaus von Biofilmen. Detailliert werden die einzelnen Schritte und die beeinflussenden Faktoren bei der Bildung des Biofilms dargestellt. Der Schwerpunkt wurde dabei auf Biofilme an Implantaten und die damit einhergehenden Probleme gelegt. Das Risiko einer Herauslösung von Bakterien aus einem Biofilm und Strategien zur Vermeidung der bakteriellen Adhäsion werden diskutiert. Ein weiterer wichtiger Punkt ist die Proteinadsorption, die normalerweise mit der Bildung eines Biofilms einher geht. Hier wurde besonderes Augenmerk auf Faktoren gelegt, die die Proteinadsorption auf Implantatoberflächen vermindern (Oberflächenmorphologie und Oberflächenchemie).

Kapitel 2 beschäftigt sich mit den bekannten Problemen die bei der Verwendung von Urogenitalkathetern auftreten: (i) bakterielle Adhäsion und (ii) Kristallablagerung auf der Katheteroberfläche. Hier werden von uns neue Wege zur Lösung dieser Probleme vorgeschlagen und praktisch umgesetzt. Unsere Methode verwendet bioabbaubare

Polymerfilme (PLGA), die mit klassichen Antibiotika und Silbernanopartikeln (Nanotoxikologie und Silberwirkung) beladen sind. Aus diesen Filmen werden Silberionen und die Antibiotika gezielt freigesetzt, um die Bakterienadhäsion wie auch die Kristallablagerung zu vermindern. Eine Freisetzung des Breitband-Antibiotikums (Norfloxacin) aus den Filmen war über einen Zeitraum von mehr als 50 Tagen in wirksamer Konzentration möglich. Zusätzlich zu Norfloxacin werden Silberionen aus den inkorporierten Silbernanopartikeln freigesetzt. Die Kombination der beiden Wirkstoffe zeigte eine große Wirksamkeit gegen die Adhäsion von *E.coli.* und der verwendeten Bakterienstammmischung. Der antibakterielle Effekt der beiden Wirkstoffe wird verstärkt durch die anti-adhäsiven Eigenschaften von archealen Tetraetherlipiden, die verwendet wurden, um eine dünne Schicht um die Silbernanopartikel aufzubauen. Die Ausbildung einer Urogenitalinfektion konnta dadurch signifikant unterdrückt werden. Eine Ablagerung von Kristallen, hervorgerufen durch pH-Erhöhung im Urin, wurde durch das Auswählen eines geeigneten Polymers für den Film vermindert. Die beim PLGA Abbau entstehen sauren Produkte neutralisieren die basischen Reste der Harnstoffhydrolyse an der Oberfläche der Filme. Dadurch wird die Biokompatibilität der Urogenitalkatheter zusätzlich verbessert.

Kapitel 3 beschreibt die Entwicklung von nanostrukturierten PLGA-Filmen mittels Eintauchmethode. Die morphologischen Eigenschaften der Filme mittels AFM charakterisiert und bezüglich ihrer Stabilität unter Durchfluss-Bedingungen getestet. Die Herstellung der halbkugligen Polymerstrukturen mit Durchmessern zwischen 100 nm und 450 nm konnte durch Veränderung der Eintauchzeit und des Aceton/Wasser-Verhältnisses der PLGA-Lösung gesteuert werden. Die Adhäsion von *E. coli* auf der Oberfläche der neuartigen PLGA Filme wurde für 30 h getestet. Bei der Auswertung der Ergebnisse zeigte sich eine starke Abhängigkeit der Bakterienadhäsion von der Größe und den Abständen der

Polymerstrukturen. Daraus konnte der Schluss gezogen werden, dass Polymerstrukturen, mit Abständen kleiner als die Breite der Bakterien, die Adhäsion dieser durch Verkleinerung der Adhäsionsfläche vermindern.

Kapitel 4 stellt die Entwicklungeiner neuen Technik zur Herstellung honigwaben-artiger Polymerfilme vor. Die Charakterisierung der erhaltenen Filme erfolgte mit dem AFM. Die Filme zeigten alle eine ähnliche Gestalt. Durch Veränderung der Herstellungsparameter konnten Porengrößen zwischen 50 und 650 nm erzeugt werden. Die Kontaktwinkel gegenüber Wasser zeigten keine signifikanten Unterschiede. In Übereinstimmung zu Kapitel 3 konnte auch hier gezeigt werden, dass die Kontaktfläche der Bakterien entscheidend ist für die Verminderung der Bakterienadhäsion. Ein Ansteigen der Porengröße führt zu einer Verkleinerung der Bakterienkontaktfläche und somit zu einer Verminderung der Bakterienadhäsion. Vergleichsexperimente mit glatten spin-gecoateten PLGA-Oberflächen unterstützen diese Hypothese. Der glatte Film hatte die schlechtesten anti-adhäsiven Eigenschaften, da er die größte Kontaktfläche bot.

Kapitel 5 beschreibt eine Methode, Dialysemembranen aus Cellulose mit thetraetherlipid-beschichteten Silbernanopartikeln zu überziehen. Eine Ablagerung von Bakterien und Proteinen auf diesen Membranen führt zu einem erhöhten Infektionsrisiko und einer erhöhten Rate von Membranfehlfunktionen. Ein Ziel dieser Arbeit ist die Herstellung antibakterieller und antiadhäsiver Schichten unter Verwendung einer Kombination von Silbernanopartikeln als Silberionendepot und Tetraetherlipiden. Silberionen sind als antibakterieller Wirkstoff etabliert. In diesem Kapitel wird beschrieben, wie die Beschichtung der Silbernanopartikel mit Tetraetherlipiden zu einer erhöhten antiadhäsiven Wirkung gegen Proteine führt. Die Tetraetherlipid-beschichteten Silbernanopartikel lagern sich selbständig auf der

Dialysemembran an. Unterschiede in der Partikelkonzentration und den Inkubationszeiten führten zu verschiedenen Oberflächenbedeckungen. Die verschiedenen Filme wurden bezüglich ihrer Effektivität der Reduktion der Proteinadsorption untersucht.

Kapitel 6 zeigt die Nutzung von N-succinyl-chitosan zum Aufbau von Nanofasern als Implantatmaterialbeschichtungen aus Polyurethan. Die Topographie der Filme wurde mit Raster-Kraft-Mikroskopie untersucht, wobei die Organisation der faser-artigen Nanostrukturen sichtbar wurde. Die Proteinadsorption und Wechselwirkung auf diesen Oberflächen wurde mit der Raster-Kraft-Mikroskopie / Kraftspektroskopie analysiert. Zur Herstellung eines Nanosensors konnte mit dem bivalenten Linker Cyanurchlorid humanes Serumalbumin an die AFM-Spitze gebunden werden. Kraftmessungen mit der modifizierten Spitze wurden auf den N-succinyl-chitosan Oberflächen durchgeführt. Die antiadhäsiven Eigenschaften der N-succinyl-chitosan Filme wurden im Vergleich zu reinem Polyurthan, Silicon und Titanoberflächen charakterisiert. Die berechneten Adhäsionskräfte zeigen die deutlich verminderte molekulare Adhäsivität der Schichten.

Kapitel 7 beschreibt eine Technik der kolloidalen Lithographie zur Veränderung der Oberflächentopographie von Silizium durch Deposition von wirkstoffbeladenen PLGA-Nanopartikeln. Die negativ geladenen Partikel konnten auf die positiv geladene Siliziumoberfläche gebunden werden. Die Herstellungsparameter wurden so lange optimiert, bis eine Oberflächenbedeckung von bis zu 100 % erreicht wurde. Wie aus ***Kapitel 6*** bekannt, spielt der Abstand der Oberflächenstrukturen eine entscheidende Rolle bei der Bakterienadhäsion. Daher wird in diesem Kapitel durch Veränderung der Herstellungsparameter versucht, Filme mit verschiedenen Partikelabständen herzustellen. Die dabei verwendete Technik beinhaltet entscheidende Vorteile, da die Partikel mit Wirkstoffen

beladen als „controlled release system“ dienen können. Diese Kombination von zwei Mechanismen (Nanostrukturierung der Oberflächen und Freisetzung von Wirkstoffen) ist eine vielversprechende Möglichkeit die Bakterienadhäsion durch die Oberflächeneigenschaften der Katheter bzw. Implantatmaterialien zu reduzieren und gleichzeitig die Bakterien durch Freisetzung von Wirkstoffen zu verringern.

Ausblick

In den letzten Jahren führte die Entwicklung der Medizin und der Medizintechnik zu neuen Implantattypen mit mehr Funktionen und verbesserter Biokompatibilität. Trotz der schnellen Entwicklung von Materialien, Funktionen und Eigenschaften der Implantate sind die Adsorption von Biofilmen und Proteinen immer noch ungelöste Probleme im Bereich der Implantate. In dieser Arbeit wurde versucht Lösungen für diese Problem zu finden. Es konnten verschiedene Methoden zur Reduktion der Bakterien Adhäsion und Proteinadsorption vorgestellt werden. Die Bakterienadhäsion wurde mit drei unterschiedlichen Strategien vermindert: (i) es wurden Materialien wie Tetraetherlipide verwendet, die der Adhäsion von Bakterien entgegenwirken; (ii) nanostrukturierte Filme wurden hergestellt und (iii) außerdem Polymerfilme mit antibakteriellen Wirkstoffen beladen. Die Effektivität jeder Methode wurde einzeln mit vielversprechenden Ergebnissen untersucht. An dieser Stelle muss allerdings gesagt werden, dass durch unsere Entwicklungen die Bakterien Adhäsion und damit verbundene mögliche Infektion nur zeitlich begrenzt verhindert werden können, da die Eigenschaft der Bakterien neue Stämme zu entwickeln und Spezies mit höher „Virulenz“ und gesteigerter Adhäsionsfähigkeit zu verschiedenen Materialien zu schaffen, sehr groß ist. Daher sollte eine Kombination der drei von uns beschriebenen Methoden zu einem besseren Ergebnis führen, als jede Methode allein dies vermag.

Die Reduktion der Proteinadsorption wurde durch Konstruktion nanostrukturierter Filme und Verwendung Proteinabwehrender Materialien erreicht. Das Phänomen das eine nanostrukturierte Oberfläche die Proteinadsorption reduziert konnte deutlich nachgewiesen werden, der mechanistische Grund dafür ist bisher nicht vollständig geklärt. Ein stärkerer Fokus auf die molekularen Vorgänge der Proteinadsorption könnte unser Wissen auf diesem Gebiet vermehren und die Produktion neuer Biomaterialien mit verbesserten Eigenschaften gegen Proteinadsorption fördern.

Appendices

Abbreviations

APTES	(3-Aminopropyl)triethoxysilane
AF	5-Aminofluorescein
AFM	Atomic force microscopy
CUTI	Catheter-associated urinary tract infections
CLA	Centre line average
CLSM	Confocal laser scanning microscopy
EDTA	Ethylenediaminetetracetic acid
ECM	Extracellular matrix
EPS	Extracellular polymeric substances
FDA	Food and Drug Administration
FTIR	Fourier transform infrared spectroscopy
HAS	Human serum albumin
LBL	Layer-by-layer
R_p	Maximum height of peaks
R_v	Maximum height of valleys
NF	Norfloxacin
NSCS	*N*-succinyl-chitosan
PTMS	Phenylthrimethoxysilane
PBS	Phosphate buffered saline
PCS	Photon correlation spectroscopy
PDI	Polydispersity index
PEI	Poly(ethylene imine)
PEO	Poly (ethylene oxide)
PET	Polyethylene terephthalate
PLGA	Poly(lactic-co-glycolic acid)

PLL	Poly($_L$-lysine)
PTFE	Polytetrafluoroethylene
PUR	Polyurethane
R_a	Arithmetic average height
RCO	Rat calvarial osteoblasts
R_q	Root mean square roughness
R_z	Ten-point height
SEM	Scanning Electron Microscopy
SDS	Sodium dodecyl sulfate
TEL	Tetraether lipids
TSB	Trypic Soy Broth

List of publications

1. Eyas Dayyoub, Johannes Sitterberg, Ulrich Rothe, Udo Bakowsky.New Antibacterial, Antiadhesive Films Based on Self Assemblies of Modified Tetraetherlipids.Advances in Science and Technology 2008;57:188-194.

2. Eyas Dayyoub, Udo Bakowsky. Self-Assembled N-Succinyl-Chitosan Nanofibers for Reduced Protein Adhesion.Advances in Science and Technology 2010;76:36-41.

3. Eyas Dayyoub, Elvira Belz, Nina Dassinger, Michael keusgen, Udo Bakowsky. A novel method for designing nanostructured polymer surfaces for reduced bacteria adhesion. Physica Status Solidi (a) 2011;28:1279-1283.

4.Eyas Dayyoub, Marion Frant, Klaus Liefeith, Udo Bakowsky. Anti-bacterial and Anti-encrustation Hydrophobic Biodegradable Polymer Coating for Urinary Catheter.In preparation for journal of controlled release.

5.Eyas Dayyoub, Christian Hobler, Pierina Nonnweiler, Michael Keusgen, Udo Bakowsky. Nanostructured Medical Device Coatings Based on Self-assembled Poly(lactic-co-glycolic acid) Nanoparticles. Submitted to Colloids and Surfaces B: Biointerfaces.

6. Eyas Dayyoub, Elvira Belz, Nina Dassinger, Jens Schäfer, Johannes Sitterberg, Michael Keusgen, Udo Bakowsky. Highly ordered self-organized polymer coatings for reduced bacteria adhesion. In preparation for Acta Biomaterialia.

7. Juliane Nguyen, Regina Reul, Thomas Betz, Eyas Dayyoub, Thomas Schmehl, Tobias Gessler, Udo Bakowsky, Werner Seeger, Thomas Kissel. Nanocomposites of lung surfactant and biodegradable cationic nanoparticles improve transfection efficiency to lung cells. Journal od Controlled Release 2009;140:47-54.

8. Juliane Nguyen, Regina1 Reul, Susanne Roesler, Eyas Dayyoub, Thomas Schmehl, Tobias Gessler, Werner Seeger, Thomas Kissel. Amine-Modified Poly(Vinyl Alcohol)s as Non-viral

Vectors for siRNA Delivery: Effects of the Degree of Amine Substitution on Physicochemical Properties and Knockdown Efficiency. Pharmaceutical Research 2010;27:2670-2682.

9. Aybike Ozcetin, Eyas Dayyoub, Christian Hobler, Michael Keusgen, Udo Bakowsky. Selective interactions of concanavalin A-modified tetraether lipid liposomes.. Physica Status Solidi (c) 2011;8:1985-1989.

10. Nina Dassinger, Doru Vornicescu , Stefan Merkl, Marcus Kehrel, Eyas Dayyoub, Udo Bakowsky , Michael Keusgen. A fusion protein for regenerative surfaces.Submitted toPhysica Status Solidi (a).

Curriculum Vitae

Name: Eyas Dayyoub
Geboren am 29.11.1979 in Latakia/Syrien
Staatsangehörigkeit: Syrisch
Familienstand: ledig

Schulische Ausbildung:

1985-1991 Grundschule in Latakia
1991-1994 Mittelschule in Latakia
1994-1998 Sekundarschule in Latakia und Abitur mit dem Prädikat "ausgezeichnet"und einer Durschschnittsnote von 88%.

Studium:

1998- 2003 Studium der Pharmazie an der Tischrin-Universität Latakia, Bachelor-Abschluss mit dem Prädikat "gut".

Berufstätigkeit:

2003-2005 Tätigkeit als Landapotheker in meiner eigenen Apotheke in Latakia/Syrien.
März 2006 – März 2012 Anfertigung der vorliegenden Dissertation unter Leitung von Herren prof. Dr. Udo Bakowsky, Institut für pharmazeutische Technologie und Biopharmazie.

Marburg 02.02.2012

E R K L Ä R U N G

Ich versichere, daß ich meine Dissertation

„**Anti-bacterial and Anti-adhesive Nanostructured Coatings for Improved Implant Biocompatibility**“

selbständig ohne unerlaubte Hilfe angefertigt und mich dabei keiner anderen als der von mir ausdrücklich bezeichneten Quellen bedient habe.

Die Dissertation wurde in der jetzigen oder einer ähnlichen Form noch bei keiner anderen Hochschule eingereicht und hat noch keinen sonstigen Prüfungszwecken gedient.

Marburg, den 14.02.2012

Eyas Dayyoub